Glucose Transport and Metabolism in Polycystic Kidney Disease

---

Dissertation

zur

Erlangung der naturwissenschaftlichen Doktorwürde

(Dr. sc. nat.)

vorgelegt der Mathematisch-naturwissenschaftlichen Fakultät der Universität Zürich

von

Daniel Rodríguez Gutiérrez

aus

Spanien

Promotionskomitee

Prof. Dr. Arnold von Eckardstein (Vorsitz)

Prof. Dr. Rudolf P. Wüthrich (Leiter der Dissertation)

Prof. Dr. Carsten Wagner

Prof. Dr. Ian James Frew

Zürich, 2016

Summary

Glucose transport and metabolism in polycystic kidney disease

Polycystic kidney disease (PKD) is one of the most common inherited disorders, being the fourth leading cause of kidney failure in humans. PKD is characterized by the formation of multiple cysts in the kidney. The expansion and proliferation of cysts play a key role in reducing kidney function and leading to chronic renal failure. There are two rat models of PKD: Han:SPRD rats which phenotypically resemble human autosomal dominant polycystic kidney disease (ADPKD), and PCK rats which are an orthologous model of autosomal recessive polycystic kidney disease (ARPKD). Han:SPRD develop cortical cysts which originate from proximal tubules of the nephrons, whereas PCK develop medullary cysts which originate from the collecting duct.

The aim of this thesis was to examine whether the transport and the metabolism of glucose in the kidney play a pathogenic role in cyst proliferation and expansion in these two rat models of PKD. We hypothesized that the generation of an osmotic diuresis by inhibition of sodium-glucose cotransporters (SGLT) in the proximal tubules will force the fluid transport from cysts to the tubular lumen, thereby reducing cyst expansion and improving the decline in renal function. Furthermore, based on the knowledge of an increased demand of glucose by aerobic glycolysis in proliferating epithelial cells in PKD (Warburg effect) we selectively blocked glucose metabolism with the glucose analog 2-deoxyglucose (2DG) to test its beneficial effect in PKD.

We first tested the dual SGLT inhibitor phlorizin in Han:SPRD rats and found a significant positive effect, i.e. phlorizin ameliorated the cyst expansion and improved the decline in renal function and reduced albuminuria. We then tested the selective SGLT2 inhibitor dapagliflozin (DAPA) in Han:SPRD rats and found that DAPA did not reduce cyst expansion but had a slight positive effect on renal function and also reduced albuminuria. In contrast, DAPA unexpectedly increased cyst expansion and accelerated the functional decline of renal function and increased albuminuria in PCK rats, presumably because of a strong osmotic effect in the collecting duct.

We then investigated the energy metabolism in cystic tissues of Han:SPRD rats and confirmed the upregulation of genes involved in glycolysis and the downregulation of genes involved in gluconeogenesis, thus demonstrating that the Warburg effect is present in the cystic kidneys of Han:SPRD rats. When using 2DG to block glycolysis we found an important reduction of cyst growth and a slower decline of renal function and less albuminuria.

Altogether our experimental studies in two different rat models of PKD show that glucose transport and metabolism play an important role for cyst growth and expansion. This sets the basis for using these potential targets in the future treatment of PKD.

Zusammenfassung

Transport und Metabolismus von Glukose bei polyzystischer Nierenkrankheit

Die polyzystische Nierenerkrankung (PKD) ist eine der häufigsten genetisch bedingten Erkrankungen und ist der vierthäufigste Grund für das chronische Nierenversagen beim Menschen. PKD charakterisiert sich durch die Bildung von multiplen Zysten in der Niere. Die Expansion und Proliferation der Zysten spielen eine entscheidende Rolle bei der Abnahme der Nierenfunktion und führen zu Nierenversagen. Es gibt zwei PKD-Rattenmodelle: Han:SPRD Ratten, welche phänotypisch der menschlichen autosomal dominanten polyzystischen Nierenerkrankung (ADPKD) ähneln, und PCK Ratten, welche ein orthologes Modell der autosomal rezessiven polyzystischen Nierenerkrankung (ARPKD) sind. Han:SPRD entwickeln kortikale Zysten, welche im proximalen Tubulus der Nephronen entstehen, während PCK medulläre Zysten entwickeln, die im Sammelrohr entstehen.

Das Ziel dieser Arbeit war es, herauszufinden, ob in diesen zwei PKD-Rattenmodellen der Glukosetransport und –metabolismus in der Niere eine pathogene Rolle bei der Zystenproliferation und –expansion spielt. Wir stellten die Hypothese auf, dass die Erzeugung einer osmotischen Diurese durch die Inhibition der Natrium-Glukose Cotransporter (SGLT) in den proximalen Tubuli, den Flüssigkeitstransport von den Zysten in das tubuläre Lumen erzwingt und somit die Zystenexpansion reduziert und den Nierenfunktionsabfall verbessert. Ausserdem, basierend auf dem Wissen, dass es eine erhöhte Glukosenachfrage durch anärobe Glykolyse in proliferierenden Epithelzellen in PKD gibt (Warburg-Effekt), blockierten wir selektiv den Glukosemetabolismus mit dem Glukoseanalogon 2-Deoxyglucose (2DG), um seine vorteilhaften Effekte in PKD zu testen.

Zuerst testeten wir den dualen SGLT Inhibitor Phlorizin in Han:SPRD Ratten und fanden einen signifikanten positiven Effekt, z.B. verbesserte Phlorizin die Zystenexpansion, den Nierenfunktionsabfall und die Albuminurie. Dann testeten wir den selektiven SGLT2 Inhibitor Dapagliflozin (DAPA) in Han:SPRD Ratten und fanden, dass DAPA die Zystenexpansion nicht verbesserte, aber einen leicht positiven Effekt auf den Nierenfunktionsabfall und die Albuminurie aufwies. In der PCK Ratte bewirkte DAPA unerwarteter Weise eine signifikante Erhöhung des Zystenvolumens, und verschlechterte den Nierenfunktionsabfall und die Albuminurie, vermutlich wegen dem starken osmotischen Effekt im Sammelrohr.

Wir untersuchten dann den Energiemetabolismus im zystischen Nierengewebe von Han:SPR Ratten. Wir fanden eine Hochregulation von Genen, welche in der Glykolyse involviert sind, und eine Herunterregulation von Genen, welche in der Glukoneogenese involviert sind. Dies demonstriert, dass der Warburg-Effekt in zystischem Gewebe von Han:SPRD präsent ist. Bei Behandlung mit 2DG, um die Glykolyse zu blockieren, fanden wir eine wesentliche Reduktion des Zystenwachstums und einen langsameren Nierenfunktionsabfall und weniger Albuminurie.

Unsere Studien in zwei verschiedenen PKD-Rattenmodellen zeigen auf, dass Glukosetransport und –metabolismus für das Zystenwachstum und die Zystenexpansion sehr wichtig sind. Dies bildet die Basis, um diese Vorgänge als potenzielle Ziele für zukünftige PKD Behandlungen weiter zu entwickeln.

Contents

Chapter 1

General Introduction and Thesis Outline

Contents

General introduction

Polycystic kidney disease (PKD) is a common genetic renal syndrome that may lead to end-stage renal disease (ESRD) in children and adults. PKD is characterized by the accumulation of fluid filled cysts in the kidneys and other organs. Cysts originate from epithelial cells in the nephron and are characterized by a single layer of cells with an increased rate of proliferation.

PKD patients present with massively enlarged kidneys with cysts of variable size, ranging from around 40 µm to several centimeters in diameter. The PKDs are classified among the ciliopathies, since primary cilia play an important pathogenic role in the disease, expressing the mutated proteins involved in the various forms of PKD (PC1, PC2 and fibrocystin) (1, 2). PKD can be subdivided in two major forms: autosomal dominant polycystic kidney disease (ADPKD) and autosomal recessive polycystic kidney disease (ARPKD).

Autosomal dominant polycystic kidney disease

ADPKD is the most common hereditary cystic kidney disease and one of the most common hereditary disorders in humans. It has a prevalence of 1:400 to 1:1000. The disease manifests typically around the fourth decade of life, with ESRD occurring in 50% of the cases at the age of 60 years and in 75% at the age of 70 years. However, ADPKD already starts in children. The age adjusted male/female sex ratio is 1.2-1.3 (3).

Most patients (85%) are affected by the most severe form, caused by mutations in the PKD1 gene which is located on chromosome 16p13.3, causing a defective polycystin-1 protein. Mutations in the PKD2 gene, located on chromosome 4q21-23, cause a defective polycystin-2 protein that leads to ADPKD in 15% of all cases of ADPKD (4, 5).

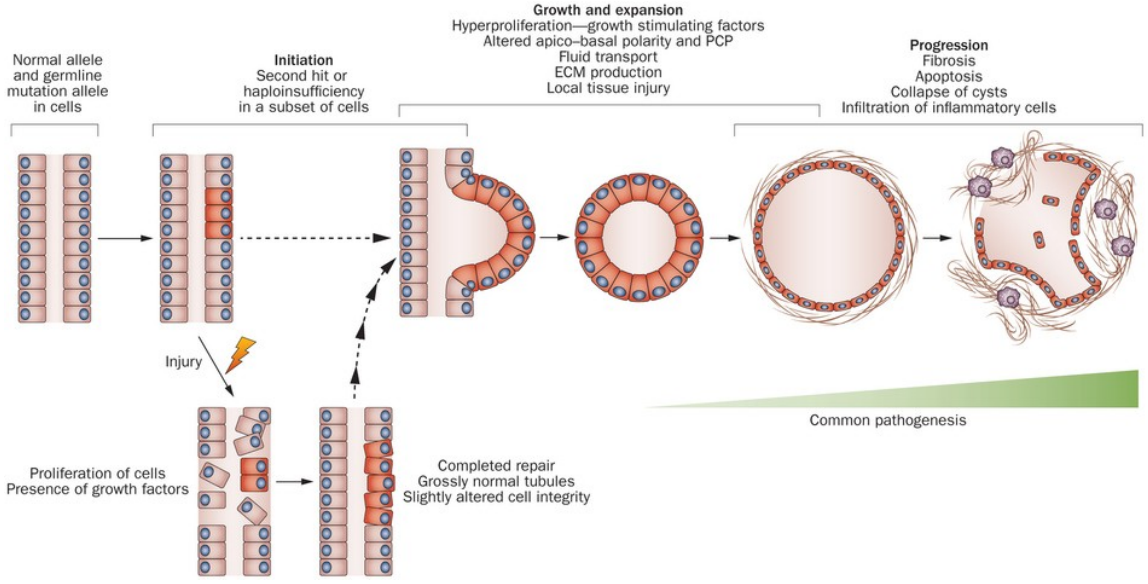

Figure 1.1: ADPKD progression. Image extracted from Happé H, Peters D.J.M. Translational research in ADPKD: lessons from animal models. Nature Reviews Nephrology 2014 (10): 587–601

ADPKD is characterized by progressive development and expansion of fluid-filled cysts in tiny segments of the nephron (Figure 1.1). The kidney gets progressively deformed by the cyst expansion within the renal cortex. Cyst progression leads to kidney failure by compression of the healthy renal parenchyma. Among the extrarenal manifestations cysts in the liver, pancreas and ovaries are well known and frequent. Intracranial aneurysms are also associated with ADPKD and can lead to cerebral hemorrhage when rupturing (6, 7). Thus, ADPKD can be considered a systemic disease.

Autosomal recessive polycystic kidney disease

ARPKD is 20 times less common than the autosomal dominant form. Considered a rare ciliopathy, its incidence rate is 1:20000. Nevertheless, it is one of the most important nephropathies in neonates and children (8).

The gene affected, PKHD1, is located in chromosome 6p21.1-p12 (9). Mutations in PKHD1 lead to malformations on the fibrocystin (also termed polyductin) protein, a transmembrane protein present on collecting ducts in the kidney and biliary ducts in the liver (10). At the ultrastructural level this protein localizes to the primary cilia membrane and centrosomes in renal epithelial cells. Fibrocystin function is associated with terminal differentiation of the collecting ducts and the maintaining of normal tubular architecture of renal and biliary tubules (11, 12).

Fibrocystin mutations lead to a non-obstructive fusiform dilation of the collecting ducts. The tubular dilation causes kidney expansion but the reniform shape of the kidney is maintained (13). ARPKD may lead to premature death, mainly because of severe hypertension and kidney failure. Patients with ARPKD also have congenital hepatic fibrosis and portal hypertension which is caused by cyst dilation of the biliary ducts.

The PKD proteins: fibrocystin and polycystins

Polycystins

The proteins which are encoded by the PKD1 and PKD2 genes are termed polycystin-1 and polycystin-2, respectively. This family of proteins plays important roles in many biological processes including, mechanosensation, fertilization and ion transport across membranes.

Polycystin-1 (PC1) is an integral membrane protein which is found in primary cilia, cytoplasmic vesicles and plasma membranes. It contains 11 transmembrane-spanning domains, a large extracellular N-terminal domain and a short cytosolic C-terminal domain (Figure 1.2). The extracellular domain contains several other domains such as leucine-rich repeats (LRRs), a C-type lectin domain, a low density lipoprotein class A repeat (LDL-A) region, multiple Ig-like domains and PKD domains. PC1 has a molecular weight of about 500’000 Da, with 4303 amino acids. When PC1 is not bound to PC2, the C-terminal cytosolic domain stably binds and activates heterotrimeric G-proteins (14, 15).

Polycystin-2 (PC2), encoded by the PKD2 gene, is also a transmembrane protein. It is composed by 968 amino acids. PC2 has 6 transmembrane-spanning domains and both N- and C-terminal cytoplasmic domains (Figure 1.2). It is also a member of the transient receptor potential (TRP) ion-channel family. PC2 works as a nonselective channel for Ca^{2+},

Na^+, and K^+. PC2 also localizes to primary cilia, centrosomes and plasma membranes, but is mainly found in the endoplasmic reticulum (ER).

PC1 and PC2 form a complex trough their C-terminal domains. Many other proteins interact with this complex. When PC1 and PC2 interact, the PC1 activation of G proteins is strongly decreased (16). The activation of the complex by a mechanical stimulus leads to conformational changes that trigger the PC1-mediated G protein signaling and the PC2 calcium channel activity (17).

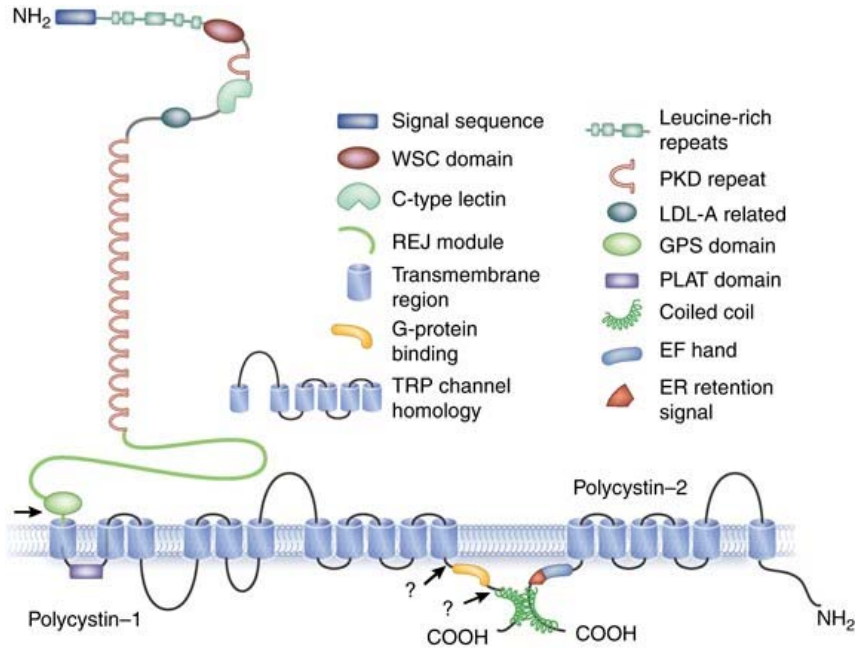

Figure 1.2: Polycystin structure. Graph is from Torres VE, Harris PC. Autosomal dominant polycystic kidney disease: the last 3 years. Kidney Int. 2009 Jul;76(2):149-68

Fibrocystin/polyductin

The protein encoded by the PKHD1 gene is termed fibrocystin or polyductin (FPC). It is composed by 4074 amino acids. FPC is a membrane protein with a large extracellular domain (more than 3800 amino acids), a unique transmembrane segment and a short C-terminal cytosolic tail that includes phosphorylation sites for cAMP/cGMP (possibly important for its function).

FPC is localized to the plasma membrane and the primary cilium of epithelial cells from the collecting duct (18, 19). Its exact function remains unclear, however it is known that FPC interacts with PC2 and modulates renal tubular formation (20).

Pathways involved in PKD progression

As stated above, one of the most important locations of polycystins is the primary cilium. In the kidney, primary cilia play a sensory role in response to urine flow. The PC1-PC2 complex localized on the base of cilia translates the mechanical stimulation into calcium influx trough PC2-channels. The increased concentration of calcium in the cell is followed by a calcium-induced calcium release from intracellular IP3-dependent stores (21). Intracellular calcium regulates the cAMP level in the cell by inhibition of adenylyl cyclase 6 (AC-VI), which is responsible for cAMP production; and by stimulation of phosphodiesterases (PDE) which degrade cAMP to AMP. Conversely, depletion of calcium in the endoplasmic reticulum (ER) results in the translocation of a calcium sensor to the ER membrane: the stromal interaction molecule 1 (STIM1). This sensor regulates several store-operated channels and AC-VI. STIM1-induced AC-VI activity increases cAMP levels in the cytosol. This pathway is known as store-operated cAMP signalling (SOcAMPS)(22).

Because of mutations in the PKD1 or PKD2 genes, PC1 or PC2 are malformed and dysregulate (i.e. increase) the production of cAMP. On the other hand, AC-VI is known to form a complex on the basal membrane with several proteins, including the vasopressin type 2 receptor (V2R). Vasopressin is one of the main hormonal modulators of AC-VI function in the collecting duct. Vasopressin is mainly regulated by plasma osmolality and was found to be elevated in hypertensive ADPKD patients (23). Vasopressin stimulates the production of cAMP via AC-VI (24). Intracellular calcium levels are not enough to inhibit the activity of AC-VI and cAMP is accumulated via SOcAMPS and V2R.

The abnormal accumulation of cAMP leads to the activation of protein kinase A (PKA). PKA plays an important regulatory role in many processes in the cell, such as glycogenesis, gluconeogenesis and lipid metabolism. PKA also phosphorylates several transepithelial fluid transport proteins such as aquaporin 2 (AQP2) and epithelial ion channels including CFTR (25). In addition, PKA stimulates the PC2 channels on the ER and leads to the release of calcium from intracellular stores (26). The reduction of these calcium stores triggers the translocation of STIM1 to the plasma membrane and the consequent activation of AC-VI (27) (Figure 1.3).

PKA is implicated in most of the processes involved in PKD progression, from cyst proliferation (activating transcription factors via MAPK/ERK signaling) to the fluid secretion (directly increasing CFTR activity). In PKD patients, the increased activity of PKA stimulates the extracellular signal-regulated kinases (ERK) via MEK, B-Raf, Ras, and Src (28). Phosphorylation of ERK leads to the inhibition of tuberous sclerosis complex proteins (TSC1/2) directly and indirectly (via LKB1, which inhibits the activity of AMPK) (3, 29). AMPK has been related with a tonic inhibition of CFTR and its reduction seems to increase fluid secretion (30). ERK also causes activation of transcription factors, both directly and indirectly (via ribosomal S6 kinase [RSK]), stimulating cell growth, proliferation and de-differentiation in affected cells (Figure 1.3). In normal conditions, TSC1/2 are found in a complex with Rheb, GDP and mTOR, binding to the cytosolic C-terminal end of PC1. The complex maintains a tonic inhibition over Rheb (31, 32). When PC-1 is absent, TSC2 is phosphorylated, triggering a further activation of Rheb and mTORC1 complex (33, 34). Activated mTORC1 boosts aerobic glycolysis, stimulates ATP synthesis and inhibits AMPK activity together with ERK, which increases mTOR signaling in a positive feedback loop (27, 29) (Figure 1.3).

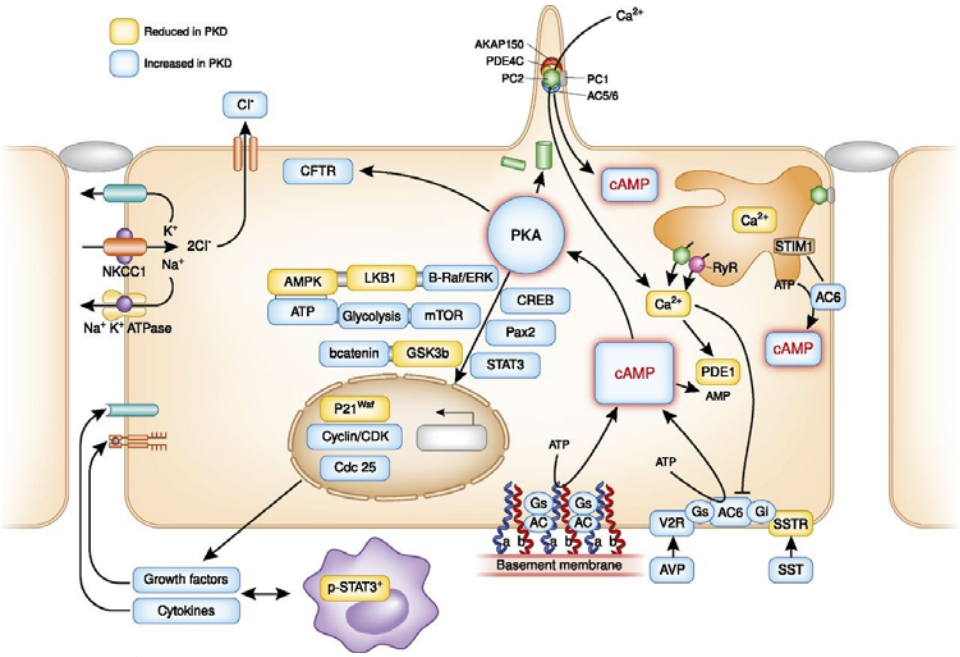

Figure 1.3: Pathways of up- or downregulated molecules in polycystic kidney disease and potential drug targets. Figure is from Torres VE, Harris PC. Strategies targeting cAMP signaling in the treatment of polycystic kidney disease. J Am Soc Nephrol. 2014, 25: 18–32.

It is well known that mTOR regulates the balance between cell growth and autophagy. In favorable conditions, activation of mTOR leads the protein synthesis and growth (34, 35). In PKD cells, activation of mTOR stimulates cell growth and promotes cyst expansion.

Rat models for PKD

There are numerous animal models of PKD (mice, rats, cats) which can be either orthologous to the human disease (i.e. with mutations in PKD1 or PKD2 or PKHD1) or non-orthologous (i.e. involving genes which are different from PKD1, PKD2 and PKHD1). The most commonly studied mouse models of PKD include the cpk, bpk, orpk, pck, pcy and $Pkd2^{ws25/-}$ strains. The most commonly studied rat strains include the PCK and the Han:SPRD rats. All these models have strengths and limitations, and none of them is both genetically orthologous and reproduces the human phenotype of PKD (36, 37).

Han:SPRD rats

The Han:SPRD (Cy) rat strain was described by Kaspareit-Rittinghausen et al in 1989 as a spontaneous mutation of Sprague-Dawley rats and the original colony was established in Hanover, Germany (38). Despite of being a non-orthologous model, Han:SPRD rats are used as a model of ADPKD because it reproduces the typical phenotype of human ADPKD. Han:SPRD kidneys are characterized by formation of numerous cyst from proximal tubules. The disease is caused by a point mutation of the Pkdr1 (ANKS6) gene. Currently, new studies found that mutations in human ANKS6 are related with a nephronophthisis-like phenotype (39).

Two different genotypes show renal cysts. The homozygous genotype (Cy/Cy) has a rapid disease progression with marked cystic dilation in all tubular segments. Cysts are less

pronounced in the inner medulla. The disease leads to early death in 3-weeks (40). The heterozygotes (Cy/+) develop a slower disease with a life span of less than 1 year in males and around 2 years in females. The disease progression in Cy/+ is more severe in males than females. Among others, a factor that can explain the increased severity in males are androgens. These hormones stimulates the disease progression via androgen receptors with the activation of MAPK pathways in males (41).

The phenotype in heterozygous Cy/+ is characterized by cyst proliferation from proximal tubules mainly from juxtamedullary nephrons. Some areas of the affected proximal tubules show inmature cellular phenotype with loss of epithelial differentiation and variability in the microvilli (42). Interstitial fibrosis and an increase in inflammatory cells are also characteristic in Cy/+ rats. No extrarenal manifestations have been observed in this model (42, 43).

PCK Rats

The PCK strain was also isolated from a Sprague-Dawley colony by Katsuyama et al in 2000 (44). The disease is originated in the Pkhd1 gene, orthologous to the gene responsible of human ARPKD. However, it has a milder phenotype than Han:SPRD rat with several phenotypical features of ADPKD. In contrast with Han:SPRD animals, in PCK rats the cysts are originated by dilation of collecting ducts in the outer medulla. The disease leads to death approximately at 1.5 years. Interstitial fibrosis and inflammation are frequent after approximately 1 month. A common extrarenal manifestation of this phenotype is the cyst formation in liver and pancreas. In liver, dilated intrahepatic bile ducts lead to fibrotic cysts in later stages (37, 40).

Current treatments and novel therapies for PKD

Current treatments in PKD are focused on treating the symptoms derived from complications of the disease. Among others, current therapies include blood pressure control, treatments for anemia or hyperlipidemia, dietary supplementation, and reduced sodium and protein intake (45-47). Nephrectomy and transplantation are the choices in patient who reach end stage renal disease (ESRD).

The work carried out to identify the cellular mechanisms that are involved in the cyst expansion and proliferation has resulted in the discovery of novel targets. New animal models have allowed the development of many preclinical studies to test potential therapies.

The major cause of cAMP accumulation in the cell is the activity of AC-VI. It is know that vasopressin, through the action of V2R, increases AC-VI activity. Thus, V2R antagonists become crucially important as potential drugs. Mozavaptan (OPC-31260) and more recently tolvaptan (OPC-41061) have been used in mouse and rat models of PKD. Recently, clinical trials in phase II and III have been completed using tolvaptan in PKD patients (NCT01214421 and NCT02160145). OPC-41061 effectively ameliorates the cyst progression, slows the increase in kidney volume growth, and improves the decline in kidney function. As side-effects, tolvaptan causes dose-dependent aquaresis (48).

High water intake (HWI) was proposed as another way to reduce the action of vasopressin in the cAMP generation. HWI was beneficial in PCK rats but did not reduce the severity of

disease in Han:SPRD rats (49). The applicability for ADPKD patients is still controversial and should be restricted to non-severe patients (eGFR>60) (24, 50).

AC-VI can also be inhibited by blocking the somatostatin receptors (SSTR), reducing the levels of cAMP in cytoplasm. Somatostatin analogues (lanreotide and octreotide) were shown to have beneficial effects on kidney volume increase and slowed the cyst progression in patients (51). Octreotide and lanreotide are well tolerated and can be administered via intramuscular injections on the hip. The most common adverse reaction is diarrhea.

The mTOR pathway is involved in several human diseases including diabetes mellitus, cancer and PKD. Inhibitors of mTOR like rapamycin (sirolimus) and everolimus were quite promising for the treatment of PKD, reducing cyst growth and ameliorating kidney function by preventing epithelial cell proliferation in mice and rats (52, 53). However, when clinical trials were conducted with both sirolimus and everolimus in PKD patients, no beneficial effects were found (54, 55).

Many other potential targets have been subjected to preclinical and clinical testing. Triptolide, Scr inhibitors, a TNF antagonist, CFTR inhibitors, metformin or CDK inhibitors among others demonstrated a variable efficacy to slow down the disease progression but none of them resulted in a real cure (56-59).

SGLT inhibitors

The kidney plays a key role in glucose homeostasis in the body. The sodium-glucose cotransporters (SGLT) are a family of membrane proteins responsible for the transport of glucose from the lumen into the epithelial cells. The SGLTs which have been found in the kidney are SGLT1 and SGLT2, managing transport of glucose and sodium across the proximal tubular epithelium (60). SGLT1 transports two molecules of glucose with every one sodium whereas SGLT2 transports only one glucose per sodium (61).

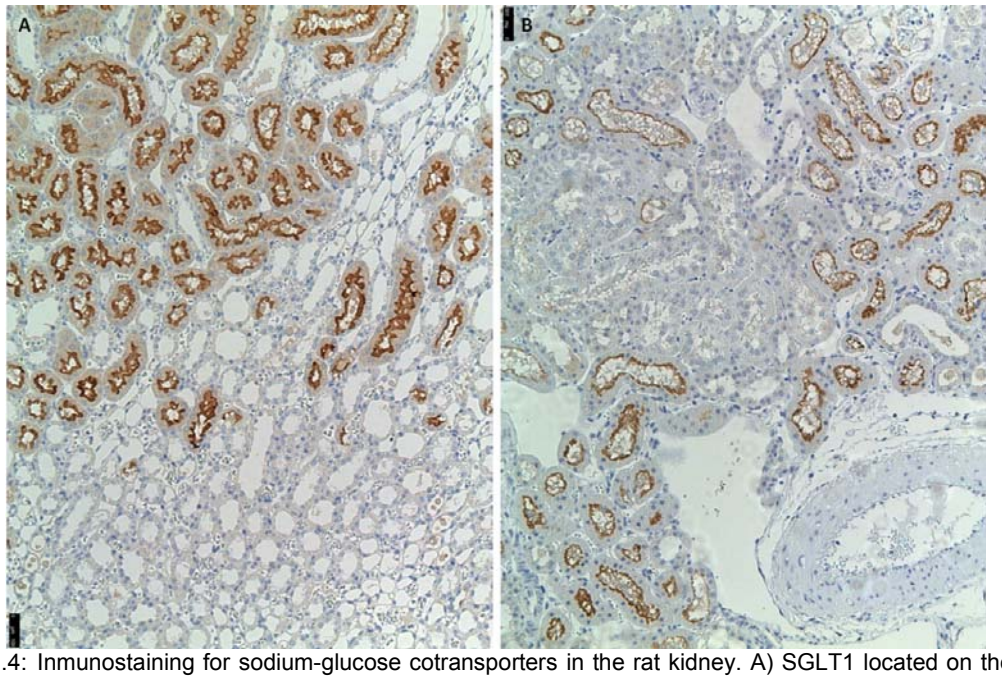

Figure 1.4: Inmunostaining for sodium-glucose cotransporters in the rat kidney. A) SGLT1 located on the brush border of S3 segment of proximal tubules. B) SGLT2 located on segments S1 and S2 of proximal tubules.

SGLT1, located in the third segment (S3) of the proximal renal tubule, is a low-capacity, high-affinity sodium-glucose cotransporter, responsible for 10% of glucose reabsorption. SGLT2 in contrast is located in the S1 segment and is a high-capacity, low-affinity transporter, mediating around 90% of glucose reabsorption in the kidney (62, 63) (Figure 1.5).

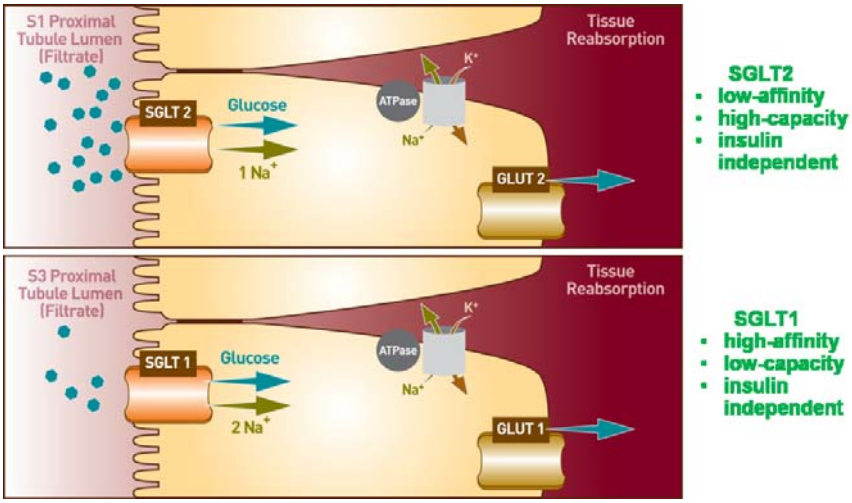

Figure 1.5: Sodium-glucose cotransporters (SGLT1/2) are located on the apical side in the proximal tubules of the kidney. SGLTs and GLUTs form transport pairs (SGLT1/GLUT1 and SGLT2/GLUT2) who manage glucose reabsorption in the different segments of proximal tubules.

Due to its main role in glucose reabsorption in the kidney, SGLTs have been a potential target for diabetes mellitus treatments. By blocking SGLT actions, SGLT inhibitors strongly inhibit glucose reabsorption form the lumen of the proximal tubules which leads to glucosuria and osmotic diuresis.

Phlorizin, a non selective SGLT inhibitor extracted from the root bark of the apple tree, is known to lower glucose reabsorption (64). Phlorizin is poorly absorbed from the gastrointestinal tract and should be administered via subcutaneous injections. In addition to inhibiting SGLT2, phlorizin also inhibits SGLT1 which is mainly located in the gastrointestinal tract, leading to glucose and galactose malabsorption, dehydration, and diarrhea (65). Thus, its potential use in the treatment of diabetics is limited. Several studies with dapagliflozin (DAPA), a novel selective SGLT2 inhibitor, demonstrated excellent efficacy in diabetes mellitus type 2 patients correcting hyperglycemia and reducing hemoglobin A_{1c} effectively (66). In contrast to phlorizin, DAPA can be administered orally and is well tolerated in humans. Many other SGLT inhibitors, both selective and non-selective, are being developed for the treatment of type 2 diabetics (67, 68).

The balance between fluid secretion and reabsorption into the lumen of cyst is slightly skewed in the direction of secretion (23). By increasing glucose concentration in the lumen of tubules, SGLT inhibitors may produce an osmotic gradient from adjacent cyst to the epithelial lumen, counteracting the cyst expansion by fluid secretion.

Glucose metabolism and 2-deoxyglucose

A study by Rowe et al. has shown that aerobic glycolysis was elevated in the absence of PC1 in a mouse model of ADPKD and also in kidney tissues from patients with ADPKD (29). It is well known that cancer cell and proliferative tissues increase their glucose intake and, unlike normal tissue, use fermentation to decompose glucose even in the presence of enough oxygen (aerobic glycolysis)(69). This phenomenon was named Warburg effect (Figure 1.6).

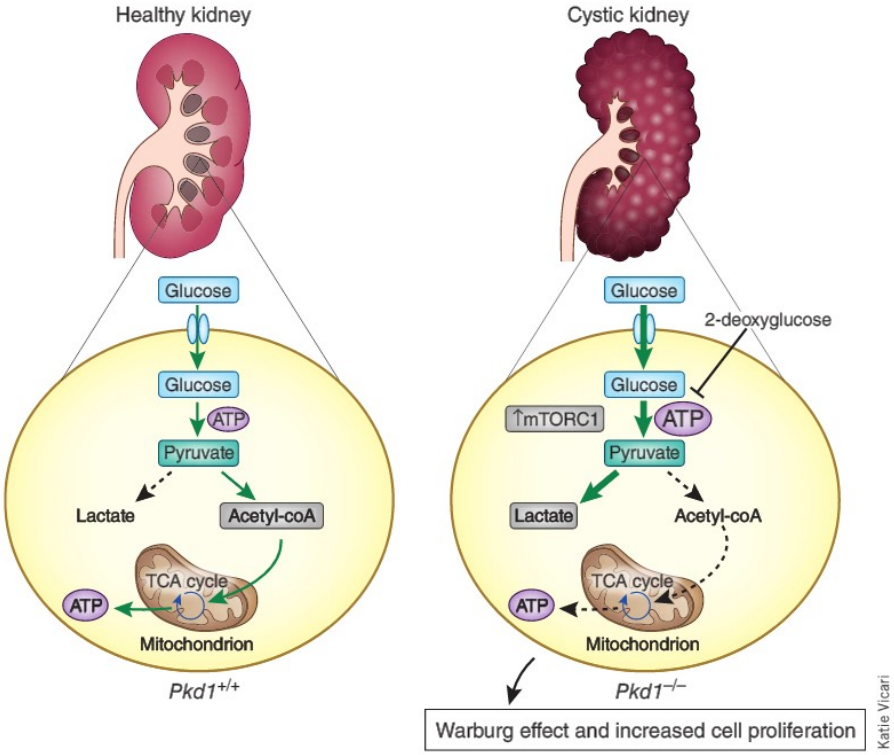

Figure 1.6: Metabolic alterations in PKD kidneys by Warburg effect. On the left, normal kidney cells metabolize glucose into ATP via tri-carboxylic acid (TCA) cycle. On the right, cystic kidney stimulates generation of lactate via aerobic glylcolysis (Warburg effect). From Priolo C, Henske EP. Metabolic reprogramming in polycystic kidney disease. Nature Medicine. 2013. 19, 407–409

The increased demand of glucose by proliferative cells may be used therapeutically by target cystic tissue. A possible way to use this target is with analogs of glucose that cannot be metabolized, thus blocking the glycolysis pathway and reducing considerably cyst proliferation. Previous studies with 2-deoxyglucose (2DG) found that cyst growth could be inhibited in mouse models of PKD (29, 70). So far, there were no experiments conducted in rat models with a slower disease progression.

Aims of this thesis

Despite the fact that many different therapies were tested, there is currently no effective treatment for such a complex disease as PKD. Glucose transport and metabolism in the kidney has emerged as an important factor that promotes PKD disease. Targeting glucose transport and metabolism may thus represent a promising strategy to treat PKD.

We hypothesized that by generating the osmotic diuresis and glycosuria, SGLT inhibitors produce an osmotic gradient from the lumen of cysts to the renal tubules, reducing the cyst expansion and ameliorating the disease progression in PKD rat models.

We also hypothesized that to reduce glucose metabolism in cystic cells, the glucose analogue 2-deoxy-glucose may have beneficial effects in rat models of PKD.

Thesis outline

Chapter 2 describes a study of the effects of the SGLT inhibitor phlorizin in the Han:SPRD rat model of ADPKD. Phlorizin effectively reduced kidney volume and ameliorated the decline in kidney function. Furthermore, phlorizin had a beneficial effect on proliferation. Following the promising results from Chapter 2, a novel, selective SGLT2 inhibitor, dapagliflozin (DAPA), was tested on Han:SPRD rats (Chapter 3). DAPA caused renal glycosuria and improved the renal function in Han:SPRD rats but, unexpectedly, had no effect on the cyst progression or proliferation. In Chapter 4, we tested dapagliflozin in an ARPKD rat model, the PCK rat. DAPA caused a significant expansion of cysts in PCK and led to a reduction in kidney function and increased albuminuria. The novel technique of high resolution ultrasound imaging was used in Chapter 4 and is described in greater detail in Chapter 5. Changing the way to approach the disease, Chapter 6 is focused on the inhibition of aerobic glycolysis by 2-deoxyglucose (2DG) in Han:SPRD rats. 2DG reduced considerably the activity of enzymes involve on glucose degradation and ameliorated the cyst expansion. Treated rats displayed improved kidney function and a reduced cyst epithelial cell proliferation. Chapter 7 is focused on the eGFR prediction in a Swiss ADPKD patient cohort with up to 10 years of follow-up. Finally, the results exposed in the individual chapters of this thesis are concluded with a summarizing discussion in Chapter 8.

References

1. Nauli SM, Alenghat FJ, Luo Y, Williams E, Vassilev P, Li X, et al. Polycystins 1 and 2 mediate mechanosensation in the primary cilium of kidney cells. Nat Genet. 2003 Feb;33(2):129-37.
2. Xu C, Rossetti S, Jiang L, Harris PC, Brown-Glaberman U, Wandinger-Ness A, et al. Human ADPKD primary cyst epithelial cells with a novel, single codon deletion in the PKD1 gene exhibit defective ciliary polycystin localization and loss of flow-induced Ca2+ signaling. Am J Physiol Renal Physiol. 2007 Mar;292(3):F930-45.
3. Torres VE, Harris PC. Autosomal dominant polycystic kidney disease: the last 3 years. Kidney Int. 2009 Jul;76(2):149-68.
4. Pei Y, Watnick T. Diagnosis and screening of autosomal dominant polycystic kidney disease. Adv Chronic Kidney Dis. 2010 Mar;17(2):140-52.
5. Hateboer N, v Dijk MA, Bogdanova N, Coto E, Saggar-Malik AK, San Millan JL, et al. Comparison of phenotypes of polycystic kidney disease types 1 and 2. European PKD1-PKD2 Study Group. Lancet. 1999 Jan 9;353(9147):103-7.
6. Alvaro D, Onori P, Alpini G, Franchitto A, Jefferson DM, Torrice A, et al. Morphological and functional features of hepatic cyst epithelium in autosomal dominant polycystic kidney disease. Am J Pathol. 2008 Feb;172(2):321-32.
7. Schievink WI, Torres VE, Piepgras DG, Wiebers DO. Saccular intracranial aneurysms in autosomal dominant polycystic kidney disease. J Am Soc Nephrol. 1992 Jul;3(1):88-95.
8. Zerres K, Mucher G, Becker J, Steinkamm C, Rudnik-Schoneborn S, Heikkila P, et al. Prenatal diagnosis of autosomal recessive polycystic kidney disease (ARPKD): molecular genetics, clinical experience, and fetal morphology. Am J Med Genet. 1998 Mar 5;76(2):137-44.
9. Igarashi P, Somlo S. Genetics and pathogenesis of polycystic kidney disease. J Am Soc Nephrol. 2002 Sep;13(9):2384-98.
10. Cramer MT, Guay-Woodford LM. Cystic kidney disease: a primer. Adv Chronic Kidney Dis. 2015 Jul;22(4):297-305.
11. Adeva M, El-Youssef M, Rossetti S, Kamath PS, Kubly V, Consugar MB, et al. Clinical and molecular characterization defines a broadened spectrum of autosomal recessive polycystic kidney disease (ARPKD). Medicine (Baltimore). 2006 Jan;85(1):1-21.
12. Bergmann C, Senderek J, Windelen E, Kupper F, Middeldorf I, Schneider F, et al. Clinical consequences of PKHD1 mutations in 164 patients with autosomal-recessive polycystic kidney disease (ARPKD). Kidney Int. 2005 Mar;67(3):829-48.
13. Hartung EA, Guay-Woodford LM. Autosomal recessive polycystic kidney disease: a hepatorenal fibrocystic disorder with pleiotropic effects. Pediatrics. 2014 Sep;134(3):e833-45.
14. Parnell SC, Magenheimer BS, Maser RL, Rankin CA, Smine A, Okamoto T, et al. The polycystic kidney disease-1 protein, polycystin-1, binds and activates heterotrimeric G-proteins in vitro. Biochem Biophys Res Commun. 1998 Oct 20;251(2):625-31.
15. Parnell SC, Magenheimer BS, Maser RL, Zien CA, Frischauf AM, Calvet JP. Polycystin-1 activation of c-Jun N-terminal kinase and AP-1 is mediated by heterotrimeric G proteins. J Biol Chem. 2002 May 31;277(22):19566-72.
16. Delmas P, Nomura H, Li X, Lakkis M, Luo Y, Segal Y, et al. Constitutive activation of G-proteins by polycystin-1 is antagonized by polycystin-2. J Biol Chem. 2002 Mar 29;277(13):11276-83.
17. Ong AC, Harris PC. Molecular pathogenesis of ADPKD: the polycystin complex gets complex. Kidney Int. 2005 Apr;67(4):1234-47.
18. Wang S, Luo Y, Wilson PD, Witman GB, Zhou J. The autosomal recessive polycystic kidney disease protein is localized to primary cilia, with concentration in the basal body area. J Am Soc Nephrol. 2004 Mar;15(3):592-602.
19. Ward CJ, Yuan D, Masyuk TV, Wang X, Punyashthiti R, Whelan S, et al. Cellular and subcellular localization of the ARPKD protein; fibrocystin is expressed on primary cilia. Hum Mol Genet. 2003 Oct 15;12(20):2703-10.

20. Kim I, Fu Y, Hui K, Moeckel G, Mai W, Li C, et al. Fibrocystin/polyductin modulates renal tubular formation by regulating polycystin-2 expression and function. J Am Soc Nephrol. 2008 Mar;19(3):455-68.
21. Kotsis F, Boehlke C, Kuehn EW. The ciliary flow sensor and polycystic kidney disease. Nephrol Dial Transplant. 2013 Mar;28(3):518-26.
22. Lefkimmiatis K, Srikanthan M, Maiellaro I, Moyer MP, Curci S, Hofer AM. Store-operated cyclic AMP signalling mediated by STIM1. Nat Cell Biol. 2009 Apr;11(4):433-42.
23. Terryn S, Ho A, Beauwens R, Devuyst O. Fluid transport and cystogenesis in autosomal dominant polycystic kidney disease. Biochim Biophys Acta. 2011 Oct;1812(10):1314-21.
24. Torres VE, Bankir L, Grantham JJ. A case for water in the treatment of polycystic kidney disease. Clin J Am Soc Nephrol. 2009 Jun;4(6):1140-50.
25. Cantero Mdel R, Velazquez IF, Streets AJ, Ong AC, Cantiello HF. The cAMP signaling pathway and direct protein kinase A phosphorylation regulate polycystin-2 (TRPP2) channel function. J Biol Chem. 2015 Sep 25;290(39):23888-96.
26. Torres VE. Therapies to slow polycystic kidney disease. Nephron Exp Nephrol. 2004;98(1):e1-7.
27. Torres VE, Harris PC. Strategies targeting cAMP signaling in the treatment of polycystic kidney disease. J Am Soc Nephrol. 2014 Jan;25(1):18-32.
28. Shibazaki S, Yu Z, Nishio S, Tian X, Thomson RB, Mitobe M, et al. Cyst formation and activation of the extracellular regulated kinase pathway after kidney specific inactivation of Pkd1. Hum Mol Genet. 2008 Jun 1;17(11):1505-16.
29. Rowe I, Chiaravalli M, Mannella V, Ulisse V, Quilici G, Pema M, et al. Defective glucose metabolism in polycystic kidney disease identifies a new therapeutic strategy. Nat Med. 2013 Apr;19(4):488-93.
30. King JD, Jr., Fitch AC, Lee JK, McCane JE, Mak DO, Foskett JK, et al. AMP-activated protein kinase phosphorylation of the R domain inhibits PKA stimulation of CFTR. Am J Physiol Cell Physiol. 2009 Jul;297(1):C94-101.
31. Inoki K, Corradetti MN, Guan KL. Dysregulation of the TSC-mTOR pathway in human disease. Nat Genet. 2005 Jan;37(1):19-24.
32. Shillingford JM, Murcia NS, Larson CH, Low SH, Hedgepeth R, Brown N, et al. The mTOR pathway is regulated by polycystin-1, and its inhibition reverses renal cystogenesis in polycystic kidney disease. Proc Natl Acad Sci U S A. 2006 Apr 4;103(14):5466-71.
33. Dere R, Wilson PD, Sandford RN, Walker CL. Carboxy terminal tail of polycystin-1 regulates localization of TSC2 to repress mTOR. PLoS One. 2010;5(2):e9239.
34. Huber TB, Walz G, Kuehn EW. mTOR and rapamycin in the kidney: signaling and therapeutic implications beyond immunosuppression. Kidney Int. 2011 Mar;79(5):502-11.
35. Wullschleger S, Loewith R, Hall MN. TOR signaling in growth and metabolism. Cell. 2006 Feb 10;124(3):471-84.
36. Torres VE, Harris PC. Polycystic kidney disease: genes, proteins, animal models, disease mechanisms and therapeutic opportunities. J Intern Med. 2007 Jan;261(1):17-31.
37. Lager DJ, Qian Q, Bengal RJ, Ishibashi M, Torres VE. The pck rat: A new model that resembles human autosomal dominant polycystic kidney and liver disease. Kidney International. 2001 Jan;59(1):126-36.
38. Kaspareit-Rittinghausen J, Rapp K, Deerberg F, Wcislo A, Messow C. Hereditary polycystic kidney disease associated with osteorenal syndrome in rats. Vet Pathol. 1989 May;26(3):195-201.
39. Taskiran EZ, Korkmaz E, Gucer S, Kosukcu C, Kaymaz F, Koyunlar C, et al. Mutations in ANKS6 cause a nephronophthisis-like phenotype with ESRD. J Am Soc Nephrol. 2014 Aug;25(8):1653-61.
40. Nagao S, Kugita M, Yoshihara D, Yamaguchi T. Animal models for human polycystic kidney disease. Exp Anim. 2012;61(5):477-88.
41. Nagao S, Kusaka M, Nishii K, Marunouchi T, Kurahashi H, Takahashi H, et al. Androgen receptor pathway in rats with autosomal dominant polycystic kidney disease. J Am Soc Nephrol. 2005 Jul;16(7):2052-62.

42. Cowley BD, Jr., Gudapaty S, Kraybill AL, Barash BD, Harding MA, Calvet JP, et al. Autosomal-dominant polycystic kidney disease in the rat. Kidney Int. 1993 Mar;43(3):522-34.
43. Schafer K, Gretz N, Bader M, Oberbaumer I, Eckardt KU, Kriz W, et al. Characterization of the Han:SPRD rat model for hereditary polycystic kidney disease. Kidney Int. 1994 Jul;46(1):134-52.
44. Katsuyama M, Masuyama T, Komura I, Hibino T, Takahashi H. Characterization of a novel polycystic kidney rat model with accompanying polycystic liver. Exp Anim. 2000 Jan;49(1):51-5.
45. Schrier RW, Abebe KZ, Perrone RD, Torres VE, Braun WE, Steinman TI, et al. Blood pressure in early autosomal dominant polycystic kidney disease. N Engl J Med. 2014 Dec 11;371(24):2255-66.
46. Torres VE, Abebe KZ, Chapman AB, Schrier RW, Braun WE, Steinman TI, et al. Angiotensin blockade in late autosomal dominant polycystic kidney disease. N Engl J Med. 2014 Dec 11;371(24):2267-76.
47. Turner JM, Bauer C, Abramowitz MK, Melamed ML, Hostetter TH. Treatment of chronic kidney disease. Kidney Int. 2012 Feb;81(4):351-62.
48. Torres VE, Chapman AB, Devuyst O, Gansevoort RT, Grantham JJ, Higashihara E, et al. Tolvaptan in patients with autosomal dominant polycystic kidney disease. N Engl J Med. 2012 Dec 20;367(25):2407-18.
49. Nagao S, Nishii K, Katsuyama M, Kurahashi H, Marunouchi T, Takahashi H, et al. Increased water intake decreases progression of polycystic kidney disease in the PCK rat. J Am Soc Nephrol. 2006 Aug;17(8):2220-7.
50. Higashihara E, Nutahara K, Tanbo M, Hara H, Miyazaki I, Kobayashi K, et al. Does increased water intake prevent disease progression in autosomal dominant polycystic kidney disease? Nephrol Dial Transplant. 2014 Sep;29(9):1710-9.
51. Ruggenenti P, Remuzzi A, Ondei P, Fasolini G, Antiga L, Ene-Iordache B, et al. Safety and efficacy of long-acting somatostatin treatment in autosomal-dominant polycystic kidney disease. Kidney Int. 2005 Jul;68(1):206-16.
52. Shillingford JM, Piontek KB, Germino GG, Weimbs T. Rapamycin ameliorates PKD resulting from conditional inactivation of Pkd1. J Am Soc Nephrol. 2010 Mar;21(3):489-97.
53. Wahl PR, Serra AL, Le Hir M, Molle KD, Hall MN, Wuthrich RP. Inhibition of mTOR with sirolimus slows disease progression in Han:SPRD rats with autosomal dominant polycystic kidney disease (ADPKD). Nephrol Dial Transplant. 2006 Mar;21(3):598-604.
54. Serra AL, Poster D, Kistler AD, Krauer F, Raina S, Young J, et al. Sirolimus and kidney growth in autosomal dominant polycystic kidney disease. N Engl J Med. 2010 Aug 26;363(9):820-9.
55. Walz G, Budde K, Mannaa M, Nurnberger J, Wanner C, Sommerer C, et al. Everolimus in patients with autosomal dominant polycystic kidney disease. N Engl J Med. 2010 Aug 26;363(9):830-40.
56. Yang B, Sonawane ND, Zhao D, Somlo S, Verkman AS. Small-molecule CFTR inhibitors slow cyst growth in polycystic kidney disease. J Am Soc Nephrol. 2008 Jul;19(7):1300-10.
57. Dell KM, Nemo R, Sweeney WE, Jr., Levin JI, Frost P, Avner ED. A novel inhibitor of tumor necrosis factor-alpha converting enzyme ameliorates polycystic kidney disease. Kidney Int. 2001 Oct;60(4):1240-8.
58. Leuenroth SJ, Bencivenga N, Igarashi P, Somlo S, Crews CM. Triptolide reduces cystogenesis in a model of ADPKD. J Am Soc Nephrol. 2008 Sep;19(9):1659-62.
59. Takiar V, Nishio S, Seo-Mayer P, King JD, Jr., Li H, Zhang L, et al. Activating AMP-activated protein kinase (AMPK) slows renal cystogenesis. Proc Natl Acad Sci U S A. 2011 Feb 8;108(6):2462-7.
60. Wright EM. Renal Na(+)-glucose cotransporters. Am J Physiol Renal Physiol. 2001 Jan;280(1):F10-8.
61. Mackenzie B, Loo DD, Panayotova-Heiermann M, Wright EM. Biophysical characteristics of the pig kidney Na+/glucose cotransporter SGLT2 reveal a common mechanism for SGLT1 and SGLT2. J Biol Chem. 1996 Dec 20;271(51):32678-83.
62. Mather A, Pollock C. Renal glucose transporters: novel targets for hyperglycemia management. Nat Rev Nephrol. 2010 May;6(5):307-11.
63. Vallon V, Platt KA, Cunard R, Schroth J, Whaley J, Thomson SC, et al. SGLT2 mediates glucose reabsorption in the early proximal tubule. J Am Soc Nephrol. 2010 Jan;22(1):104-12.

64. Rossetti L, Smith D, Shulman GI, Papachristou D, DeFronzo RA. Correction of hyperglycemia with phlorizin normalizes tissue sensitivity to insulin in diabetic rats. J Clin Invest. 1987 May;79(5):1510-5.
65. Ehrenkranz JR, Lewis NG, Kahn CR, Roth J. Phlorizin: a review. Diabetes Metab Res Rev. 2005 Jan-Feb;21(1):31-8.
66. List JF, Woo V, Morales E, Tang W, Fiedorek FT. Sodium-glucose cotransport inhibition with dapagliflozin in type 2 diabetes. Diabetes Care. 2009 Apr;32(4):650-7.
67. Ferrannini E, Seman L, Seewaldt-Becker E, Hantel S, Pinnetti S, Woerle HJ. A Phase IIb, randomized, placebo-controlled study of the SGLT2 inhibitor empagliflozin in patients with type 2 diabetes. Diabetes Obes Metab. 2012 Aug;15(8):721-8.
68. Zambrowicz B, Freiman J, Brown PM, Frazier KS, Turnage A, Bronner J, et al. LX4211, a dual SGLT1/SGLT2 inhibitor, improved glycemic control in patients with type 2 diabetes in a randomized, placebo-controlled trial. Clin Pharmacol Ther. 2012 Aug;92(2):158-69.
69. Warburg O. On the origin of cancer cells. Science. 1956 Feb 24;123(3191):309-14.
70. Chiaravalli M, Rowe I, Mannella V, Quilici G, Canu T, Bianchi V, et al. 2-Deoxy-d-glucose ameliorates PKD progression. J Am Soc Nephrol. 2015 Nov 3.

Chapter 2

Targeting of sodium–glucose cotransporters with phlorizin inhibits polycystic kidney disease progression in Han:SPRD rats

Xueqi Wang[1,2,3], Suhua Zhang[1,2,4], Yang Liu[2], Daniela Spichtig[2], Sarika Kapoor[1,2], Hermann Koepsell[5], Nilufar Mohebbi[1,2], Stephan Segerer[1,2], Andreas L. Serra[1,2], Daniel Rodriguez[2], Olivier Devuyst[1,2], Changlin Mei[3] and Rudolf P. Wüthrich[1,2]

[1]Division of Nephrology, University Hospital, Zürich, Switzerland
[2]Institute of Physiology, University of Zürich, Zürich, Switzerland
[3]Department of Nephrology, Kidney Institute of PLA, Shanghai Changzheng Hospital, Second Military Medical University, Shanghai, PRC
[4]Department of Nephrology, Shanghai Renji Hospital, School of Medicine, Shanghai Jiaotong University, Shanghai, PRC
[5]Institute of Anatomy and Cell Biology, University of Würzburg, Würzburg, Germany

Kidney International (2013) 84, 962–968

Contribution by Daniel Rodriguez:

Western blot analysis for phosphorylated ERK and total ERK in response to phlorizin and analysis of data.

http://www.kidney-international.org

Targeting of sodium–glucose cotransporters with phlorizin inhibits polycystic kidney disease progression in Han:SPRD rats

Xueqi Wang[1,2,3,6], Suhua Zhang[1,2,4,6], Yang Liu[2], Daniela Spichtig[2], Sarika Kapoor[1,2], Hermann Koepsell[5], Nilufar Mohebbi[1,2], Stephan Segerer[1,2], Andreas L. Serra[1,2], Daniel Rodriguez[2], Olivier Devuyst[1,2], Changlin Mei[3] and Rudolf P. Wüthrich[1,2]

[1]Division of Nephrology, University Hospital, Zürich, Switzerland; [2]Institute of Physiology, University of Zürich, Zürich, Switzerland; [3]Department of Nephrology, Kidney Institute of PLA, Shanghai Changzheng Hospital, Second Military Medical University, Shanghai, PRC; [4]Department of Nephrology, Shanghai Renji Hospital, School of Medicine, Shanghai Jiaotong University, Shanghai, PRC and [5]Institute of Anatomy and Cell Biology, University of Würzburg, Würzburg, Germany

Renal tubular epithelial cell proliferation and transepithelial cyst fluid secretion are key features in the progression of polycystic kidney disease (PKD). As the role of the apical renal sodium–glucose cotransporters in these processes is not known, we tested whether phlorizin inhibits cyst growth and delays renal disease progression in a rat model of PKD. Glycosuria was induced by subcutaneous injection of phlorizin in male heterozygous (Cy/þ) and wild-type Han:SPRD rats. Phlorizin induced immediate and sustained glycosuria and osmotic diuresis in these rats. Cy/þ rats treated with phlorizin for 5 weeks showed a significant increase in creatinine clearance, a lower 2-kidneys/body weight ratio, a lower renal cyst index, and reduced urinary albumin excretion as compared with vehicle-treated Cy/þ rats. Measurement of Ki67 staining found significantly lower cell proliferation in dilated tubules and cysts of Cy/þ rats treated with phlorizin, as well as a marked inhibition of the activated MAP kinase pathway. In contrast, the mTOR pathway remained unaltered. Phlorizin dose dependently inhibited MAP kinase in cultured tubular epithelial cells from Cy/þ rats. Thus, long-term treatment with phlorizin significantly inhibits cystic disease progression in a rat model of PKD. Hence, induction of glycosuria and osmotic diuresis (glycuresis) by renal sodium–glucose cotransporters inhibition could have a therapeutic effect in polycystic kidney disease.

Correspondence: Changlin Mei, Department of Nephrology, Kidney Institute of PLA, Shanghai Changzheng Hospital, Second Military Medical University, Shanghai, 20003, P.R China. E-mail: chlmei1954@126.com or Rudolf P. Wüthrich, Division of Nephrology, University Hospital, Rämistrasse 100, Zurich, 8091, Switzerland, E-mail: rudolf.wuethrich@usz.ch

[6]These authors contributed equally to this work.

Part of this work has been presented in abstract form at the annual meeting of the American Society of Nephrology in November 2012 in San Diego.

Received 10 September 2012; revised 9 March 2013; accepted 21 March 2013; published online 29 May 2013

Kidney International (2013) 84, 962–968; doi:10.1038/ki.2013.199; published online 29 May 2013

KEYWORDS: polycystic; phlorizin; rat; sodium–glucose cotransport

Autosomal dominant polycystic kidney disease (ADPKD) is characterized by the development of innumerable renal cysts which originate from the tubular epithelium of various nephron segments.[1] Cystogenesis in ADPKD reflects epithelial dedifferentiation, increased proliferation, and abnormal fluid secretion.[2] The compression of healthy adjacent parenchyma by the expanding cysts leads to progressive renal failure, with more than 50% of the patients reaching end-stage renal disease during their lifetime.[3] Insights into the pathophysiological processes that govern cyst development led to a growing number of drug candidates in ADPKD. In particular, several drugs targeting epithelial cell proliferation or the transport processes that contribute to intracystic fluid secretion have recently been proposed. These drugs include mammalian target of rapamycin (mTOR) inhibitors, somatostatin, and vasopressin type 2 receptor antagonists.[4,5]

The dihydrochalcone phlorizin is a natural product and dietary constituent which is found in a number of fruit trees.[6] For decades, it has been extensively used as a tool for physiological research. Phlorizin's principal pharmacological action is to produce renal glycosuria and—to a lesser degree—to block intestinal glucose absorption through inhibition of the Na^+–glucose cotransporters (SGLTs) located apically in the proximal tubules of the kidneys and the small intestinal mucosa. The administration of phlorizin to experimental animal models results in profound inhibition of the renal SGLTs in renal proximal tubules, resulting in marked glycosuria.[6]

To the best of our knowledge, the role of SGLTs in the pathogenesis of polycystic kidney disease (PKD) has never been examined. We hypothesized that induction of glycosuria and osmotic diuresis by inhibiting renal SGLTs could slow cystogenesis and renal disease progression. To test this

hypothesis, we treated heterozygous (Cy/þ) Han:SPRD rats with phlorizin and investigated the effects of chronic glycuresis on parameters of renal function and cystogenesis. Our data demonstrate that phlorizin effectively retarded renal functional loss and cyst volume growth in this rat model of PKD.

RESULTS

Phlorizin treatment induces glycosuria and osmotic diuresis in Han:SPRD rats

Treatment of 5-week-old male heterozygous (Cy/þ) and wild-type (þ/þ) Han:SPRD rats with phlorizin (400 mg/kg/day subcutaneous in propylene glycol) induced an immediate and sustained glycosuria. The glycosuria was accompanied by a threefold increase in urine output, reflecting the increased osmolar excretion (Table 1; Figure 1a and b). In contrast, Cy/þ and þ/þ rats injected with the vehicle (propylene glycol) did not develop glycosuria. Plasma glucose levels did not change in response to phlorizin (Table 1). Despite the massive polyuria, plasma osmolality and plasma sodium and chloride concentrations were stable in Cy/þ rats at days 17 and 35 of treatment, suggesting that the animals adequately compensated for the osmotic diuresis and did not get dehydrated. Of note, phlorizin-treated Cy/þ rats displayed a slightly enhanced urinary sodium and chloride excretion rate compared with vehicle-treated rats, as well as a 6.7% weight difference at the end of the treatment period (Table 1).

Effect of phlorizin treatment on renal function

After 5 weeks of treatment with phlorizin, the plasma creatinine was 28% lower in male Cy/þ rats compared with the vehicle-treated group, and the creatinine clearance was 56% higher (Table 2; Figure 1c and d). Thus, despite increased urine output and lower body weight, the decline in renal function was significantly attenuated in the phlorizin-treated rats.

Plasma blood urea nitrogen values increased to a greater extent upon treatment of Cy/þ rats with phlorizin compared with vehicle (Table 2). However, blood urea nitrogen values also increased upon treatment with phlorizin in þ/þ control rats. This is consistent with an enhanced tubular reabsorption of urea upon induction of osmotic diuresis.

As albuminuria is a marker of renal disease severity in the Han:SPRD model of PKD, we determined the amount of urinary albumin in Cy/þ and þ/þ rats treated with phlorizin or vehicle by enzyme-linked immunosorbent assay (ELISA) and SDS–polyacrylamide gel electrophoresis. Figure 2 shows that albumin excretion was higher in Cy/þ compared with wild-type þ/þ rats, as expected. The excretion of urinary albumin was significantly reduced upon treatment of Cy/þ rats with phlorizin. After 5 weeks of treatment, the albumin excretion amounted to 2.7± 0.7 mg/day in vehicle-treated Cy/þ rats vs. 1.0± 0.4 mg/day in phlorizin-treated animals (63.1% less in the phlorizin-treated group compared with the vehicle-treated group, P○ 0.01).

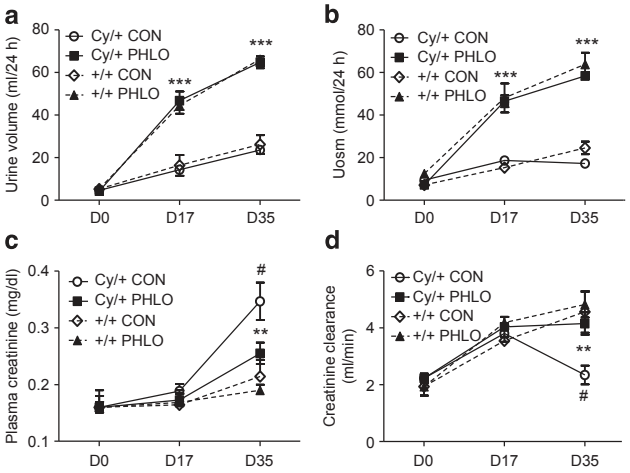

Figure 1 | Diuresis, osmolar excretion, and renal function in control (þ/þ) and cystic (Cy/þ) male Han:SPRD rats treated with vehicle (propylene glycol; CON) or phlorizin (PHLO). (a) Course of diuresis, (b) 24-h osmolar excretion, (c) plasma creatinine, and (d) creatinine clearance from baseline to days 17 and 35 of treatment. **P○ 0.01, ***P○ 0.001 when comparing Cy/þ CON and Cy/þ PHLO at each time point. #P○ 0.05 when comparing Cy/þ and þ/þ group.

Table 1 | Effect of phlorizin treatment on body weight, diuresis, and fluid and electrolyte parameters in Cy/þ rats

		Day 17		Day 35	
	Baseline	CON	PHLO	CON	PHLO
Number of animals (n)	17	7	10	7	10
Age (in weeks)	5	7.5	7.5	10	10
Total body weight (g)	94.5± 2.5	212.8± 8.7	186.7± 7.3*	304.7± 9.4	284.2± 5.5*
Diuresis (ml/day)	4.5± 0.4	14.3± 1.4	47.6± 3.8***	23.6± 2.9	65.0± 2.2***
P_{osm} (mosm/l)	300.5± 16.4	306.3± 5.5	306.7± 7.9	310.2± 4.1	314.2± 16.9
P_{Na^+} (mmol/l)	143.7± 2.8	144.9± 3.6	144.4± 3.1	144.3± 3.7	144.7± 8.8
P_{Cl^-} (mmol/l)	104.8± 2.3	102.6± 1.3	103.4± 2.5	104.7± 4.7	104.6± 6.8
$P_{glucose}$(mmol/l)	9.3± 0.8	11.3± 1.2	11.1± 1.6	12.9± 3.0	13.0± 3.8
U_{osm} (mosm/day)	8.3± 2.4	18.7± 4.0	47.0± 7.3***	17.2± 2.3	49.1± 13.6***
$U_{glucose}$ (mmol/day)	○ 0.1	0.1± 0.0	21.5± 2.9***	0.1± 0.0	18.0± 4.6***
U_{Na^+} (mmol/day)	0.6± 0.2	1.2± 0.2	1.7± 0.1**	1.1± 0.2	1.9± 0.8**
U_{Cl^-} (mmol/day)	1.3± 0.4	2.7± o.6	3.1± 0.5	2.2± 0.4	3.4± 1.1***

Abbreviations: CON, vehicle (propylene glycol) treated; PHLO, phlorizin.
*P○ 0.05, **P○ 0.01, ***P○ 0.001 when comparing CON and PHLO at each time point.

Table 2 | Effect of phlorizin on parameters of renal function in Cy/þ and þ/þ rats

Group	Time point (day)	BUN (mg/dl)		Creatinine (mg/dl)		Creatinine clearance (ml/day)	
		CON	PHLO	CON	PHLO	CON	PHLO
Cy/þ	Baseline	39.7± 5.6	41.0± 4.7	0.14± 0.03	0.15± 0.03	2.04± 0.50	1.67± 0.68
	D17	53.8± 4.4$^{\#\#\#}$	65.0± 8.1$^{*\#\#}$	0.18± 0.04	0.17± 0.03	3.40± 0.37	3.86± 0.93
	D35	77.8± 14.8$^{\#\#}$	76.6± 13.0$^{\#\#}$	0.35± 0.08$^{\#}$	0.25± 0.05*	2.34± 0.81$^{\#}$	4.15± 0.14*
þ/þ	Baseline	38.3± 3.9	35.2± 4.1	0.15± 0.02	0.17± 0.01	1.64± 0.39	1.99± 0.15
	D17	38.2± 4.3	50.3± 12.4	0.18± 0.01	0.16± 0.02	3.50± 0.12	4.18± 0.37
	D35	36.1± 2.3	53.1± 10.8*	0.22± 0.03	0.21± 0.03	4.56± 1.26	4.82± 1.01

Abbreviations: BUN, blood urea nitrogen; CON, vehicle (propylene glycol) treated; PHLO, phlorizin.
*P○ 0.05 when comparing CON and PHLO at each time point. $^{\#}$P○ 0.05; $^{\#\#}$P○ 0.01; $^{\#\#\#}$P○ 0.001 when comparing Cy/þ and þ/þ at each time point for the same treatment.

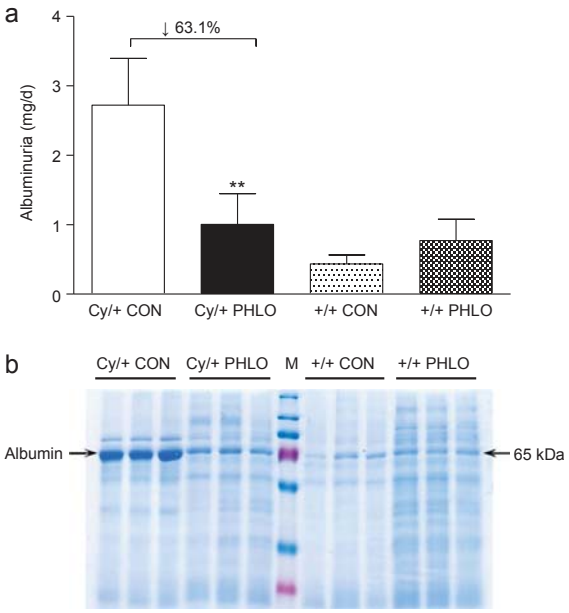

Figure 2 | Albumin excretion in Cy/þ and þ/þ rats after 5 weeks of treatment with vehicle (propylene glycol; CON) or phlorizin (PHLO). (a) Urine albumin concentration (Cy/þ CON: n¼7; Cy/þ PHLO: n¼10; þ/þ CON: n¼5; þ/þ PHLO: n¼3). **P○ 0.01; (b) Urine sample SDS-polyacrylamide gel electrophoresis. Each lane shows a urine sample of a single rat, each group shows representative samples from three rats. Loading volumes were corrected for diuresis and amounted to 15 ml for vehicle-treated rats, and 45 ml for phlorizin-treated rats. Arrow shows the band for albumin. M, marker.

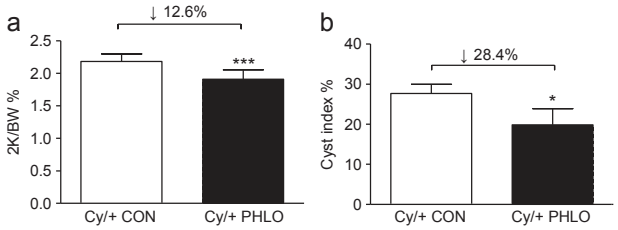

Figure 3 | Effect of phlorizin on kidney weight and cyst index. Ratio of (a) 2-kidneys/body weight (2K/BW) and (b) cyst index in male Cy/þ rats treated daily for 5 weeks with vehicle (propylene glycol; CON; n¼7) or phlorizin (PHLO, n¼10). *P○ 0.05, ***P○ 0.001.

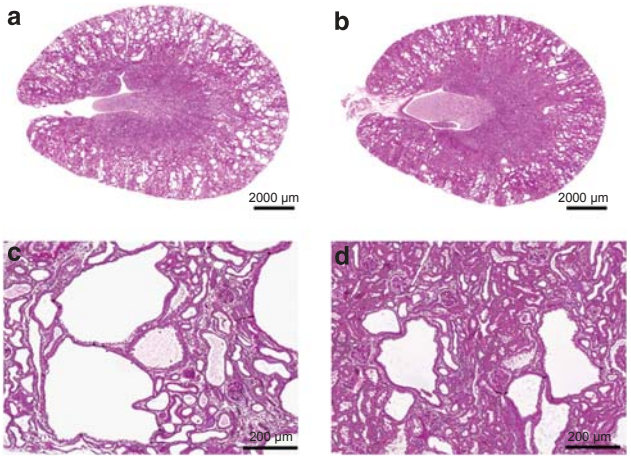

Figure 4 | Effect of phlorizin on renal histology. Renal histology (periodic acid–Schiff) in (a, c) vehicle-treated (propylene glycol; CON) and (b, d) phlorizin-treated (PHLO) male Cy/þ rats. Scale bar is 2000 mm in a and b, and 200 mm in c and d.

This suggests that the accompanying glomerular and proximal tubular damage was strongly attenuated in phlorizin-treated Cy/þ.

Effect of phlorizin treatment on kidney weight and morphology

After 5 weeks of treatment with phlorizin or vehicle, rats were killed and the kidneys were excised and decapsulated for weight determination and morphological analysis. The total weight of both kidneys amounted to 6.96± 0.59 g in vehicle-treated Cy/þ (n¼7) vs. 5.66± 0.35 g in phlorizin-treated Cy/þ rats (n¼10), representing a difference of 18.7% (P○ 0.001). Figure 3a shows that the 2-kidneys/body weight ratio was reduced by 12.6% in the phlorizin-treated rats (P○ 0.001). Likewise the cyst index (determined on periodic acid–Schiff-stained sections) was reduced by 28.4% in phlorizin-treated rats (P○ 0.05). The cyst index data were confirmed by further histomorphological analysis of the kidneys, which demonstrated that phlorizin-treated Cy/þ rats had fewer and smaller cyst profiles as compared with vehicle-treated rats (Figure 4).

Phlorizin inhibits proliferation of cyst epithelium

Immunostaining for Ki67 was used to examine whether phlorizin treatment had an effect on cystic epithelial cell

proliferation. Figure 5 demonstrates a marked increase in the positivity of nuclei in the cystic and non-cystic epithelium of Cy/þ kidneys in comparison with wild-type þ/þ kidneys. Quantification of the Ki67-positive nuclei revealed that the number of Ki67-positive nuclei was 39.8% lower in cystic epithelium and 23.8% lower in dilated tubules in phlorizin- versus vehicle-treated Cy/þ rats (Table 3). These data suggest that phlorizin may directly affect cell proliferation.

Effect of phlorizin treatment on mitogen-activated protein kinase and mTOR signaling pathway

We then studied the effect of phlorizin treatment on the phosphorylation of two key kinases that are known to be activated in PKD, namely extracellular signal-regulated kinase (ERK; mitogen-activated protein kinase (MAPK) pathway) and S6K (mTOR pathway). Figure 6 demonstrates that the phosphorylation and the ratio of phosphorylated to total ERK and S6K were markedly increased in Cy/þ compared with wild-type þ/þ rat kidneys. Of importance, phlorizin treatment was associated with a significant decrease in the phosphorylation of ERK, whereas the phosphorylation of S6K was unchanged. These data suggest that phlorizin differentially inhibits signaling cascades in the Cy/þ kidneys.

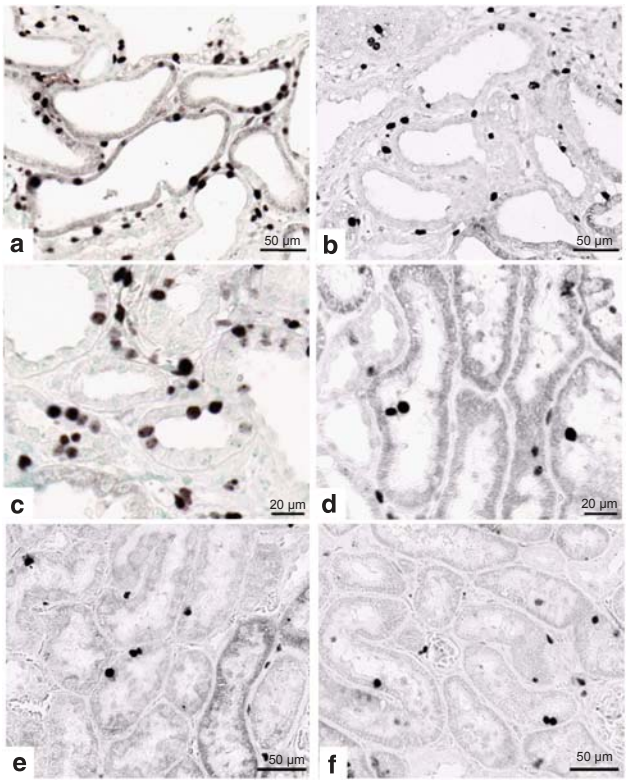

Figure 5 | Representative areas of Ki67 immunohistochemical staining in Cy/þ rat kidneys. (a) Cy/þ CON (cyst), (b) Cy/þ phlorizin (PHLO; cyst), (c) Cy/þ CON (dilated tubule), (d) Cy/þ PHLO (dilated tubule), (e) þ/þ CON, and (f) þ/þ PHLO.

Table 3 | Effect of phlorizin treatment on Ki67 staining of Cy/þ rat kidneys

Treatment	CON (n¼4)	PHLO (n¼7)	Difference (%)	P-value
Ki67-positive cells in dilated tubules	2.8± 0.7	1.9± 0.3	□23.8	0.037
Ki67-positive nuclei in cyst-lining epithelium	5.8± 2.3	3.5± 1.5	□39.8	0.029

Abbreviations: CON, vehicle (propylene glycol) treated; PHLO, phlorizin.

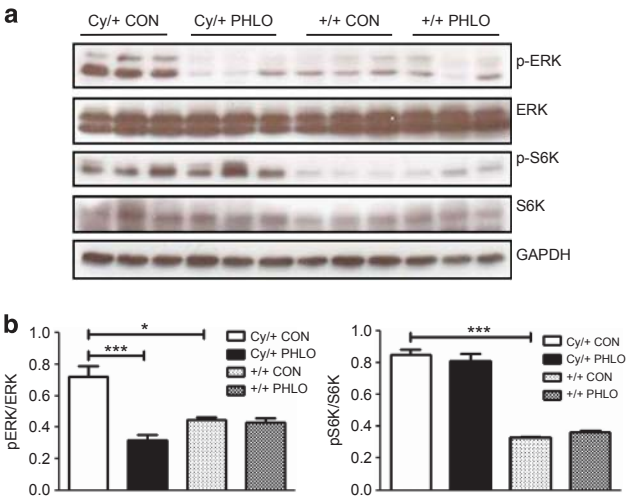

Figure 6 | Effect of phlorizin on ERK and S6K phosphorylation. (a) Western blot analysis and (b) densitometry for mammalian target of rapamycin and mitogen-activated protein kinase pathway in þ/þ and Cy/þ kidney. Cy/þ rats show enhanced phosphorylation of extracellular signal-regulated kinase (ERK) and S6K compared with wild-type þ/þ animals. In phlorizin-treated Cy/þ rats, the phosphorylation of ERK and the pERK/total ERK ratio is significantly reduced, whereas the phosphorylation of S6K and the pS6K/total S6K ratio is unchanged. CON, propylene glycol treated; GAPDH, glyceraldehyde-3-phosphate dehydrogenase; PHLO, phlorizin. *P○ 0.05, ***P○ 0.001.

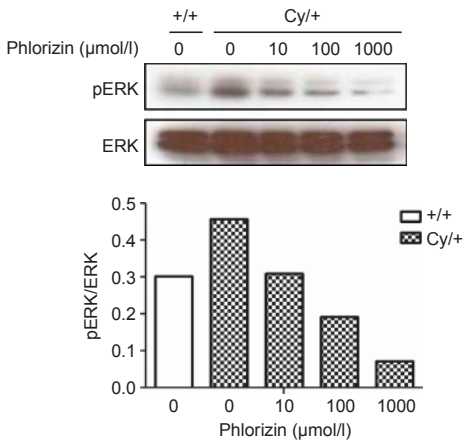

Figure 7 | Western blot analysis for phosphorylated extracellular signal-regulated kinase 1/2 (pERK; top) and total ERK (bottom) in response to phlorizin treatment (0–1000 1mol/l) in cultured Cy/þ tubular epithelial cell (TEC). TEC cultured from þ/þ kidneys served as control. Bottom bar graph shows the densitometric pERK/total ERK ratios.

Effect of phlorizin on MAPK signaling pathway

To test whether phlorizin has a direct effect on MAPK activation, we examined the effect of phlorizin in cultured tubular epithelial cells (TECs) derived from Cy/þ kidneys. Figure 7 shows that ERK phosphorylation was constitutively upregulated in TECs derived from Cy/þ cells, contrasting with the much weaker ERK phosphorylation, which is seen in TECs that are derived from wild-type þ/þ rats. Upon incubation of the cells with phlorizin (0–1000 mmol/l), there was a dose-dependent decrease of ERK phosphorylation. This suggests that phlorizin via this direct effect on the MAPK signaling pathway could directly alter TEC activation and proliferation in PKD.

DISCUSSION

Treatment strategies for PKD with drugs that aim for renal-specific targets may provide superior efficacy and fewer adverse events, compared with therapeutic agents that have a broader and less selective effect. The SGLT system may be one of these renal-specific targets in PKD, and SGLT inhibitors might have a potential benefit in PKD, either by directly affecting cell proliferation or indirectly via their osmotic diuresis effect. Drugs that specifically inhibit the kidney-specific SGLT2 are currently being developed for glycemic control in type 2 diabetes.[7,8] Most of the SGLT2 inhibitors are structurally derived from phlorizin, which is a powerful inhibitor of both SGLT1 and SGLT2, and is known to produce massive glycosuria and osmotic diuresis in the rat.[6,9]

Here, we show for the first time that chronic inhibition of SGLT and induction of glycosuria with phlorizin slows renal cystic disease progression in the Han:SPRD rat model of PKD.[10] A 5-week treatment course with phlorizin resulted in the following: (1) improved renal function, as assessed by plasma creatinine and creatinine clearance measurements; (2) a reduction in urinary albumin excretion, which is a marker of disease progression in this model; (3) a lower total kidney weight and 2-kidneys/body weight ratio, correlating morphologically with smaller cysts and a lower cyst index; (4) decreased tubular and cystic epithelial cell proliferation, as assessed by Ki67 staining; (5) inhibition of the activated MAPK pathway, as assessed by a lower p-ERK1/2 to total ERK ratio, both *in vivo* and *in vitro*. Thus, phlorizin-mediated induction of glycosuria and the subsequent occurrence of osmotic diuresis (glycuresis) were associated with reduced cystic disease progression.

The putative mechanisms by which phlorizin inhibits cystic renal disease progression may be manifold and must be discussed at several levels. *First* of all, phlorizin may directly inhibit cyst epithelial cell proliferation. This is suggested by a markedly reduced number of proliferating cyst epithelial cells in phlorizin-treated Cy/þ rats. In addition, our *in vitro* experiments with cultured Cy/þ TECs show that phlorizin has a direct effect on the MAPK pathway, which manifests as an inhibition of ERK1/2 phosphorylation. *Second*, by inducing osmotic diuresis phlorizin might change the transepithelial transport of fluid and electrolytes in a way that inhibits cyst growth. From the present studies, however, it is not possible to provide a mechanism how osmotic diuresis could reverse fluid secretion into the cysts. *Third*, a change in the hormonal environment (in particular the inhibition of insulin and insulin-like growth factor-1 production) is likely to be caused by the loss of glucose in the urine and/or by a direct effect of phlorizin on insulin secretion. As insulin and insulin-like growth factor-1 are known to be implicated in cyst epithelial cell proliferation, the reduced cyst development that is seen with phlorizin treatment could be partially explained by these hormonal changes.[11,12]

Treatment with phlorizin did not result in a stop or reversal of disease progression. The treatment was well tolerated by the rats and did not result in notable side effects, except for a threefold increase in the urine output, which was compensated by an appropriate increase in fluid intake. As the activated MAPK[13] and the mTOR pathway (reviewed in Torres *et al.*[14]) critically contribute to the pathogenesis of PKD, one could postulate that SGLT inhibitors might be ideal drugs to combine with drugs that affect different signaling pathways, such as the mTOR pathway that was not affected by phlorizin in this study. We and others have previously shown that treatment with sirolimus[15,16] or everolimus[17] significantly inhibited cyst growth and disease progression in Han:SPRD rats. The effect of mTOR inhibitors on cyst volume growth is only partial, perhaps because of the known compensatory upregulation of the MAPK pathway.[18] Combining SGLT inhibitors with mTOR inhibitors might therefore be a therapeutic strategy worthwhile pursuing in PKD.

It might be of interest to oppose the effect of phlorizin (a glycuretic drug) and the effect of the vasopressin type 2 receptor antagonist tolvaptan (an aquaretic drug), the latter of which is in phase 3 clinical development for the treatment of ADPKD.[19,20] Both drugs target highly selective renal tubular transport systems and produce a significant and sustained increase in urine output. Similar to phlorizin, tolvaptan is also known to inhibit the ERK pathway but not the mTOR pathway.[21,22] At this point, it is not known whether the vasopressin–cAMP axis is altered with phlorizin. In view of the primary increase in the osmotic clearance, treatment with phlorizin could lead to increased endogenous AVP levels—an effect similar to that observed with long-term vasopressin type 2 receptor antagonism—[23] and this could promote distal tubular cyst growth, an effect that might not be seen in Han:SPRD as the cysts are almost exclusively of proximal tubular origin, which are not supposed to be responsive to vasopressin. Of note, increasing fluid intake and urine output experimentally by providing rats with 5% glucose in the drinking water also revealed a beneficial effect on cyst growth in a distal PKD model (PCK rat) but not in the proximal model (Han:SPRD rat).[24] Thus, glycuretic and aquaretic drugs display similar and dissimilar effects on cyst volume progression and should be developed further as a future treatment for ADPKD.

By now there is no evidence that chronic SGLT inhibition may potentially be deleterious for the kidney. Results from *Sglt2*$^{-/-}$ knockout mice[25] and more recently from *Sglt1*$^{-/-}$ knockout mice[26] have revealed that there is no alteration in renal function and morphology. As in phlorizin-treated rats, *Sglt2*$^{-/-}$ mice display glycosuria, polyuria, and increased food and fluid intake without differences in plasma glucose concentrations and glomerular filtration rate compared with wild-type mice. SGLT2 deficiency is also not associated with volume depletion, as shown by similar body weight, BP, and hematocrit. Likewise, human familial renal glycosuria that results from mutations in the *SGLT2* gene is considered to be a benign condition.[27] As far as we know, the renal safety of the SGLT2 inhibitor dapagliflozin (in clinical development for type 2 diabetes) is excellent, except for a slightly higher incidence of genitourinary infections.[28]

In summary, we have shown that induction of glycosuria and osmotic diuresis (glycuresis) by inhibition of the renal SGLT with phlorizin resulted in a significant retardation of the cystic disease progression in the Han:SPRD rat model of PKD. Further studies are in progress to assess the effect of glycosuria induction in additional models of PKD, including the ARPKD model in PCK rats. Whether this experimental strategy can be translated to human ADPKD remains to be determined.

MATERIALS AND METHODS

Animals

The Han:SPRD rat colony was established in our animal facility from a litter, which was obtained from the Rat Resource and Research Center (Columbia, MO). Heterozygous cystic (Cy/+) and wild-type normal (+/+) rats were used in this study. Only male rats were used as cysts develop more rapidly in male compared with female rats. The regulatory commission for animal studies, a local government agency, approved the study protocol. Rats had free access to tap water and standard rat diet.

Study design

Treatment was started in 5-week-old male heterozygous Cy/+ or wild-type +/+ control Han:SPRD rats. Groups of 7–10 rats were used. Phlorizin (Sigma-Aldrich, Buchs, Switzerland) was dissolved in a solution of 60% propylene glycol in phosphate-buffered saline and was injected subcutaneously at a dose of 400 mg/kg/day for 5 weeks. Control rats were injected with the same volume of 60% propylene glycol in phosphate-buffered saline. The dose of the phlorizin or the vehicle was adjusted daily according to the body weight of the rats. Blood and urine were collected at baseline (before treatment), at day 17 and 35 of treatment in all animals. All samples were stored at −20 °C before measurement. Rats were killed after 5 weeks of treatment, and kidneys were harvested for further analysis.

The Synchron LX System, UniCel DxC 600/800 System, and Synchron System AQUA CAL 1 and 2 (Beckman, Brea, CA) were used for the quantitative determination of glucose, sodium, chloride, creatinine, and blood urea nitrogen concentrations in rat plasma and urine. Plasma and urine osmolalities were measured by using an Advanced freezing-point osmometer.

The GenWay (San Diego, CA) rat albumin ELISA kit was used for urine albumin concentration measurements. The urine samples were diluted 500 times in the diluent solution. One-hundred microliter aliquots of albumin standard or urine sample were added into each well of precoated plates. Plates were incubated for 30 min at room temperature and were washed four times thereafter. Plates were then incubated with horseradish peroxidase–conjugated anti-albumin solution for 30 min at room temperature in the dark, and were washed again four times. Then 100 μl of 3,3′,5,5′-tetramethylbenzidine substrate solution was added into each well, and plates were incubated in the dark for 10 min at room temperature. Then 100 μl stop solution was added, mixed well, and the absorbance at 450 nm was determined using a Tecan ELISA reader (Männedorf, Zürich, Switzerland).

Tissue sectioning, periodic acid–Schiff staining, and cyst index determination

For the histological examination, one of the kidneys from each animal was sliced perpendicularly to the long axis at ~2-mm intervals. Slices from the midportion of the kidneys were fixed in 10% buffered formalin overnight. On the next day tissues were embedded in paraffin. Three-micrometer sections were stained with periodic acid–Schiff following routine protocols. The stained sections were subjected to cyst index analysis, using the HistoQuest image analysis software (TissueGnostics, Vienna, Austria) to count the whole cortex region (total area, TA) and the cyst area (cyst area, CA) in the renal cortex. The cyst index was calculated as CA/TA×100.

Immunohistochemistry

Immunohistochemistry for Ki67 was performed on 3-μm tissue sections. In brief, the tissue sections were deparaffinized and rehydrated. The antigen retrieval was performed in an autoclave oven. As primary antibody we used a mouse anti-Ki67 antibody (BD Pharmingen, San Jose, CA). After applying the primary antibody for 1 h the sections were washed, and then incubated with the biotinylated secondary antibody (Vector, Los Angeles, CA) for 30 min. This was followed by the application of the ABC reagent (Vector), using 3,3′-diaminobenzidine with metal enhancement as the detection reagent.

For each section we randomly chose 10 cysts, counted the number of Ki67-positive nuclei, and then averaged the number of Ki67-positive nuclei per cyst. We also chose 10 areas with dilated tubules and counted the number of Ki67-positive dilated tubules and the number of positive Ki67 nuclei per tubule, and then averaged the Ki67-positive nuclei in each positive dilated tubule.

Western blot analysis

Kidneys were homogenized with ice-cold lysis buffer containing 40 mmol/l Hepes, 120 mmol/l NaCl, 1 mmol/l ethylenediaminetetraacetic acid, 10 mmol/l potassium pyrophosphate, 10 mmol/l glycerol phosphate, 50 mmol/l NaF, 0.5 mmol/l $NaVO_3$, 1% Triton-X 100, and protease inhibitor mixture (pH 7.6). Tissue lysates were cleared by centrifugation. Equal amounts of lysates were resolved by SDS–polyacrylamide gel electrophoresis, transferred to nitrocellulose membranes, and probed with antibodies against ERK1/2$^{Thr202/Tyr204}$, ERK1/2, p70 S6K Thr$^{421/Ser424}$, p70 S6K (all from Cell Signaling Technology, Danvers, MA), and glyceraldehyde-3-phosphate dehydrogenase. Sheep anti-mouse IgG-HRP and donkey anti-rabbit IgG-HRP were used as secondary antibodies. Quantification of phosphorylated ERK1/2 and p70 S6K expression was normalized for total ERK1/2 and p70 S6K, respectively, using a densitometer,

and the data are reported as ratio of phlorizin- versus vehicle-treated Cy/þ and þ/þ rats.

Primary cultures of TECs from Cy/þ rats

Primary cultures of TECs from 8-week-old þ/þ and Cy/þ kidneys were prepared by mincing the kidneys and digesting the tissues with 1 mg/ml collagenase with gentle agitation for 1 h at 37 1C. The suspension was allowed to sediment for 1 min. Cells were collected by harvesting the supernatant twice, and were then washed three times with 10% fetal bovine serum (FBS)/Hanks balanced salt solution. Isolated cells were resuspended in K1 medium (1:1 mixture of Dulbecco's modified Eagle's medium and Ham's F-12 medium supplemented with 5% FBS, 10 mmol/l HEPES, 42 mmol/l sodium bicarbonate, 50 ng/ml insulin, 50 nmol/l hydrocortisone, 50 ng/ml transferrin, 5 pmol/l triiodothyronine, 20 ng/ml rat EGF, 100 IU/ml penicillin, and 100 mg/ml streptomycin). Cells were then seeded in collagen type 1–precoated culture dishes and grown to confluence. The medium was then changed to a K1 medium with 0.5% FBS for 24 h, and the cells were then incubated with phlorizin (0–1000 mmol/l) for 24 h. Lysates were then prepared and resolved by SDS–polyacrylamide gel electrophoresis and probed by western blot analysis with antibodies against ERK1/2$^{Thr202/Tyr204}$ and total ERK1/2 as described above.

Statistical analysis

Data are presented as means± s.d. Data were tested for statistically significant differences between treatment groups by using the unpaired two-tailed *t*-test, and by using the GraphPad Prism version 5.0 software (GraphPad, San Diego, CA). $P < 0.05$ was considered to indicate statistically significant differences.

DISCLOSURE

All the authors declared no competing interests.

ACKNOWLEDGMENTS

We thank Ilka Edenhofer for helping with the tissue stainings, Julien Weber for the blood and urine sample analysis, and Zhongnong Guo for helping with the immunohistochemistry. This work is supported by the Sino Swiss Science & Technology Cooperation (SSSTC) Program (EG 14-032009 to XW, and IP2010-2012 to CM and RPW); the Hartmann-Müller Foundation; the Swiss National Science Foundation (320030-144093 to RPW; 32003B-129710 to SS; NCCR Kidney. CH to OD); the Action de Recherche Concertée; an Inter-University Attraction Pole; the Major Research Projects of Shanghai Science and Technology Commission (08dz1900600 to CM); and the National Natural Science Foundation of China (30971368 to CM).

REFERENCES

1. Torres VE, Harris PC, Pirson Y. Autosomal dominant polycystic kidney disease. Lancet 2007; 369: 1287–1301.
2. Terryn S, Ho A, Beauwens R et al. Fluid transport and cystogenesis in autosomal dominant polycystic kidney disease. Biochim Biophys Acta 2011; 1812: 1314–1321.
3. Steinman TI. Polycystic kidney disease: a 2011 update. Curr Opin Nephrol Hypertens 2012; 21: 189–194.
4. Novalic Z, van der Wal AM, Leonhard WN et al. Dose-dependent effects of sirolimus on mTOR signaling and polycystic kidney disease. J Am Soc Nephrol 2012; 23: 842–853.
5. Chang MY, Ong AC. Mechanism-based therapeutics for autosomal dominant polycystic kidney disease: recent progress and future prospects. Nephron Clin Pract 2012; 120: c25–c35.
6. Ehrenkranz JR, Lewis NG, Kahn CR et al. Phlorizin: a review. Diabetes Metab Res Rev 2005; 21: 31–38.
7. Mather A, Pollock C. Renal glucose transporters: novel targets for hyperglycemia management. Nat Rev Nephrol 2010; 6: 307–311.
8. Vallon V, Sharma K. Sodium-glucose transport: role in diabetes mellitus and potential clinical implications. Curr Opin Nephrol Hypertens 2010; 19: 425–431.
9. Rossetti L, Smith D, Shulman GI et al. Correction of hyperglycemia with phlorizin normalizes tissue sensitivity to insulin in diabetic rats. J Clin Invest 1987; 79: 1510–1515.
10. Gretz N, Kränzlin B, Pey R et al. Rat models of autosomal dominant polycystic kidney disease. Nephrol Dial Transplant 1996; 11: 46–51.
11. Aukema HM, Housini I. Dietary soy protein effects on disease and IGF-I in male and female Han:SPRD-cy rats. Kidney Int 2001; 59: 52–61.
12. Parker E, Newby LJ, Sharpe CC et al. Hyperproliferation of PKD1 cystic cells is induced by insulin-like growth factor-1 activation of the Ras/Raf signalling system. Kidney Int 2007; 72: 157–165.
13. Nagao S, Yamaguchi T, Kusaka M et al. Renal activation of extracellular signal-regulated kinase in rats with autosomal-dominant polycystic kidney disease. Kidney Int 2003; 63: 427–437.
14. Torres VE, Boletta A, Chapman A et al. Prospects for mTOR inhibitor use in patients with polycystic kidney disease and hamartomatous diseases. Clin J Am Soc Nephrol 2010; 5: 1312–1329.
15. Wahl PR, Serra AL, Le Hir M et al. Inhibition of mTOR with sirolimus slows disease progression in Han:SPRD rats with autosomal dominant polycystic kidney disease (ADPKD). Nephrol Dial Transplant 2006; 21: 598–604.
16. Tao Y, Kim J, Schrier RW et al. Rapamycin markedly slows disease progression in a rat model of polycystic kidney disease. J Am Soc Nephrol 2005; 16: 46–51.
17. Wu M, Wahl PR, Le Hir M et al. Everolimus retards cyst growth and preserves kidney function in a rodent model for polycystic kidney disease. Kidney Blood Press Res 2007; 30: 253–259.
18. Carracedo A, Ma L, Teruya-Feldstein J et al. Inhibition of mTORC1 leads to MAPK pathway activation through a PI3K-dependent feedback loop in human cancer. J Clin Invest 2008; 118: 3065–3074.
19. Higashihara E, Torres VE, Chapman AB et al. TEMPO Formula and 156-05-002 Study Investigators. Tolvaptan in autosomal dominant polycystic kidney disease: three years' experience. Clin J Am Soc Nephrol 2011; 6: 2499–2507.
20. Torres VE, Chapman AB, Devuyst O et al. the TEMPO 3:4 Trial Investigators. Tolvaptan in patients with autosomal dominant polycystic kidney disease. N Engl J Med 2012; 367: 2407–2418.
21. Wang X, Gattone V 2nd, Harris PC et al. Effectiveness of vasopressin V2 receptor antagonists OPC-31260 and OPC-41061 on polycystic kidney disease development in the PCK rat. J Am Soc Nephrol 2005; 16: 846–851.
22. Reif GA, Yamaguchi T, Nivens E et al. Tolvaptan inhibits ERK-dependent cell proliferation, chloride secretion, and in vitro cyst growth of human ADPKD cells stimulated by vasopressin. Am J Physiol Renal Physiol 2011; 301: F1005–F1013.
23. Ho TA, Godefroid N, Gruzon D et al. Autosomal dominant polycystic kidney disease is associated with central and nephrogenic defects in osmoregulation. Kidney Int 2012; 82: 1121–1129.
24. Nagao S, Nishii K, Katsuyama M et al. Increased water intake decreases progression of polycystic kidney disease in the PCK rat. J Am Soc Nephrol 2006; 17: 2220–2227.
25. Vallon V, Platt KA, Cunard R et al. SGLT2 mediates glucose reabsorption in the early proximal tubule. J Am Soc Nephrol 2011; 22: 104–112.
26. Gorboulev V, Schürmann A, Vallon V et al. $Na^{þ}$-D-glucose cotransporter SGLT1 is pivotal for intestinal glucose absorption and glucose-dependent incretin secretion. Diabetes 2012; 61: 187–196.
27. Santer R, Calado J. Familial renal glucosuria and SGLT2: from a mendelian trait to a therapeutic target. Clin J Am Soc Nephrol 2010; 5: 133–141.
28. Bailey CJ, Gross JL, Pieters A et al. Effect of dapagliflozin in patients with type 2 diabetes who have inadequate glycaemic control with metformin: a randomised, double-blind, placebo-controlled trial. Lancet 2010; 375: 2223–2233.

Chapter 3

Inhibition of sodium-glucose cotransporter 2 with dapagliflozin in Han: SPRD rats with polycystic kidney disease

Daniel Rodriguez[a,b,c] Sarika Kapoor[a,b] Ilka Edenhofer[a,b] Stephan Segerer[a,b] Meliana Riwanto[a,b] Anja Kipar[d] Ming Yang[e] Changlin Mei[e] Rudolf P. Wüthrich[a,b]

[a]Division of Nephrology, University Hospital, Zürich, Switzerland [b]Institute of Physiology, University of Zürich, Switzerland
[c]Competence Center for Personalized Medicine, Zürich, Switzerland [d]Laboratory for Animal Model Pathology, Institute of Veterinary Pathology, Vetsuisse Faculty, University of Zürich, Zürich, Switzerland
[e]Department of Nephrology, Shanghai Changzheng Hospital, Second Military Medical University, Shanghai, P.R. China

Kidney Blood Press Res 2015;40:638-647

Contribution by Daniel Rodriguez:

Hypothesis proposal, breeding and genotyping, animal treatment and collection of urinary and blood samples, histological analysis with image analysis software HistoQUANT, statistical analysis and interpretation of data, writing of the first draft of the manuscript.

Kidney & Blood Pressure Research

Kidney Blood Press Res 2015;40:638-647
DOI: 10.1159/000368540
Published online: December 19, 2015
Accepted: November 25, 2015

Original Paper

Inhibition of Sodium-Glucose Cotransporter 2 with DapagliÁozin in Han: SPRD Rats with Polycystic Kidney Disease

Daniel Rodriguez[a,b,c] Sarika Kapoor[a,b] Ilka Edenhofer[a,b] Stephan Segerer[a,b] Meliana Riwanto[a,b] Anja Kipar[d] Ming Yang[e] Changlin Mei[e] Rudolf P. Wüthrich[a,b]

[a]Division of Nephrology, University Hospital, Zürich, Switzerland; [b]Institute of Physiology, University of Zürich, Switzerland; [c]Competence Center for Personalized Medicine, Zürich, Switzerland; [d]Laboratory for Animal Model Pathology, Institute of Veterinary Pathology, Vetsuisse Faculty, University of Zürich, Zürich, Switzerland; [e]Department of Nephrology, Shanghai Changzheng Hospital, Second Military Medical University, Shanghai, P.R. China

Key Words
Cyst • DapagliÁozin • Glucosuria • Polycystic kidney disease (PKD) • Sodium glucose cotransporter (SGLT)

Abstract
Background/Aims: DapagliÁozin (DAPA) is a selective inhibitor of the sodium-glucose cotransporter 2 (SGLT2) which induces glucosuria and osmotic diuresis. The therapeutic effect of DAPA in progressing stages of polycystic kidney disease (PKD) has not been studied. Methods: We examined the effect of DAPA in the Han: SPRD rat model of PKD. DAPA (10 mg/kg/day) or vehicle (VEH) was administered orally via gavage to 5 week old male Han: SPRD (Cy/+) or control (+/+) rats (n = 8-9 per group) for 5 weeks. Blood and urine were collected at baseline and after 2.5 and 5 weeks of treatment to assess renal function and albuminuria. At the end of the treatment, rats were sacriÀced and kidneys were excised for histological analysis. Results: After 5 weeks of treatment, DAPA-treated Cy/+ and +/+ rats exhibited signiÀcantly higher glucosuria, water intake and urine output than VEH-treated rats. DAPA-treated Cy/+ rats also exhibited signiÀcantly higher clearances for creatinine and BUN and less albuminuria than VEH-treated Cy/+ rats. DAPA treatment for 5 weeks resulted in a signiÀcant increase of the kidney weight in Cy/+ rats but no change in cyst growth. The degree of tubular epithelial cell proliferation, macrophage inÀltration and interstitial Àbrosis was also similar in DAPA- and VEH-treated Cy/+ rats. Conclusion: The induction of glucosuria with the SGLT2-speciÀc inhibitor DAPA was associated with improved renal function and decreased albuminuria, but had no effect on cyst growth in Cy/+ rats. Overall the beneÀcial effects of DAPA in this PKD model were weaker than the previously described effects of the combined SGLT1/2 inhibitor phlorizin.

Rudolf P. Wüthrich, MD, FASN
Division of Nephrology, University Hospital, Rämistrasse 100, 8091 Zürich, (Switzerland)
Tel. +41 44 255 33 84, Fax +41 44 255 45 93, E-Mail rudolf.wuethrich@usz.ch

Kidney Blood Press Res 2015;40:638-647
DOI: 10.1159/000368540
Published online: December 19, 2015

www.karger.com/kbr

Introduction

Autosomal Dominant Polycystic Kidney Disease (ADPKD) is the most common form of cystic renal diseases, affecting all ethnic groups worldwide, with an incidence of 1:400-1:1.000 [1, 2]. The disease is caused by a mutation in the PKD1 or the PKD2 genes that encode for the proteins polycystin-1 (PC1) and polycystin-2 (PC2) [3]. Altered function and/or a decrease of PC1 or PC2 levels below a certain threshold lead to slow and continuous development of fluid-filled cysts [4], resulting in bilateral renal enlargement and end-stage renal disease (ESRD) in approximately half of the patients [5].

Since ADPKD is relentlessly progressing, effective and specific long-term therapies are needed to halt disease progression. Several drugs are being tested in clinical trials, and some are emerging to be effective in selected patients [6]. Tolvaptan, in particular, is an aquaretic drug which inhibits the vasopressin V_2 receptor in the distal nephron and causes a massive increase in diuresis, thereby suppressing the renal cAMP production and its stimulatory effect on cyst growth [7].

The sodium-glucose cotransporters (SGLTs) are a family of membrane proteins which are involved in the transepithelial transport of glucose in the kidneys and the gut. Within the kidney, SGLT1 is located in the S3 segment of the proximal renal tubule, whereas SGLT2 is found in the S1 segment [8]. SGLT1 is a low-capacity, high-affinity sodium-glucose cotransporter, responsible for 10% of glucose reabsorption, whereas SGLT2 is a high-capacity, low-affinity transporter which mediates 90% of glucose reabsorption [9]. The pharmacological inhibition of SGLTs leads to glucosuria which is accompanied by a constant increase in diuresis. In analogy to the tolvaptan-induced increase in diuresis which has beneficial effects in PKD we speculated that the increase in diuresis which is caused by SGLT inhibitors could also decrease cyst growth in PKD. In a previous study, we have already demonstrated that phlorizin, a dual SGLT1/2 inhibitor, reduced cyst growth and slowed the decline of renal function in the Han:SPRD rat model of PKD [10]. The inhibition of SGLTs was associated with a decrease in ERK1/2 phosphorylation and tubular epithelial cell (TEC) proliferation in the polycystic kidneys.

Dapagliflozin (DAPA) is a selective SGLT2 inhibitor that is clinically used to control glycemia in patients with type 2 diabetes mellitus [11]. DAPA is well absorbed when given by the oral route, whereas phlorizin needs to be applied parenterally since it is only minimally absorbed when applied orally [12]. By causing glucosuria, DAPA effectively corrects hyperglycemia and reduces hemoglobin A_{1c} in patients with type 2 diabetes mellitus [13]. We hypothesized that - similar to phlorizin - DAPA might also have a therapeutic effect in PKD. The purpose of the present study was therefore to assess whether DAPA can reduce cyst growth and improve renal function in heterozygous (Cy/+) Han:SPRD rats.

Materials and Methods

Animals

The Han:SPRD rat colony was established in our animal facility from a litter which was obtained from the Rat Resource and Research Center (Columbia, MO, USA). Heterozygous cystic (Cy/+) and wild-type normal (+/+) rats were used in this study. Only male rats were used since cysts develop more rapidly in male than in female rats. The regulatory commission for animal studies, a local government agency, approved the study protocol. Rats had free access to tap water and standard rat diet.

Study design

Treatment was started in 5-week old male Cy/+ and wild-type +/+ control Han:SPRD rats. Groups of 8-9 rats were used. DAPA was dissolved in 45% propylene glycol + 45% H_2O + 10% ethanol and was

given daily by gavage at a dose of 10 mg/kg for 5 weeks. Control rats were treated with vehicle (45% propylene glycol + 45% H_2O + 10% ethanol) alone. Blood and 24 h urines were collected from each animal at baseline (before treatment), and after 2.5 and 5 weeks of treatment. Blood was taken from the sublingual vein, centrifuged and the plasma collected. Urines were collected in metabolic cages over a 24 h period. All samples were stored at -80°C prior to further examination. In the plasma glucose, creatinine, blood urea nitrogen (BUN), sodium and chloride concentrations were determined, and the urine was tested for glucose, creatinine and BUN concentrations, using standard clinical chemistry methods. After 5 weeks of treatment, rats were euthanatized with isoflurane (Attane, Piramal Healthcare Limited, India) and both kidneys were excised, decapsulated, weighed and fixed in 10% buffered formalin for 2 days for histological analysis.

Urine albumin determination

A rat albumin ELISA kit was used for the measurement of urine albumin concentration (GenWay, San Diego, California). The urine samples were diluted 500 times in the diluent solution. Albumin standard or urine sample were added to the pre-coated plates (100 µl/well). Plates were incubated for 30 min at room temperature and washed 4 times thereafter with phosphate-buffered saline (PBS). Plates were then incubated with horseradish peroxidase-conjugated anti-albumin solution for 30 min at room temperature in the dark, and washed again 4 times. Then 100 µl 3,3′,5,5′-tetramethylbenzidine substrate solution was added into each well, and plates were incubated in the dark for 10 min at room temperature. Then 100 µl stop solution was added, mixed well, and the absorbance at 450 nm was determined using a Tecan ELISA reader (Tecan Group Ltd, Männedorf, Switzerland).

Histology and immunohistology

One kidney was longitudinally cut in half and approximately 2 mm thick slices were embedded in paraffin wax. Consecutive sections (3-5 µm) were prepared and stained with hematoxylin-eosin, the PAS reaction and Gomori's Blue Trichrome using the Artisan Link stainer (Dako, Baar, Switzerland).

Immunohistology was used to stain for Ki67-positive (proliferating) TEC and CD68-positive infiltrating macrophages, using a Dako Autostainer (Dako) and the streptavidin horseradish peroxidase (HRP) method. After deparaffinization and rehydration, sections were incubated in citrate buffer (pH 6.0) for 20 min at 95°C in a pressure cooker. After washing in TBS-Tween, slides were incubated for 60 min at room temperature with the primary antibodies (mouse anti-rat Ki67 [clone MIB-5, Dako], mouse anti-rat CD68 [clone ED1, AbD Serotec, Kidlington, UK]) at a dilution of 1:10 and 1:500 in dilution buffer (Dako), respectively. This was followed by incubation with the secondary antibody for 15 min, the peroxidase blocking solution for 10 min, and the streptavidin HRP for 15 min. After washing, the reaction was visualized by incubation with 3, 3'-diaminobenzidine for 10 min, followed by counterstaining with hemalaun (Merck, Darmstadt, Germany).

Histomorphometry

PAS-stained sections were subjected to cyst index analysis, using the HistoQuant image analysis software (3DHISTECH Kft., Budapest, Hungary) to assess the cortical cystic area (CCA) within the entire cortex (total area, TA). The cyst index was calculated as CCA/TA*100. We counted the total number of cysts detected in 2 full longitudinal sections of each kidney and then averaged the total number of cysts. We calculated the area of each cyst, then counted and arranged them by size. For each section stained for the expression of Ki67, the total number of Ki67-positive nuclei was counted, from which an average number of Ki67-positive nuclei per mm^2 of tissue was calculated. For each section stained for the expression of CD68, the total number of CD68-positive cells was counted, from which an average number of CD68-positive nuclei per mm^2 of tissue was calculated. The extent of fibrosis was determined on Gomori's Blue Trichrome stained sections by measuring the collagen stained area in mm^2 and dividing it by the total area of tissue in mm^2.

Statistical analysis

Data are presented as means ± SD. Statistical differences between treatment groups were assessed by the unpaired two-tailed t-test using Graph Pad Prism version 5.0 (Graph Pad, San Diego, CA, USA). $P < 0.05$ was considered to be statistically significant.

Results

DAPA induced glucosuria and increased diuresis

Treatment with DAPA effectively induced glucosuria and increased the urine output in Cy/+rats (Table 1). Alongside the increased diuresis, an increase in water intake was observed with DAPA treatment. The body weight gain was not altered with DAPA in Cy/+. A mild increase in urine Na^+ and Cl^- was seen upon treatment with DAPA in Cy/+ (Table 1).

DAPA preserved the decline of the creatinine and BUN clearances in Cy/+rats

With increasing age, the clearances for creatinine and BUN increased in VEH- and DAPA-treated +/+ rats to a similar level (Table 2). In VEH-treated Cy/+ rats, creatinine and BUN clearances decreased during the 5-week treatment phase, in parallel with the development of renal cysts. In contrast, DAPA treatment in Cy/+ rats led to preservation of the creatinine and BUN clearances at 2.5 and 5 weeks of treatment (Table 3).

DAPA reduced albuminuria in Cy/+rats

Albuminuria increased signi cantly in VEH-treated Cy/+ rats between baseline and week 5. However, DAPA-treated Cy/+ rats showed a signi cantly lower urine albumin excretion than the VEH-treated rats after 5 weeks of treatment (Table 1).

Table 1. Effects of DAPA on body weight, diuresis, and uid and electrolyte parameters in Cy/+rats. Results are expressed as mean ± SD. Comparisons are made between DAPA and VEH groups at the same time point. Abbreviations: VEH, vehicle; DAPA, dapagli ozin; P, plasma; U, urine. *P < 0.05, ** P < 0.01, ***P < 0.001 when comparing DAPA vs. VEH at each time point

	Baseline		2.5 weeks			5 weeks		
	Cy/+ VEH	Cy/+ DAPA	Cy/+ VEH	Cy/+ DAPA		Cy/+ VEH	Cy/+ DAPA	
Number of animals (n)	9	9	9	9		9	9	
Body weight (g)	152.1 ± 12.9	174.6 ± 42.3	278.2 ± 18.9	278.7 ± 31.6		340.5 ± 26.1	341.0 ± 30.9	
Urine volume (ml/day)	10.2 ± 2.5	10.4 ± 7.1	18.2 ± 6.6	35.9 ± 8.4	**	27.5 ± 5.4	42.7 ± 7.0	***
Water intake (ml/day)	30.0 ± 4.4	29.3 ± 8.4	44.2 ± 6.3	62.9 ± 8.1	***	55.6 ± 10.8	75.7 ± 11.0	**
P glucose (mmol/l)	9.0 ± 0.9	9.9 ± 0.6	9.9 ± 1.3	10.2 ± 1.8		13.9 ± 3.2	12.8 ± 2.5	
P Na^+(mmol/l)	139.8 ± 1.3	143.0 ± 4.0	136.0 ± 14.6	139.6 ± 11.1		142.1 ± 1.5	143.4 ± 6.8	
P Cl^- (mmol/l)	103.0 ± 1.0	100.6 ± 3.8	98.1 ± 12.3	96.3 ± 12.0		99.9 ± 6.2	96.9 ± 6.2	
U glucose (mmol/day)	0.0 ± 0.0	0.0 ± 0.0	0.2 ± 0.3	11.8 ± 3.4	***	0.2 ± 0.0	15.8 ± 4.5	***
U Na^+ (mmol/day)	0.9 ± 0.1	1.2 ± 0.9	1.1 ± 0.2	1.3 ± 0.3		1.3 ± 0.4	1.7 ± 0.3	*
U Cl^- (mmol/day)	1.6 ± 0.3	2.0 ± 1.4	1.8 ± 0.4	2.0 ± 0.5		1.9 ± 0.4	2.5 ± 0.4	*
U albumin (µg/day)	0.1 ± 0.0	0.1 ± 0.1	0.4 ± 0.1	0.5 ± 0.3		3.8 ± 0.9	2.2 ± 0.4	**

Table 2. Effect of DAPA on parameters of renal function in +/+ rats. Results are expressed as mean ± SD. Comparisons are made between DAPA and VEH groups at the same time point. Abbreviations: BUN, blood urea nitrogen; VEH, vehicle; DAPA, dapagli ozin; P, plasma; U, urine. *P < 0.05, ***P < 0.001 when comparing DAPA vs. VEH at each time point

	Baseline		2.5 weeks			5 weeks		
	+/+ VEH	+/+ DAPA	+/+ VEH	+/+ DAPA		+/+ VEH	+/+ DAPA	
Number of animals (n)	8	9	8	9		8	9	
P BUN (urea) (mg/dl)	17.6 ± 2.1	15.5 ± 1.8	17.1 ± 1.9	23.0 ± 3.4	***	18.7 ± 1.2	28.0 ± 12.1	*
P creatinine (mg/dl)	0.3 ± 0.0	0.3 ± 0.1	0.3 ± 0.0	0.3 ± 0.1		0.4 ± 0.0	0.4 ± 0.1	
BUN clearance (ml/min)	0.6 ± 0.1	0.8 ± 0.3	0.9 ± 0.1	0.9 ± 0.1		1.1 ± 0.1	1.2 ± 0.5	
Creatinine clearance (ml/min)	1.7 ± 0.3	1.2 ± 0.8	2.2 ± 0.2	2.1 ± 0.5		2.6 ± 0.3	2.9 ± 0.1	

Table 3. Effect of DAPA on parameters of renal function in Cy/+ rats. Results are expressed as mean ± SD. Comparisons are made between DAPA and VEH groups at the same time point. Abbreviations: BUN, blood urea nitrogen; VEH, vehicle; DAPA, dapagli□ozin; P, plasma; U, urine. ** P < 0.01, *** P < 0.001 when comparing DAPA vs. VEH at each time point

	Baseline		2.5 weeks		5 weeks		
	Cy/+ VEH	Cy/+ DAPA	Cy/+ VEH	Cy/+ DAPA	Cy/+ VEH	Cy/+ DAPA	
Number of animals (n)	9	9	9	9	9	9	
P BUN(urea) (mg/dl)	23.2 ± 11.5	14.8 ± 4.1	25.5 ± 7.8	25.8 ± 4.0	41.7 ± 6.9	32.8 ± 11.6	
P creatinine (mg/dl)	0.3 ± 0.1	0.2 ± 0.2	0.4 ± 0.1	0.4 ± 0.0	0.6 ± 0.1	0.4 ± 0.0	**
BUN clearance (ml/min)	0.6 ± 0.2	0.9 ± 0.5	0.6 ± 0.1	0.7 ± 0.3	0.5 ± 0.1	0.9 ± 0.3	**
Creatinine clearance (ml/min)	1.9 ± 0.3	1.7 ± 1.0	1.8 ± 0.5	2.0 ± 0.3	1.5 ± 0.5	2.3 ± 0.2	***

Table 4. Effect of DAPA on kidney weight in 10-week old +/+ and Cy/+ rats after 5 weeks of treatment. Results are expressed as mean ± SD. Comparisons are made between DAPA and VEH groups at the same time point. Abbreviations: VEH, vehicle; DAPA, dapagli□ozin; 2KW, two-kidneys weight; BW, body weight. ** P < 0.01, ***P < 0.001 when comparing DAPA vs. VEH at each time point

	+/+ VEH	+/+ DAPA		Cy/+ VEH	Cy/+ DAPA	
Number of animals (n)	8	9		9	9	
Kidney Weight (g)	2.3 ± 0.2	3.1 ± 0.3	***	6.8 ± 0.9	8.0 ± 1.3	
2KW/BW (%)	0.7 ± 0.0	0.9 ± 0.1	**	2.0 ± 0.2	2.3 ± 0.2	**

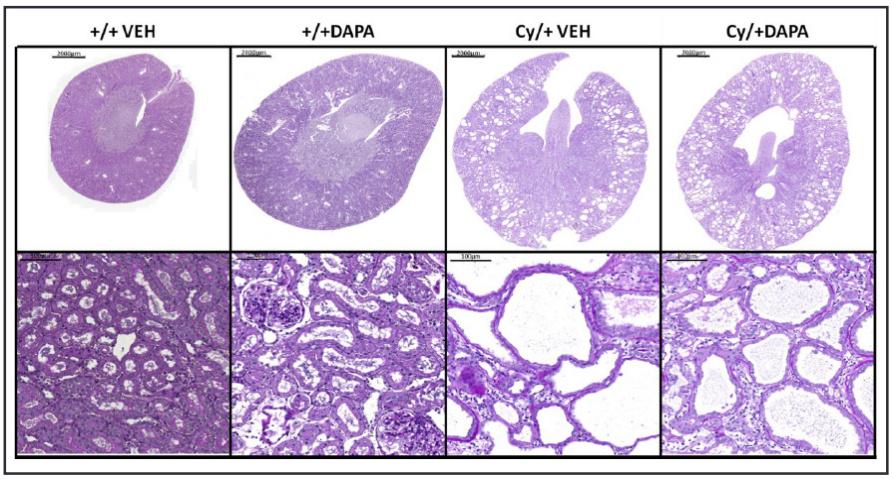

Fig. 1. PAS staining of kidney sections. Sections are from 10 week old Cy/+ and +/+ rats treated with DAPA or VEH for 5 weeks; scale bar is 2000 µm in upper images and 100 µm in lower images.

DAPA increased kidney weight without effect on cyst growth

In +/+ and Cy/+ rats, treatment with DAPA for 5 weeks led to a signi□icant increase in the kidney weight and the 2-kidneys/body weight ratio (2KW/BW) compared to VEH-treated rats (Table 4). The histological examination of the kidneys revealed a slightly higher amount of non-cystic parenchyma but a similar cyst burden in DAPA-treated Cy/+ rats (Fig. 1). Histomorphometric quanti□ication of the cyst burden revealed a similar cyst index in DAPA- and VEH-treated Cy/+ rats (20.3 ± 1.4 vs 21.9 ± 1.2%, P = 0.55) (Fig. 2A), a similar total number of cysts (1056 ± 225 vs. 994 ± 229, P = 0.67; Fig. 2B) and a similar size pro□ile of the cysts (Fig. 2C). Altogether these data suggests that there was a higher amount of non-cystic tissue in DAPA-treated Cy/+ rats.

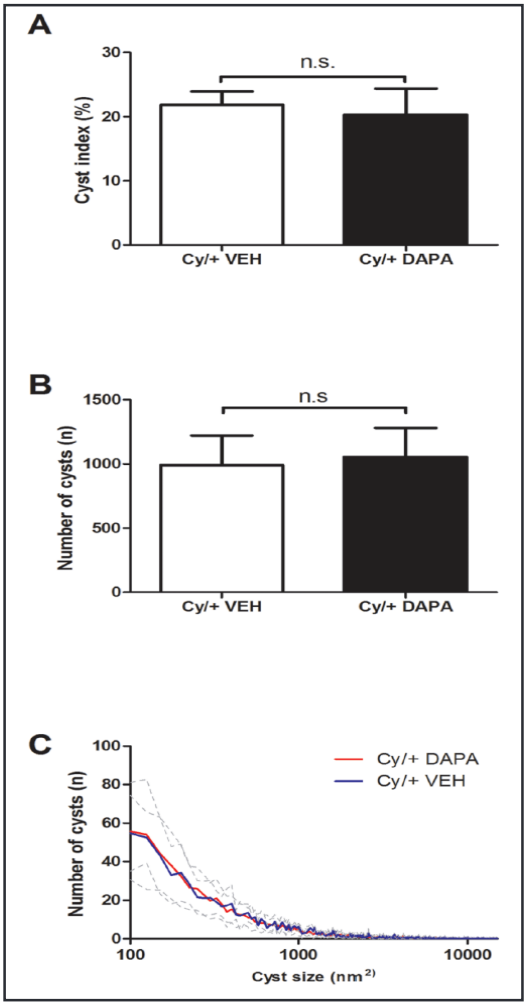

Fig. 2. Histomorphometric analysis of cyst growth. PAS-stained kidney sections of 10 week old Cy/+ rats treated with DAPA or VEH for 5 weeks. (A) Cyst index (%). (B) Number of cysts (n). (C) Cyst classification by size, grey lines represent ranges for ± 1 SD.

DAPA had no effect on renal tubular epithelial cell proliferation

The immunohistological staining for Ki67-positive tubular epithelial cells (TEC) showed that the number of Ki67-positive TECs was higher in Cy/+ than +/+ rats, suggesting enhanced TEC proliferation in Cy/+ rats (Fig. 3). The difference in the number of Ki67-positive TECs between DAPA- and VEH-treated +/+ rats was not significant (139 ± 87 vs. 163 ± 63 cells/ mm^2, P = 0.67). DAPA-treated Cy/+ rats exhibited less proliferating TECs than VEH-treated animals (237 ± 109 vs. 327±60 Ki67-positive cells/ mm^2), but the difference was also not significant (P=0.28) (Fig. 4A).

DAPA had no effect on renal macrophages infiltration

The degree of infiltration with macrophages was assessed by staining kidney sections for CD68. The number of CD68-positive cells was significantly higher in Cy/+ compared to +/+ rats (20 ± 8 vs. 11 ± 6 CD68-positive cells/ mm^2, P = 0.03). However, there was no difference between DAPA- and VEH-treated Cy/+ rats (19 ± 8 vs. 20 ± 8 ED-1-positive cells/ mm^2, P = 0.85) (Fig. 4B).

DAPA had no effect on interstitial fibrosis

Using Gomori's Blue Trichrome staining we quantified the degree of renal interstitial fibrosis in Cy/+ and +/+ rats. The renal collagen index was slightly higher in Cy/+ vs. +/+ rat kidneys (5.3 ± 2.0 vs. 4.0 ± 0.8%, P = 0.12). DAPA treatment did not significantly change the collagen index in +/+ (2.9 ± 1.7 vs. 4.0 ± 0.8%, P = 0.11) and Cy/+ rats (4.5 ± 1.8 vs. 5.3 ± 2.0%, P = 0.46) (Fig. 4C).

Discussion

Increasing water intake and diuresis was shown to have beneficial effects on the cystic disease progression in different rodent models of PKD [14-17]. The increased water intake suppresses vasopressin and reduces the translocation of aquaporin 2 from intracellular vesicles to the luminal membrane of the collecting duct, leading to increased diuresis [18]. Furthermore, in the case of PKD, inhibiting vasopressin with tolvaptan at the level of the V_2 receptor in the collecting duct also increases diuresis and reduces intrarenal cAMP, thereby inhibiting cyst epithelial cell proliferation via MAP kinase [19]. The pharmacological inhibition of SGLTs leads to glucosuria which is also accompanied by a significant increase in

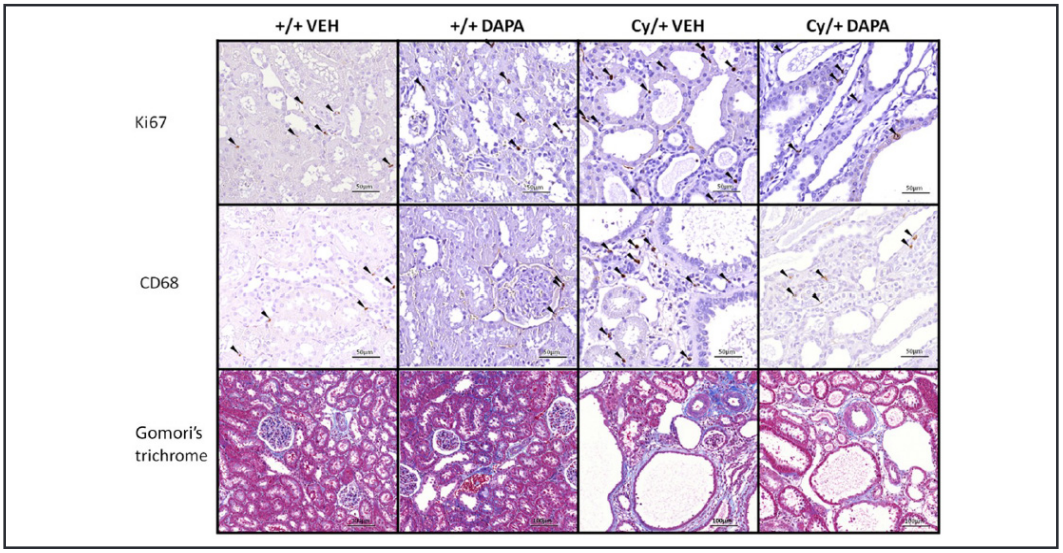

Fig. 3. Histological analysis for Ki67, CD68 and interstitial fibrosis. Kidney sections were analyzed for TEC proliferation (immunostaining for Ki67), macrophage infiltration (immunostaining for CD68) and interstitial fibrosis (Gomori's Blue Trichrome). Arrowheads mark Ki67- or CD68-positive cells. Scale bar is 50 μm for Ki67 and CD68 stainings, and 100 μm in Gomori's Blue Trichrome staining.

Fig. 4. Histomorphometric analysis for Ki67, CD68 and interstitial fibrosis. (A) Ki67 quantification (Ki67-positive cells/ mm²). (B) CD68 quantification (CD68-positive cells/ mm²). (C) Fibrosis quantification (collagen index in %).

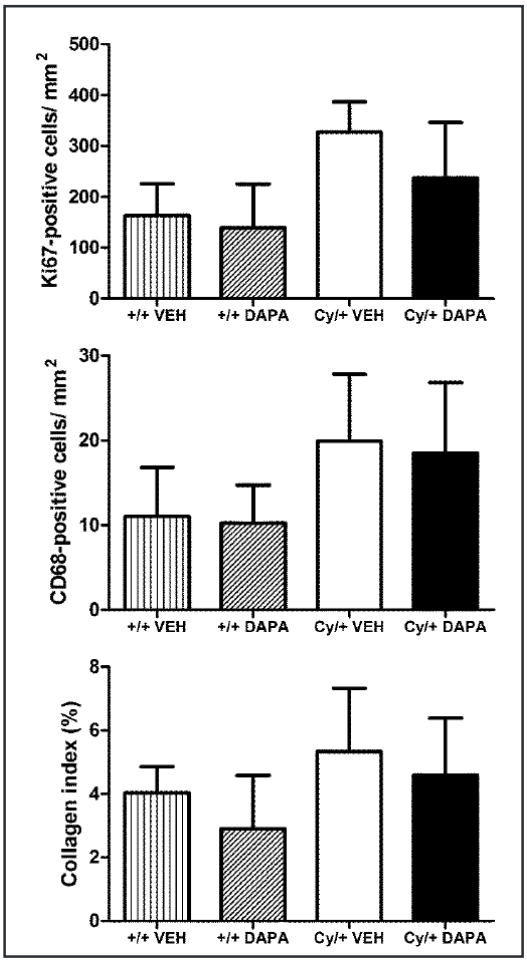

diuresis. In analogy to the tolvaptan-induced increase in diuresis which has beneficial effects in PKD we speculated that the increase in diuresis which is caused by SGLT inhibitors could also decrease cyst growth in PKD. Thus, by inducing osmotic diuresis and increasing urinary flow to the collecting duct with the SGLT1/2 inhibitor phlorizin, we recently have shown that cyst growth, renal function and albuminuria improved in the Han:SPRD rat model of PKD [10].

In the present study, we examined the effect of DAPA, a selective SGLT2 inhibitor, on the cystic disease process in Han: SPRD rats. DAPA effectively induced glucosuria and osmotic diuresis but was less potent than the previously tested phlorizin. While DAPA improved the decline of renal function and improved albuminuria it did not decrease cyst growth, macrophage infiltration and interstitial fibrosis in Han: SPRD rats. All in all, the beneficial effects of the SGLT2-selective inhibitor DAPA appeared to be

limited in Cy/+ rats, and are in contrast to the more important effects of the dual SGLT1/2 inhibitor phlorizin.

Of interest, DAPA led an unexpected kidney enlargement which was not due to an increase in the cyst growth. An increase of kidney weight has also been noticed in Sglt2 -/- knockout mice [20]. Although we do not know the mechanisms behind this increase in kidney weight our histological analysis suggests that it is most likely caused by widening of the tubular lumen due to the increased diuresis. In addition there may also be a certain degree of tubular hypertrophy which could be related to an increase of the SGLT1-mediated glucose reabsorption in the S2 and S3 segment of the proximal tubules [21]. In a different setting, namely in SGLT1-transfected cardiomyocytes a hypertrophic response has also been noticed, suggesting that SGLT1-mediated enhanced glucose uptake may indeed affect cell size [22].

DAPA was developed as a selective SGLT2 inhibitor [23-25] and is in clinical use for the control of glycemia in patients with type 2 diabetes [26, 27]. Since DAPA is also known to increase diuresis [25-28], and given its oral availability and its favorable safety profile [29, 30], we felt that it might be a potentially useful drug to retard disease progression in patients with ADPKD. With DAPA's effect of increasing osmolality along the nephron we speculated that DAPA might also rebalance the transport of fluid across the cyst epithelium, thereby preventing cyst expansion. As mentioned, DAPA was a less effective glucosuric agent than phlorizin and it did not inhibit cyst growth in the Han:SPRD rat model of PKD in the present study, presumably because much of the glucose is reabsorbed by the uninhibited SGLT1 in the proximal tubule [21].

To be effective in PKD, it would be desirable to develop a less selective SGLT inhibitor, displaying strong inhibition of SGLT2 and partial inhibition of SGLT1. This would decrease the SGLT1-mediated glucose reabsorption and enhance the urinary glucose excretion. Ideally such a drug should be orally available, and should not block SGLT1 in the gut completely which might cause glucose-galactose malabsorption and diarrhea [31]. The development of dual SGLT1/2 inhibitors would of course also be predicted to have stronger effects on glycemic control in patients with type 2 diabetes [32].

We recently tested DAPA in PCK rats, an orthologous model of autosomal recessive PKD (ARPKD) [33]. Whereas Han:SPRD rats develop cysts of proximal tubular origin in the cortex, PCK rats develop cysts of distal tubular origin in the medulla. Quite unexpectedly, we found that DAPA led to an increase of the cyst growth in PCK rats. Furthermore the DAPA-treated PCK rats displayed hyperfiltration and albuminuria, eventually accelerating the decline in renal function. Although the renal function was improved with DAPA in Han:SPRD rats we did not find evidence for hyperfiltration, particularly since albuminuria was improved. Altogether the data suggest that DAPA has PKD model-specific effects, and that the effect in human ADPKD could be unpredictable.

Conclusion

The SGLT2-selective inhibitor DAPA improved the decline of renal function and the extent of albuminuria in Han:SPRD rats with PKD, but it did not have a significant effect on cyst growth and secondary renal parenchymal alterations such as macrophage infiltration and fibrosis. Dual SGLT1/2 inhibitors with a stronger glucosuric effect are under development and should be considered for future testing in PKD.

Acknowledgements

The authors are grateful to Sabina Wunderlin (Histology Laboratory, Institute of Veterinary Pathology, Vetsuisse Faculty, University of Zürich), for excellent technical

assistance. We thank Petra Seebeck, Svende Pfundstein and Stefanie Weinreich (Zürich Integrative Rodent Physiology, University of Zürich) for their professional help with the animal work. This study was supported by the Swiss National Science Foundation (320030_144093 to RPW), the Novartis Foundation and the Hartmann-Müller Foundation.

Disclosure Statement

The authors declare that they have no competing financial interest in the work presented here.

References

1 Torres VE, Harris PC: Autosomal dominant polycystic kidney disease: The last 3 years. Kidney Int 2009;76:149-168.
2 Torres VE, Harris PC, Pirson Y: Autosomal dominant polycystic kidney disease. Lancet 2007;369:1287-1301.
3 Gallagher AR, Germino GG, Somlo S: Molecular advances in autosomal dominant polycystic kidney disease. Adv Chronic Kidney Dis 2010;17:118-130.
4 Hopp K, Ward CJ, Hommerding CJ, Nasr SH, Tuan HF, Gainullin VG, Rossetti S, Torres VE, Harris PC: Functional polycystin-1 dosage governs autosomal dominant polycystic kidney disease severity. J Clin Invest 2012;122:4257-4273.
5 Grantham JJ, Torres VE, Chapman AB, Guay-Woodford LM, Bae KT, King BF, Jr., Wetzel LH, Baumgarten DA, Kenney PJ, Harris PC, Klahr S, Bennett WM, Hirschman GN, Meyers CM, Zhang X, Zhu F, Miller JP; CRISP Investigators: Volume progression in polycystic kidney disease. N Engl J Med 2006;354:2122-2130.
6 Wuthrich RP, Mei C: Pharmacological management of polycystic kidney disease. Expert Opin Pharmacother 2014;15:1085-1095.
7 Rinschen MM, Schermer B, Benzing T: Vasopressin-2 receptor signaling and autosomal dominant polycystic kidney disease: From bench to bedside and back again. J Am Soc Nephrol 2014;25:1140-1147.
8 Neumiller JJ, White JR, Jr., Campbell RK: Sodium-glucose co-transport inhibitors: Progress and therapeutic potential in type 2 diabetes mellitus. Drugs 2010;70:377-385.
9 Bakris GL, Fonseca VA, Sharma K, Wright EM: Renal sodium-glucose transport: Role in diabetes mellitus and potential clinical implications. Kidney Int 2009;75:1272-1277.
10 Wang X, Zhang S, Liu Y, Spichtig D, Kapoor S, Koepsell H, Mohebbi N, Segerer S, Serra AL, Rodriguez D, Devuyst O, Mei C, Wuthrich RP: Targeting of sodium-glucose cotransporters with phlorizin inhibits polycystic kidney disease progression in Han:SPRD rats. Kidney Int 2013;84:962-968.
11 List JF, Woo V, Morales E, Tang W, Fiedorek FT: Sodium-glucose cotransport inhibition with dapagli lozin in type 2 diabetes. Diabetes Care 2009;32:650-657.
12 Marsenic O: Glucose control by the kidney: An emerging target in diabetes. Am J Kidney Dis 2009;53:875-883.
13 Rosenstock J, Vico M, Wei L, Salsali A, List JF: Effects of dapagli lozin, an SGLT2 inhibitor, on HbA_{1c}, body weight, and hypoglycemia risk in patients with type 2 diabetes inadequately controlled on pioglitazone monotherapy. Diabetes Care 2012;35:1473-1478.
14 Gattone VH, 2nd, Wang X, Harris PC, Torres VE: Inhibition of renal cystic disease development and progression by a vasopressin V_2 receptor antagonist. Nat Med 2003;9:1323-1326.
15 Hopp K, Wang X, Ye H, Irazabal MV, Harris PC, Torres VE: Effects of hydration in rats and mice with polycystic kidney disease. Am J Physiol Renal Physiol 2015;308:F261-266.
16 Nagao S, Nishii K, Katsuyama M, Kurahashi H, Marunouchi T, Takahashi H, Wallace DP: Increased water intake decreases progression of polycystic kidney disease in the PCK rat. J Am Soc Nephrol 2006;17:2220-2227.
17 Wang X, Wu Y, Ward CJ, Harris PC, Torres VE: Vasopressin directly regulates cyst growth in polycystic kidney disease. J Am Soc Nephrol 2008;19:102-108.

18 Nielsen S, Chou CL, Marples D, Christensen EI, Kishore BK, Knepper MA: Vasopressin increases water permeability of kidney collecting duct by inducing translocation of aquaporin-CD water channels to plasma membrane. Proc Natl Acad Sci U S A 1995;92:1013-1017.
19 Devuyst O, Torres VE: Osmoregulation, vasopressin, and cAMP signaling in autosomal dominant polycystic kidney disease. Curr Opin Nephrol Hypertens 2013;22:459-470.
20 Vallon V, Rose M, Gerasimova M, Satriano J, Platt KA, Koepsell H, Cunard R, Sharma K, Thomson SC, Rieg T: Knockout of Na-glucose transporter SGLT2 attenuates hyperglycemia and glomerular hyper ltration but not kidney growth or injury in diabetes mellitus. Am J Physiol Renal Physiol 2013;304:F156-167.
21 Abdul-Ghani MA, DeFronzo RA, Norton L: Novel hypothesis to explain why SGLT2 inhibitors inhibit only 30-50% of ltered glucose load in humans. Diabetes 2013;62:3324-3328.
22 Ramratnam M, Sharma RK, D'Auria S, Lee SJ, Wang D, Huang XY, Ahmad F: Transgenic knockdown of cardiac sodium/ glucose cotransporter 1 (SGLT1) attenuates PRKAG2 cardiomyopathy, whereas transgenic overexpression of cardiac SGLT1 causes pathologic hypertrophy and dysfunction in mice. J Am Heart Assoc 2014;3:e000899.
23 Meng W, Ellsworth BA, Nirschl AA, McCann PJ, Patel M, Girotra RN, Wu G, Sher PM, Morrison EP, Biller SA, Zahler R, Deshpande PP, Pullockaran A, Hagan DL, Morgan N, Taylor JR, Obermeier MT, Humphreys WG, Khanna A, Discenza L, Robertson JG, Wang A, Han S, Wetterau JR, Janovitz EB, Flint OP, Whaley JM, Washburn WN: Discovery of dapagli ozin: A potent, selective renal sodium-dependent glucose cotransporter 2 (SGLT2) inhibitor for the treatment of type 2 diabetes. J Med Chem 2008;51:1145-1149.
24 Obermeier M, Yao M, Khanna A, Koplowitz B, Zhu M, Li W, Komoroski B, Kasichayanula S, Discenza L, Washburn W, Meng W, Ellsworth BA, Whaley JM, Humphreys WG: In vitro characterization and pharmacokinetics of dapagli ozin (BMS-512148), a potent sodium-glucose cotransporter type 2 inhibitor, in animals and humans. Drug Metab Dispos 2010;38:405-414.
25 Yao CH, Song JS, Chen CT, Yeh TK, Hung MS, Chang CC, Liu YW, Yuan MC, Hsieh CJ, Huang CY, Wang MH, Chiu CH, Hsieh TC, Wu SH, Hsiao WC, Chu KF, Tsai CH, Chao YS, Lee JC: Discovery of novel N-beta-D-xylosylindole derivatives as sodium-dependent glucose cotransporter 2 (SGLT2) inhibitors for the management of hyperglycemia in diabetes. J Med Chem 2011;54:166-178.
26 Bailey CJ, Gross JL, Pieters A, Bastien A, List JF: Effect of dapagli ozin in patients with type 2 diabetes who have inadequate glycaemic control with metformin: A randomised, double-blind, placebo-controlled trial. Lancet 2010;375:2223-2233.
27 Calado J: Dapagli ozin, an oral sodium glucose cotransporter type 2 inhibitor for the treatment of type 2 diabetes mellitus. IDrugs 2009;12:785-798.
28 Maliha G, Townsend RR: SGLT2 inhibitors: Their potential reduction in blood pressure. J Am Soc Hypertens 2015;9:48-53.
29 Anderson SL: Dapagli ozin ef cacy and safety: A perspective review. Ther Adv Drug Saf 2014;5:242-254.
30 Plosker GL: Dapagli ozin: A review of its use in patients with type 2 diabetes. Drugs 2014;74:2191-2209.
31 Wright EM, Loo DD, Hirayama BA: Biology of human sodium glucose transporters. Physiol Rev 2011;91:733-794.
32 Gallo LA, Wright EM, Vallon V: Probing SGLT2 as a therapeutic target for diabetes: Basic physiology and consequences. Diab Vasc Dis Res 2015;12:78-89.
33 Kapoor S, Rodriguez D, Riwanto M, Edenhofer I, Segerer S, Mitchell K, Wuthrich RP: Effect of sodium-glucose cotransport inhibition on polycystic kidney disease progression in PCK rats. PLoS One 2015;10:e0125603.

Chapter 4

Effect of sodium-glucose cotransport inhibition on polycystic kidney disease progression in PCK rats

Sarika Kapoor[1,2], Daniel Rodriguez[1,2], Meliana Riwanto[1,2], Ilka Edenhofer[1,2], Stephan Segerer[1,2], Katharyn Mitchell[3] and Rudolf P. Wüthrich[1,2]

[1] Division of Nephrology, University Hospital, Zürich, Switzerland,
[2] Institute of Physiology, University of Zürich, Zürich, Switzerland,
[3] Clinic for Equine Internal Medicine, Vetsuisse Faculty, University of Zürich, Zürich, Switzerland

PLoS ONE 10(4): e0125603

Contribution by Daniel Rodriguez:

Animal treatment, histological analysis, statistical analyses (t-test comparisons) and interpretation of data.

PLOS | ONE

RESEARCH ARTICLE

Effect of Sodium-Glucose Cotransport Inhibition on Polycystic Kidney Disease Progression in PCK Rats

Sarika Kapoor[1,2], Daniel Rodriguez[1,2], Meliana Riwanto[1,2], Ilka Edenhofer[1,2], Stephan Segerer[1,2], Katharyn Mitchell[3], Rudolf P. Wüthrich[1,2]*

1 Division of Nephrology, University Hospital, Zürich, Switzerland, 2 Institute of Physiology, University of Zürich, Zürich, Switzerland, 3 Clinic for Equine Internal Medicine, Vetsuisse Faculty, University of Zürich, Zürich, Switzerland

* rudolf.wuethrich@usz.ch

Citation: Kapoor S, Rodriguez D, Riwanto M, Edenhofer I, Segerer S, Mitchell K, et al. (2015) Effect of Sodium-Glucose Cotransport Inhibition on Polycystic Kidney Disease Progression in PCK Rats. PLoS ONE 10(4): e0125603. doi:10.1371/journal.pone.0125603

Academic Editor: Eric Feraille, University of Geneva, SWITZERLAND

Received: January 15, 2015

Accepted: March 24, 2015

Published: April 30, 2015

Data Availability Statement: All relevant data are within the paper.

Funding: Supported by the Swiss National Science Foundation (grant number 320030_144093 to RPW) and by the Hartmann Müller Foundation (to SK). The funders had no role in study design, data collection and analysis, decision to publish, or preparation of the manuscript.

Competing Interests: The authors have declared that no competing interests exist.

Abstract

The sodium-glucose-cotransporter-2 (SGLT2) inhibitor dapagliflozin (DAPA) induces glucosuria and osmotic diuresis via inhibition of renal glucose reabsorption. Since increased diuresis retards the progression of polycystic kidney disease (PKD), we investigated the effect of DAPA in the PCK rat model of PKD. DAPA (10 mg/kg/d) or vehicle was administered by gavage to 6 week old male PCK rats (n=9 per group). Renal function, albuminuria, kidney weight and cyst volume were assessed after 6 weeks of treatment. Treatment with DAPA markedly increased glucose excretion (23.6 ± 4.3 vs 0.3 ± 0.1 mmol/d) and urine output (57.3 ± 6.8 vs 19.3 ± 0.8 ml/d). DAPA-treated PCK rats had higher clearances for creatinine (3.1 ± 0.1 vs 2.6 ± 0.2 ml/min) and BUN (1.7 ± 0.1 vs 1.2 ± 0.1 ml/min) after 3 weeks, and developed a 4-fold increase in albuminuria. Ultrasound imaging and histological analysis revealed a higher cyst volume and a 23% higher total kidney weight after 6 weeks of DAPA treatment. At week 6 the renal cAMP content was similar between DAPA and vehicle, and staining for Ki67 did not reveal an increase in cell proliferation. In conclusion, the inhibition of glucose reabsorption with the SGLT2-specific inhibitor DAPA caused osmotic diuresis, hyperfiltration, albuminuria and an increase in cyst volume in PCK rats. The mechanisms which link glucosuria to hyperfiltration, albuminuria and enhanced cyst volume in PCK rats remain to be elucidated.

Introduction

Polycystic kidney diseases (PKD) are the most frequent entities among the genetically determined renal syndromes [1]. The autosomal dominant form of PKD (ADPKD) is twenty times more frequent than the autosomal recessive form (ARPKD) [2]. Approximately 5–8% of all patients with end-stage renal disease (ESRD) suffer from ADPKD [3]. Although progress has recently been made in the development of treatments which retard the cystic growth, no therapy was shown to be effective in delaying the occurrence of ESRD [4].

It has been shown that renal cAMP is a major driver of cyst growth in PKD [5]. The excessive cAMP production is a consequence of the genetic defect which underlies PKD [6]. Due to an early loss of the urine concentrating capability the production of vasopressin is upregulated in PKD, stimulating the production of cAMP directly through its V_2 receptor in the distal renal epithelium [7]. Therapeutic strategies which decrease the vasopressin-driven cAMP production have been successful in decreasing renal cyst growth and in slowing the decline of renal function in PKD [8–11]. Thus, treatment of mice, rats and humans with the vasopressin V_2-receptor antagonist tolvaptan [12], crossing PKD rats (PCK strain) with vasopressin-deficient rats (Brattleboro strain) [13], or increasing fluid intake in rats by adding glucose to the drinking water [14] have all been effective to retard PKD disease progression. Patients with ADPKD tend to have a higher urine output because of a renal concentrating defect and a blunted release of vasopressin [15], but presumably also because drinking large amounts of water has been recommended to patients with ADPKD in an attempt to reduce cyst growth [16,17].

As mentioned, the aquaretic drug tolvaptan (vasopressin V_2 receptor antagonist) was shown to have beneficial effects on polycystic kidney disease progression. It is not known whether the induction of osmotic diuresis would also have such a beneficial effect. We have previously shown that the induction of osmotic diuresis by inhibiting renal proximal tubular sodium-glucose cotransport (SGLT) with phlorizin retards cyst growth and renal functional decline in the Han:SPRD rat model of PKD [18]. Phlorizin is a nonselective SGLT inhibitor which inhibits SGLT1 and SGLT2. In recent years, selective SGLT2 inhibitors have been developed and are now in clinical use for the treatment of hyperglycemia in patients with type 2 diabetes mellitus [19]. To evaluate whether the selective inhibition of SGLT2 is capable of retarding cyst volume progression and delaying renal functional loss, we tested the effect of oral dapagliflozin (DAPA) administration in PCK rats, an orthologous model of ARPKD.

Materials and Methods

Ethics statement

All animal work was conducted according to relevant national and international guidelines. The protocol was approved by the committee on the Ethics of Animal Experiments at the University of Zürich (Permit Number: 175–2012). All efforts were made to minimize any suffering to animals.

Animals

PCK rats (an orthologous model of autosomal recessive polycystic kidney disease) and normal Sprague-Dawley (SD) rats were used in this study. PCK rats (originally derived from SD rats) were obtained from Charles River Laboratories (Sulzfeld, Germany) while SD rats were obtained from the Rat Resource and Research Center (Columbia, MO, USA). All rats had free access to tap water and were fed a standard rat diet. Only male rats were used in this study as cysts develop more rapidly in male compared with female rats.

Experimental design

DAPA (Bristol-Myers Squibb, Princeton, New Jersey) was dissolved in a vehicle of polypropylene glycol, water and ethanol (45:45:10, v/v/v). At 5–6 weeks of age, male PCK or normal control SD rats (n = 8–9 per group) were given DAPA (10 mg/kg/d) or vehicle by gavage for 5–6 weeks. The doses of the drug and the vehicle were adjusted daily according to the body weight of the rats. Blood was drawn and 24 h urine was collected at baseline and after 2–3 and 5–6 weeks of treatment to assess different parameters of renal function. At the end of the treatment

phase (at 12 week of age), the PCK rats were examined by ultrasound to determine the kidney and cyst volume *in vivo*. All rats were then sacrificed and the kidneys were excised, decapsulated and weighed to calculate the two kidneys to total body weight (2K/TBW) ratios. Kidney slices were fixed in 10% buffered formalin and were then embedded in paraffin for subsequent histological examinations.

Plasma and urine analyses

Plasma and urine aliquots were rapidly frozen and stored at -80°C until their measurement. Glucose, sodium, chloride, creatinine and blood urea nitrogen (BUN) concentrations were determined in plasma and urine using a Cobas 8000 Modular Analyzer from Roche Diagnostics AG (Rotkreuz, Switzerland). Plasma and urine osmolality were measured by using an Advanced Osmometer Model 2020 (Advanced Instruments Inc., Norwood, MA, USA). The urine protein content was analyzed by SDS-PAGE and Coomassie blue staining, adjusting the loading volumes of the samples to the 24 h urine volume. The GenWay rat albumin ELISA kit (San Diego, CA, USA) was used to measure urine albumin concentration, according to the instructions provided by the manufacturer.

Ultrasound imaging of rat kidneys

PCK rats were anesthetized with isoflurane (1.5–2%) in oxygen. Physiological variables (heart rate, respiratory rate, rectal temperature) were continuously monitored by using a VisualSonics Advanced Physiological Monitoring Unit (Toronto, Ontario, Canada). The abdomen was clipped and all hair was removed using Veet hair removal cream. Acoustic coupling was ensured using ultrasound coupling gel. Ultrasound images of the kidneys were acquired using a high resolution ultrasound system (Vevo 2100, VisualSonics) equipped with a 18–38 MHz probe (MS400). Following image optimization, transverse 2D and power Doppler images of both kidneys were acquired with the aid of an automated 3D motor head. Care was taken to include the cranial and caudal poles of the kidney where possible (maximum scan distance 28 mm). The slice thickness between scanning planes was 0.072 mm with a maximum of 500 slices. The images were captured in digital raw format (RF). Offline processing of 3D reconstructions was performed using Vevo 2100 software (v1.6.0) on a dedicated workstation. The resulting 3D model was used to determine the total kidney and cyst volumes and the number of cysts.

Tissue sectioning, PAS staining, and cystic index determination

For histological examination, one of the kidneys from each rat was sliced perpendicularly to the long axis at approximately 2 mm intervals. Slices from the midportion of the kidneys were fixed in 10% buffered formalin overnight, and tissues were then embedded in paraffin. Three μm sections were stained with periodic acid-Schiff (PAS) following a routine protocol. The stained sections were subjected to cystic index analysis, using the HistoQuest image analysis software (TissueGnostics, Vienna, Austria). The total kidney area (TKA) and the medullary cystic area (MCA) were determined, and the cystic index was calculated in percent as MCA/TKA□100.

Immunohistochemical analysis

Immunohistochemistry for Ki67 was performed on 3 μm tissue sections which were deparaffinized and rehydrated. Antigen retrieval was performed in an autoclave oven. Mouse anti-Ki67 antibody (BD Pharmingen, San Jose, CA, USA) was applied for 1 hour. Sections were washed

and incubated with the biotinylated secondary antibody (Vector Laboratories Inc. Burlingame, CA, USA) for 30 minutes. After washing, the ABC reagent (Vector) was applied to the sections using 3,3'-diaminobenzidine with metal enhancement as the detection reagent. The percentage of Ki-67 positive cells was determined from the total number of cells in cysts and non-cystic tubules from each kidney section. We counted the total number of cells in 10 random fields containing cysts and 10 random fields of non-cystic tissue in each kidney section of each PCK rat using HistoQuest image analysis software (TissueGnostics, Vienna, Austria).

Determination of cAMP content of whole kidneys

The frozen kidneys were ground to fine powder under liquid nitrogen in a stainless steel mortar. After the liquid nitrogen had evaporated, tissue was weighed and homogenized in 10 volumes of 0.1 M HCl. After centrifugation at 600 g for 10 min at room temperature, the supernatants were collected and assayed for cAMP without acetylation using an enzyme immunoassay kit (Sigma-Aldrich, Inc., St. Louis, MO, USA). The protein content was determined by using the BCA protein assay kit from Pierce (Rockford, Illinois, USA). The results were expressed in pmol/mg of protein.

Statistics

Data are expressed as means ± SE. The individual parameters of the DAPA group were compared with those of the CON group by a two-tailed Student's t-test for unpaired data by using the GraphPad Prism version 5.0 software (GraphPad, San Diego, CA, USA). P values of < 0.05 were considered statistically significant.

Results

Effect of DAPA treatment on body weight, diuresis and electrolytes

Treatment with DAPA was well tolerated in PCK rats and they appeared healthy throughout the 6 week treatment phase. Treatment of 6-week old male PCK rats with DAPA (10 mg/kg/d) induced immediate and sustained glucosuria that was accompanied by a 2-fold increase in water intake and a 3-fold increase in urine output when compared with vehicle-treated controls (Table 1). Feces output was also increased by 23% at 3 week and by 45% at 6 week in DAPA-treated PCK rats compared with controls. Plasma glucose ($P_{glucose}$) levels did not change in response to DAPA, and plasma osmolality (P_{osm}), sodium (P_{Na^+}) and chloride (P_{Cl^-}) concentrations remained stable at 3 and 6 weeks of treatment. DAPA-treated PCK rats displayed a slightly enhanced urine sodium and chloride excretion rate compared with vehicle-treated rats. Of note, DAPA-treated rats had a 6.4% lower body weight than controls at the end of the 6 week treatment phase (Table 1 and Fig 1A). Treatment with DAPA in normal SD rats also resulted in the induction of glucosuria and an increase in water intake and urine output and a slight increase in urine sodium and chloride, whereas P_{Na^+} and P_{Cl^-} remained stable (Table 2).

Effect of DAPA treatment on renal function and albuminuria

Table 3 shows that the plasma creatinine concentrations were similar at 3 weeks but tended to increase at 6 weeks in DAPA-treated PCK rats. The plasma BUN concentrations were significantly higher at 3 and 6 weeks of DAPA treatment. The clearances of creatinine and BUN were significantly higher at 3 weeks, but the difference disappeared at 6 weeks of treatment with DAPA. Calculating the [$clearance_{creatinine}$ + $clearance_{BUN}$ / 2] confirmed that there was a higher clearance at 3 but not at 6 weeks of DAPA treatment in PCK rats (Fig 1B). Table 4 shows the data in normal SD rats. In DAPA-treated normal rats we did not see an increase in

Table 1. Effect of DAPA on body weight, fluid balance and electrolytes in PCK rats.

Time point	Baseline		Day 21		Day 42	
Treatment group	CON	DAPA	CON	DAPA	CON	DAPA
Number of animals	9	9	9	8	9	8
Age, week	6	6	9	9	12	12
Body weight, g	214 ± 5	210 ± 5	333 ± 5	324 ± 6	438 ± 6	410 ± 9*
Water intake, ml/d	31 ± 1	31 ± 1	48 ± 2	92 ± 2***	40 ± 3	86 ± 8***
Diuresis, ml/d	10 ± 1	9 ± 1	18 ± 3	53 ± 2***	19 ± 1	57 ± 7***
P_{osm}, mosm/l	294.6 ± 2.2	293.8 ± 1.2	323.0 ± 2.4	315.4 ± 2.9	341.0 ± 7.5	351.6 ± 10.2
P_{Na^+}, mmol/l	137.6 ± 1.6	139.5 ± 0.6	138.5 ± 0.4	140.8 ± 0.4	140.9 ± 0.7	138.8 ± 2.5
P_{Cl^-}, mmol/l	104.8 ± 0.8	105.5 ± 0.3	101.9 ± 0.5	103.9 ± 0.4	105.5 ± 1.6	104.0 ± 1.1
$P_{glucose}$, mmol/l	12.5 ± 1.4	10.6 ± 0.6	11.2 ± 0.4	11.3 ± 0.3	13.4 ±1.3	16.0 ± 2.7
U_{osm}, mosm/d	13.9 ± 0.7	14.2 ± 0.7	20.0 ± 2.1	57.2 ± 2.0***	23.9 ±1.0	62.5 ± 5.6***
U_{Na^+}, mmol/d	1.1 ± 0.1	1.1 ± 0.1	1.0 ± 0.1	1.5 ± 0.2*	1.2 ± 0.1	1.8 ± 0.1***
U_{Cl^-}, mmol/d	2.0 ± 0.1	2.1 ±0.1	1.9 ±0.2	2.9 ± 0.2**	2.2 ± 0.1	3.3 ± 0.1***
$U_{glucose}$, mmol/d	0.1 ± 0.0	0.0 ± 0.0	0.3 ± 0.2	24.6 ± 0.9***	0.3 ± 0.1	23.6 ± 4.3***

Data are expressed as means ± SE. CON, vehicle control; DAPA, dapagliflozin.

*P<0.05

**P<0.01

***P<0.001, when comparing DAPA and CON at each time point. P, plasma; U, urine.

doi:10.1371/journal.pone.0125603.t001

the creatinine and BUN clearances, and the [$clearance_{creatinine}$ + $clearance_{BUN}$ / 2] was also similar between DAPA- vs. vehicle-treated SD rats. These data suggest that there was transient hyperfiltration and subsequent deterioration of renal function upon treatment with DAPA in PCK but not in SD rats.

Since albuminuria correlates with disease severity in PKD we analyzed the urine protein content by SDS-PAGE and determined the urine albumin excretion by ELISA (Fig 2). SDS-PAGE of urines (adjusted for 24 h urine volumes) revealed a marked increase of albuminuria in DAPA-treated PCK at 6 weeks (Fig 2A). The ELISA showed that albumin excretion

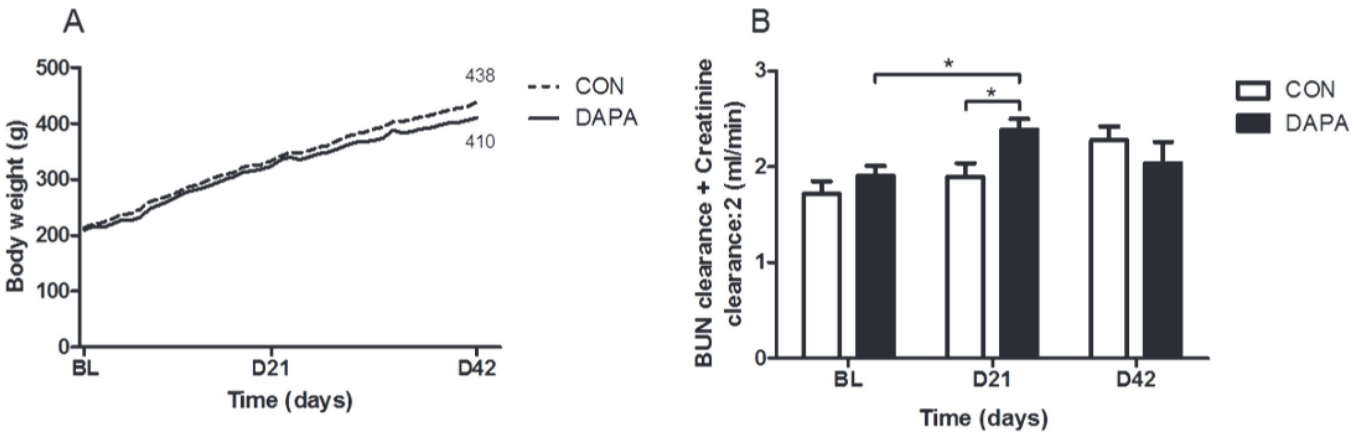

Fig 1. Effect of DAPA on body weight and renal function. Course of body weight in vehicle (CON) and dapagliflozin (DAPA) treated PCK rats during the 6 week treatment phase (A). [$Clearance_{creatinine}$ + $Clearance_{BUN}$ / 2] at baseline (BL) and after 21 and 42 days of treatment in PCK rats (B). N = 8 per group. Data are expressed as means ± SE.* P<0.05.

doi:10.1371/journal.pone.0125603.g001

Table 2. Effect of DAPA on body weight, fluid balance and electrolytes in normal SD rats.

Time point	Baseline		Day 18		Day 35	
Treatment group	CON	DAPA	CON	DAPA	CON	DAPA
Number of animals	9	9	9	9	9	8
Age, week	5	5	7.5	7.5	10	10
Body weight, g	144 ± 2	149 ± 7	285 ± 5	297 ± 7	349 ± 5	354 ± 6
Water intake, ml/d	32 ± 1	32 ± 3	41 ± 2	54 ± 2***	49 ± 3	62 ± 7*
Diuresis, ml/d	11 ± 1	12 ± 1	17 ± 2	24 ± 3*	32 ± 2	36 ± 4
P_{Na^+}, mmol/l	138.9 ± 0.4	142.3 ± 3.4	138.4 ± 0.4	133.5 ± 1.6*	141.9 ± 0.5	140.4 ± 0.6
P_{Cl^-}, mmol/l	100.9 ± 0.3	100.6 ± 1.0	100.3 ± 0.3	94.0 ± 3.0	100.9 ± 0.3	95.9 ± 2.3
$P_{glucose}$, mmol/l	10.5 ± 0.6	10.3 ± 0.2	9.9 ± 0.2	9.7 ± 0.3	13.4 ± 0.2	13.0 ± 0.5
U_{Na^+}, mmol/d	1.3 ± 0.1	1.2 ± 0.1	1.1 ± 0.1	1.4 ± 0.1	1.1 ± 0.3	1.6 ± 2.0
U_{Cl^-}, mmol/d	2.1 ± 0.1	1.8 ± 0.2	1.8 ± 0.1	2.1 ± 0.1	2.3 ± 0.1	2.4 ± 0.5
$U_{glucose}$, mmol/d	0.0 ± 0.0	0.0 ± 0.0	0.0 ± 0.0	10.6 ± 0.6***	0.0 ± 0.0	13.5 ± 2.0***

Data are expressed as means ± SE. CON, vehicle control; DAPA, dapagliflozin.

*P<0.05

**P<0.01

***P<0.001, when comparing DAPA and CON at each time point. P, plasma; U, urine.

doi:10.1371/journal.pone.0125603.t002

increased slightly at 3 weeks and a further increase was observed at 6 weeks in vehicle-treated PCK rats, as expected (Fig 2B). In DAPA-treated rats the albuminuria increased markedly at 3 weeks and more importantly at 6 weeks. After 6 weeks the albumin excretion amounted to 1.7 ± 0.3 mg/d in vehicle-treated rats and to 6.8 ± 0.7 mg/day in DAPA-treated animals (P< 0.0001). In normal SD rats, the excretion of urine albumin was lower than in PCK rats but also increased slightly upon treatment with DAPA for 5 weeks (0.4 ± 0.0 vs. 1.2 ± 0.2 mg/day, P< 0.05).

In vivo high resolution ultrasound imaging of rat kidneys

After 6 weeks of treatment, the PCK rats were anesthetized for ultrasound analysis of both kidneys. Fig 3A shows that the kidneys with the typical medullary cysts could be easily visualized

Table 3. Effect of DAPA on renal function in PCK rats.

Time point	Baseline		Day 21		Day 42	
Treatment group	CON	DAPA	CON	DAPA	CON	DAPA
Number of animals	9	9	9	8	9	8
Age, week	6	6	9	9	12	12
$P_{creatinine}$, μmol/l	18.0 ± 0.0	18.0 ± 0.0	21.9 ±0.5	21.4 ±0.5	26.9 ± 1.2	36.1 ± 6.7
$Clearance_{creatinine}$, ml/min	2.4 ± 0.2	2.7 ± 0.2	2.6 ± 0.2	3.1 ±0.1*	3.2 ± 0.2	2.7 ± 0.3
P_{BUN}, mmol/l	3.7 ± 0.1	3.9 ±0.1	4.1 ± 0.2	4.9 ± 0.2*	5.7 ± 0.1	7.1 ± 0.6*
$Clearance_{BUN}$, ml/min	1.0 ± 0.1	1.1 ± 0.1	1.2 ±0.1	1.7 ± 0.1**	1.3 ± 0.1	1.4 ± 0.1
[$Clearance_{creatinine}$ + $Clearance_{BUN}$ / 2]	1.7 ± 0.1	1.9 ± 0.1	1.8 ± 0.1	2.3 ± 0.1*	2.2 ± 0.1	2.0 ± 0.1

Data are expressed as means ± SE. CON, vehicle control; DAPA, dapagliflozin.

*P<0.05

**P<0.01, when comparing CON and DAPA at each time point. P, plasma.

doi:10.1371/journal.pone.0125603.t003

Table 4. Effect of DAPA on renal function in normal SD rats.

Time point	Baseline		Day 18		Day 35	
Treatment group	CON	DAPA	CON	DAPA	CON	DAPA
Number of animals	9	9	9	9	9	8
Age, week	5	5	7.5	7.5	10	10
$P_{creatinine}$, μmol/l	26.5 ± 0.0	26.5 ± 0.1	26.5 ± 0.0	26.5 ± 0.2	35.3 ± 2.5	35.3 ± 3.2
$Clearance_{creatinine}$, ml/min	1.7 ± 0.1	1.2 ± 0.3	2.0 ± 0.1	2.0 ± 0.2	2.6 ± 0.1	2.7 ± 0.2
P_{BUN}, mmol/l	6.6 ± 0.3	5.5 ± 0.2	6.1 ± 0.2	8.2 ± 0.4***	6.6 ± 0.1	9.9 ± 1.5*
$Clearance_{BUN}$, ml/min	0.6 ± 0.0	0.8 ± 0.1	0.8 ± 0.0	0.8 ± 0.1	1.1 ± 0.0	0.8 ± 0.2*
[$Clearance_{creatinine}$ + $Clearance_{BUN}$ / 2]	1.1 ± 0.1	1.0 ± 0.2	1.4 ± 0.1	1.2 ± 0.2	1.9 ± 0.1	1.9 ± 0.1

Data are expressed as means ± SE. CON, vehicle control; DAPA, dapagliflozin.

*P<0.05

**P<0.01

***P<0.001 when comparing CON and DAPA at each time point. P, plasma.

doi:10.1371/journal.pone.0125603.t004

in vehicle-treated male PCK rats. On the other hand, DAPA-treated rats displayed larger kidneys and had substantially bigger cysts (Fig 3B). Ultrasound-based measurements revealed a 35% higher total kidney volume (P< 0.01), a 2-fold higher cyst volume (P< 0.05) and a 47% higher cystic index (P< 0.05) in DAPA- vs. vehicle-treated rats, whereas the number of cysts was similar in both groups after 6 weeks of treatment (P = 0.841) (Fig 3C–3F).

Effect of DAPA treatment on kidney weight and morphology

After 6 weeks of treatment with DAPA the total weight of both kidneys was 23% higher in DAPA- as compared with vehicle-treated male PCK rats (4.32 ± 0.24 vs. 5.33 ± 0.20 g, P< 0.01). The two kidneys to body weight (2K/BW) ratio was also significantly increased by 34% in the DAPA-treated rats (P< 0.001). PAS-staining of kidney sections revealed that the

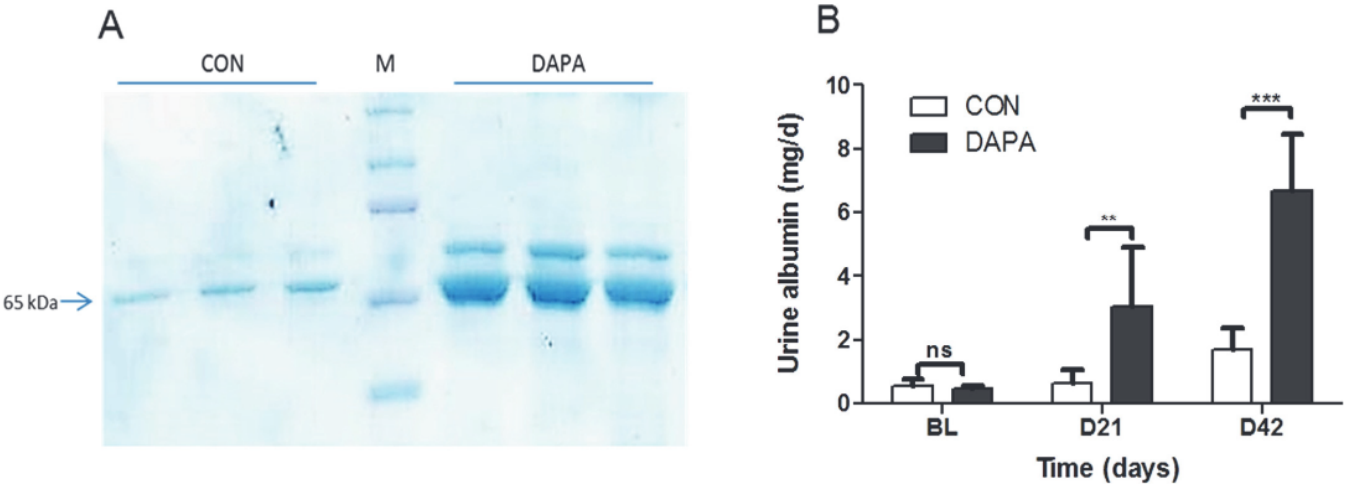

Fig 2. Effect of DAPA on albumin excretion. Urine protein analysis by SDS-PAGE from urine samples of PCK rats after 6 weeks of treatment with vehicle (CON) or dapagliflozin (DAPA). Each lane shows urine sample of a single PCK rat. Sample volumes were corrected for diuresis and amounted to 15 μl for CON and 45 μl for DAPA. Arrow shows the band for albumin. M = molecular weight marker (A). Urine albumin concentration as measured by ELISA, in mg/day (B). N = 8 per group. Columns represent means ± SE. **P<0.01, ***P<0.001 when comparing CON and DAPA at each time point, ns = non-significant.

doi:10.1371/journal.pone.0125603.g002

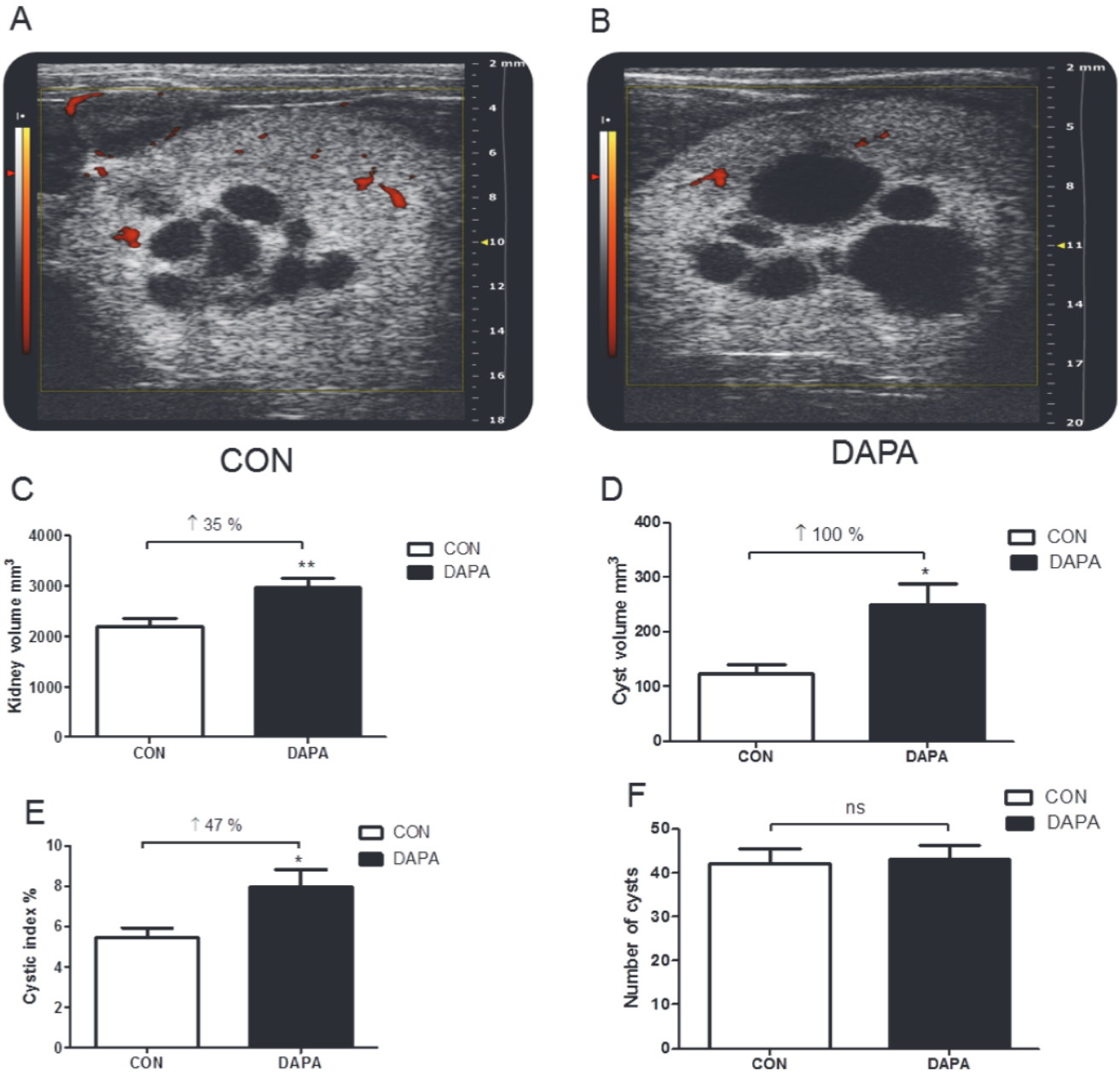

Fig 3. Effect of DAPA on kidney volume and cystic index. Typical 2D transverse power Doppler ultrasound images of a kidney in CON- and DAPA-treated PCK rats. The red areas represent a power Doppler signal consistent with blood flow within the renal vasculature. The maximum scan distance between cranial and caudal poles of the kidney was 28 mm. The slice thickness between scanning planes was 0.072 mm with a maximum of 500 slices (A, B). Change in kidney volume (C), cyst volume (D), cystic index (E) and number of cysts (F) in PCK rats. N = 6 rats or 12 kidneys per group. Columns represent means ± SE. *P<0.05, **P<0.01, ns = non-significant.

doi:10.1371/journal.pone.0125603.g003

cyst index was increased by 43% in DAPA-treated rats (P< 0.05) while the total cyst number was not significantly changed (P = 0.074) (Figs 4 and 5). In normal SD rats the total kidney weight of both kidneys was also higher in DAPA-treated rats as compared to the total kidney weight in vehicle-treated rats (3.1± 0.3 vs. 2.3 ± 0.2 g, P = 0.0002).

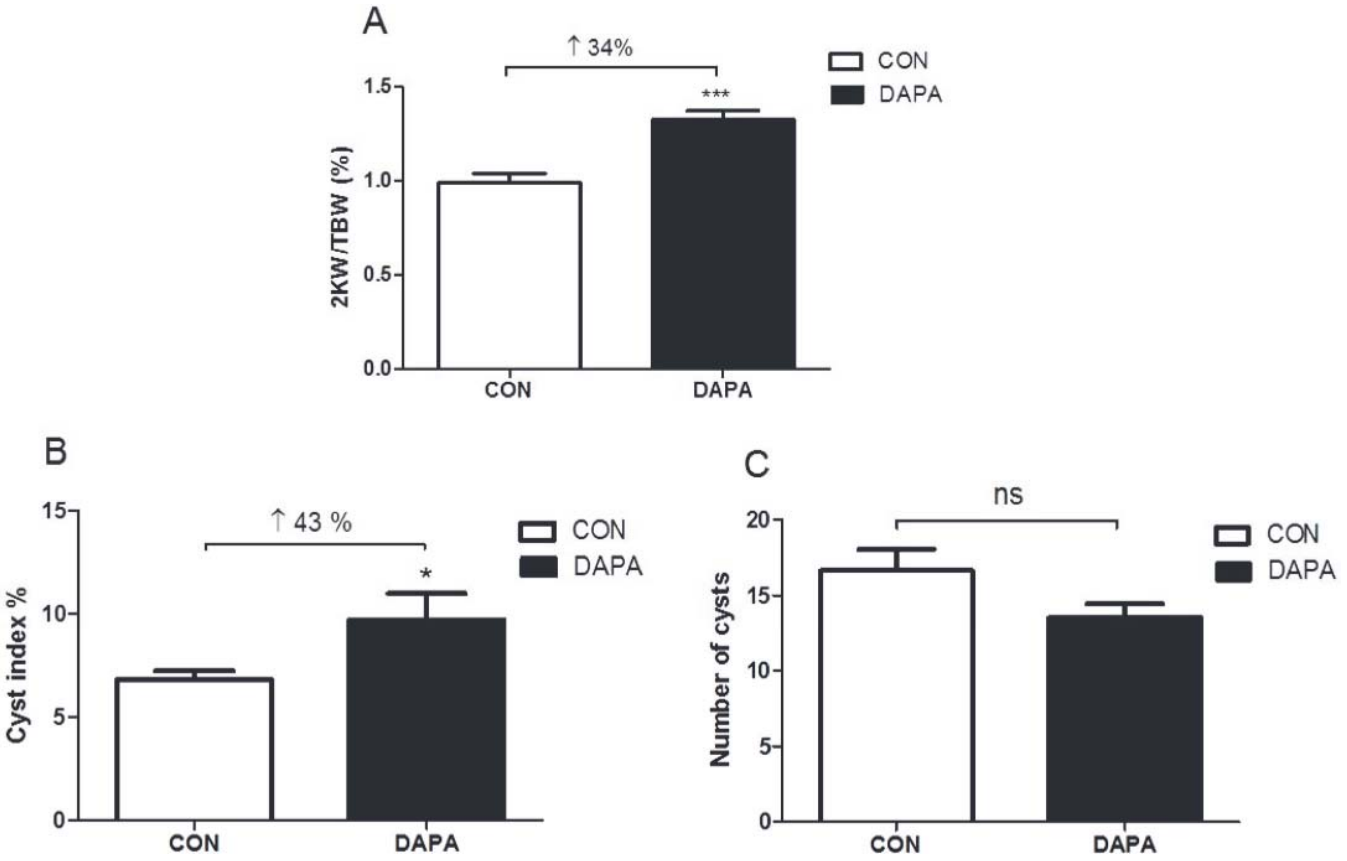

Fig 4. Effect of DAPA on kidney weight and cyst index. Ratio of two kidney weights to total body weight (2KW/TBW) (A), cyst index (B) and number of cysts (C) after 6 week treatment with vehicle (CON) or DAPA in PCK rats. N = 8 per group. Columns represent means ± SE. *P<0.05, ***P<0.001, ns = non-significant.

doi:10.1371/journal.pone.0125603.g004

Effect of DAPA treatment on renal cAMP content and renal epithelial cell proliferation

Since cAMP is a major driver of cyst growth we analyzed the content of cAMP in PCK kidney tissue by ELISA. Fig 6 shows that the amount of cAMP per mg of total protein was similar in DAPA- and vehicle-treated male PCK rats (P = 0.717).

Immunohistochemistry staining for Ki67 was then used to examine whether DAPA treatment had an effect on tubular and cystic epithelial cell proliferation. Fig 7 shows no significant change in the number of Ki67-positive nuclei in the cystic epithelium in DAPA-treated PCK rats. Quantification of the Ki67-positive nuclei confirmed that the number of Ki67-positive nuclei was not changed in cystic epithelium as well as in non-cystic epithelium in DAPA- vs. vehicle-treated PCK rats (Table 5).

Discussion

Here we show that the induction of osmotic diuresis with the SGLT2-specific inhibitor DAPA leads to an unexpected increase in the kidney and renal cyst volumes of PCK rats, an orthologous model of ARPKD. Furthermore, DAPA-treated PCK but not normal SD rats displayed a transient increase in the clearances of creatinine and BUN and a progressive increase in albuminuria which suggests that DAPA promotes hyperfiltration in PCK rats. The renal cAMP

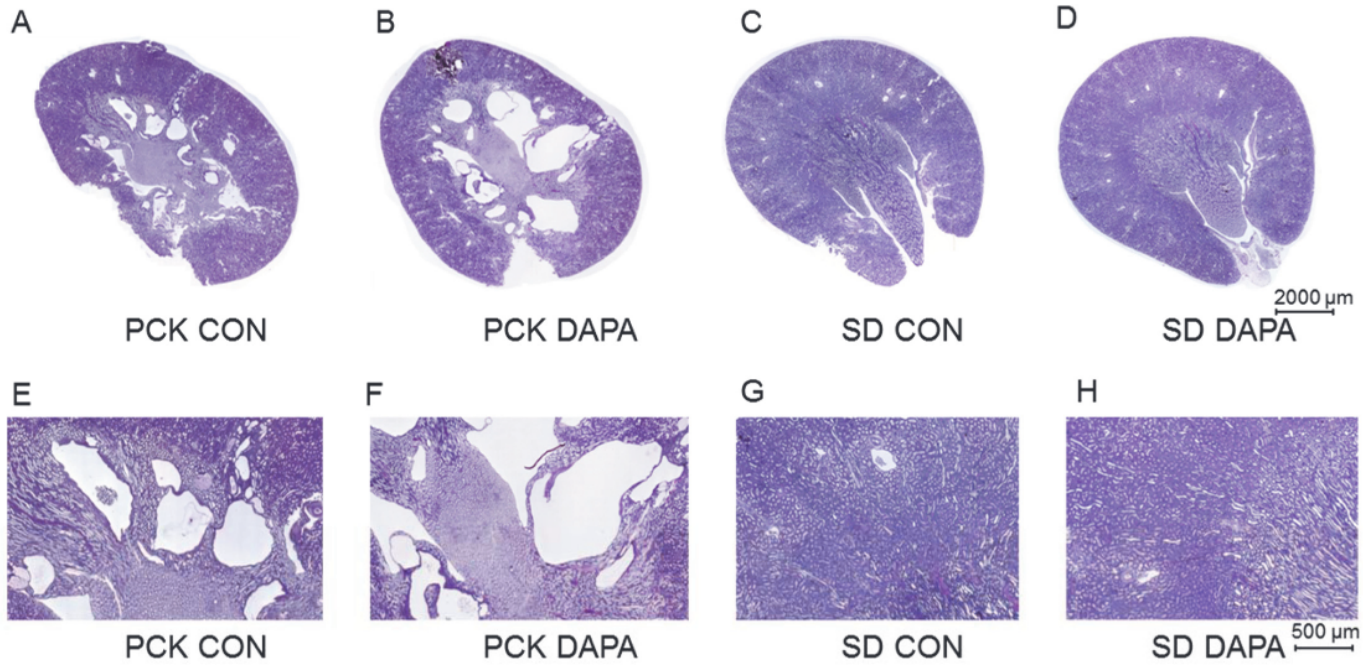

Fig 5. Effect of DAPA on renal histology. Representative renal histology by periodic acid-Schiff (PAS) staining of kidneys in vehicle- treated (CON) PCK (A,E) and normal SD (C,G) rats and in DAPA-treated PCK (B,F) and normal SD (D,H) rats. Scale bar is 2000 µm in A and B and 500 µm in C and D.

doi:10.1371/journal.pone.0125603.g005

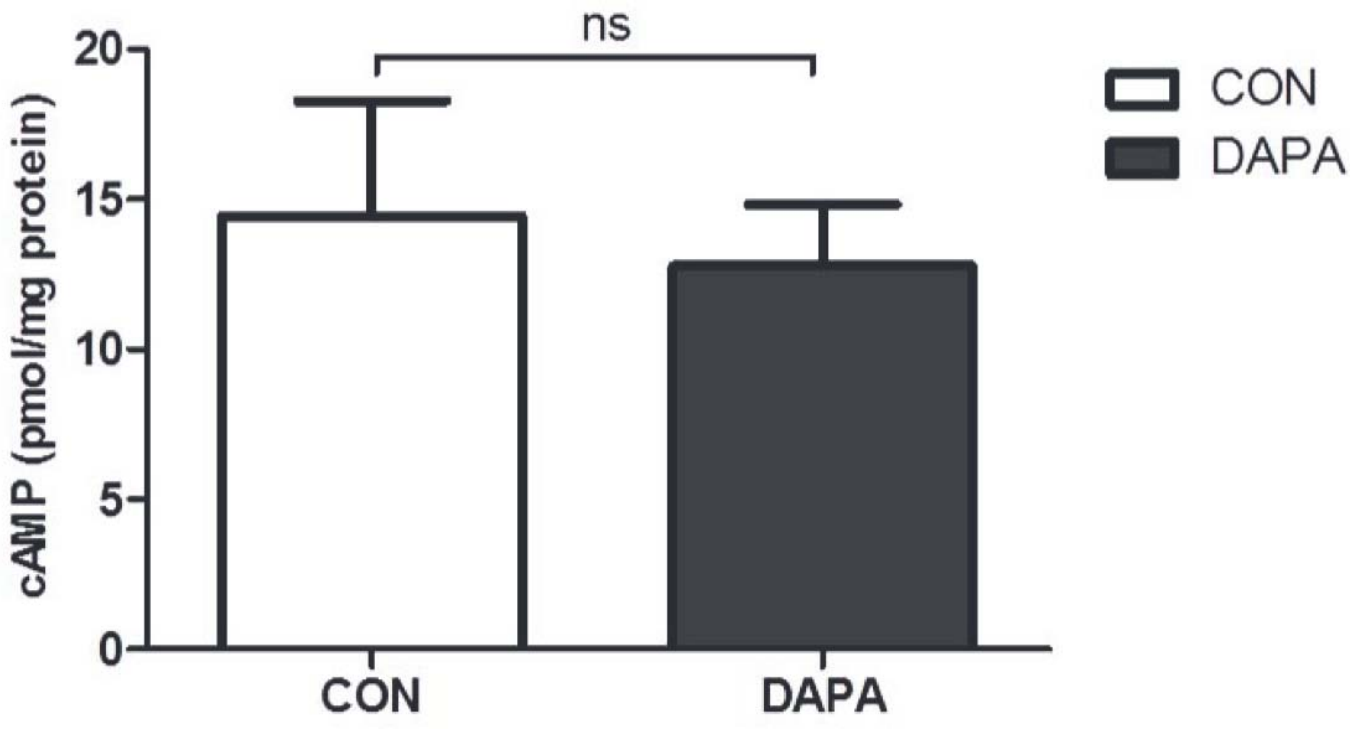

Fig 6. Effect of DAPA on renal cAMP content. Analysis of cAMP concentration per mg protein in PCK rat kidneys treated with vehicle (CON) or dapagliflozin (DAPA). N = 8 per group. Columns represent means ± SE. ns = non-significant.

doi:10.1371/journal.pone.0125603.g006

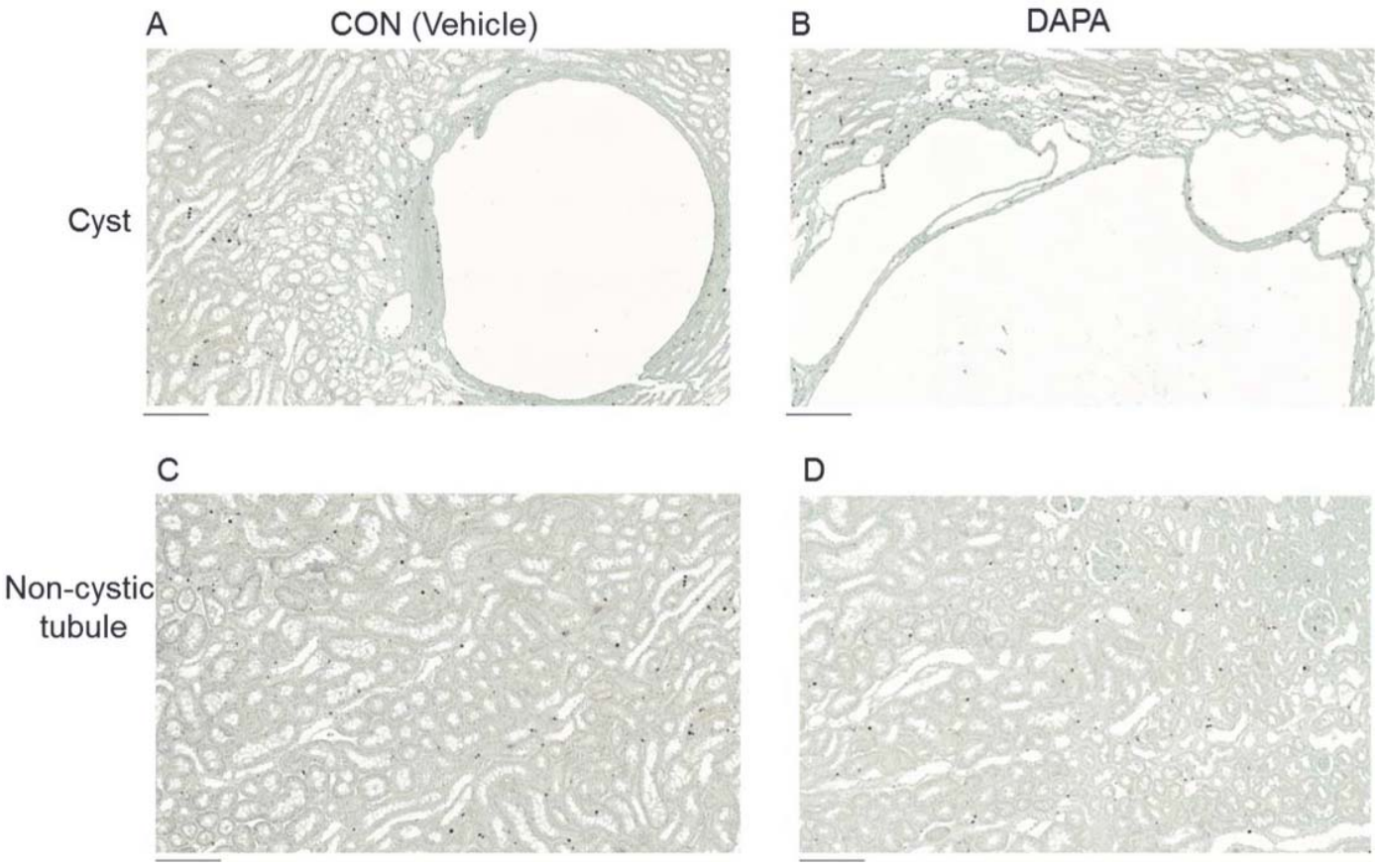

Fig 7. Effect of DAPA on cell proliferation. Representative areas of Ki67 immunohistochemical staining in PCK rat kidneys are shown. Nuclei of Ki67-positive cells were stained brown with 3,3'-diaminobenzidine and that of Ki67-negative cells appeared blue because of the counterstaining with hematoxylin. CON (cystic area) (A), DAPA (cystic area) (B), CON (non-cystic area) (C), DAPA (non-cystic area) (D). Scale bar is 200 μm in A, B, C and D.

doi:10.1371/journal.pone.0125603.g007

content was similar, and there was no evidence for heightened epithelial cell proliferation which could explain the greater cyst volume upon treatment with DAPA. Thus, the induction of glucosuria with DAPA appeared to have a negative impact on cystic disease progression in PCK rats.

The increase in glomerular filtration in response to DAPA appeared to be transient, i.e. it was seen after 3 weeks but not after 6 weeks. However it was associated with an increase in albuminuria at 3 weeks and a further increase at 6 weeks. In general, an increase in albuminuria is seen with progressing stages of PKD [20]. The increased amount of urine albumin could be

Table 5. Effect of DAPA on cell proliferation in PCK rat kidneys.

Treatment	CON	DAPA	Difference, %	P-value
Number of animals	7	7		
Ki67-positive cells (%) in cyst-lining epithelium	6.5 ± 1.3	6.7 ± 1.9	+ 3.5	0.922
Ki67-positive cells (%) in non-cystic tubules	2.5 ± 0.91	3.1 ± 1.1	+ 24.7	0.677

Morphometric analysis using Ki67, a proliferation marker in kidney medulla of vehicle (CON)- and DAPA-treated PCK rats. Data are expressed as means ± SE.

doi:10.1371/journal.pone.0125603.t005

the consequence of enhanced leakage of albumin from glomeruli, or alternatively it could be caused by decreased tubular reabsorption. Whether albuminuria is reflecting glomerular hyperfiltration damage needs to be examined further.

Treatment with SGLT2 inhibitors has been associated with a decrease in the GFR in normal and diabetic rats and in humans with type 2 diabetes mellitus [21,22]. This contrasts with our findings in PCK rats which display evidence of transient hyperfiltration. This hyperfiltration could in part be explained by the enhanced food i.e. protein intake which is seen in response to DAPA [23], since protein loading is a known stimulus for increasing glomerular filtration. However this should have been counterbalanced by the higher sodium delivery at the macula densa which normally leads to afferent arteriolar vasoconstriction [24]. Since normal rats which are treated with DAPA do not develop hyperfiltration and albuminuria [25–27], the effects that we observed appear to be specific to the PCK model of PKD.

In a previous study, we found that treatment with the SGLT1/SGLT2 inhibitor phlorizin attenuated albuminuria in Han:SPRD rats, improved GFR, and decreased cyst growth [18]. Contrasting with these results, the DAPA-treated PCK rats displayed enhanced cyst growth. Han:SPRD rats are a non-orthologous model of PKD, with cyst formation exclusively in the proximal tubules [28,29]. In contrast, PCK rats display cyst formation in the distal nephron. Typically, the cysts disconnect from the original proximal tubule in Han:SPRD, whereas in PCK rats the cysts remain connected to the distal tubule. We speculate that the increased intratubular osmotic pressure which is caused by the glucosuria could promote the dilation of distal tubular segments and cysts. This could cause compression of adjacent healthy distal tubules and provide a stimulus to enhance GFR, as it may be seen in partial obstructive uropathy [30].

The enhanced cyst growth did not appear to be the consequence of vasopressin-mediated cAMP stimulation, since the renal cAMP content was similar between DAPA- and vehicle-treated PCK rats. Despite a massive increase in the diuresis, DAPA-treated rats did not appear to be dehydrated, and the serum sodium concentrations did not increase. This suggests indirectly that vasopressin levels did not increase. Furthermore, Ki67 staining did not reveal an increase in proliferating cells in dilated tubules, and there was no change in the number of nuclei in the cysts upon DAPA treatment. This indicates again that the cysts increased in size due to osmotic pressure without affecting epithelial cell proliferation.

Diabetes may occur in patients with ADPKD and it is associated with greater cardiovascular morbidity [31]. With the possibility to treat ADPKD patients with SGLT2 inhibitors there could be a risk of albuminuria and increased cyst growth. Although such a complication has not yet been described caution should be exerted when prescribing these drugs to patients with ADPKD.

In summary, we have shown that the induction of osmotic diuresis by inhibiting SGLT2 promotes transient hyperfiltration, albuminuria and increased cyst volume in PCK rats. Further studies need to explore the mechanisms which link the enhanced glomerular filtration to the increase in cyst volume upon SGLT inhibition in this model of PKD.

Acknowledgments

We thank Prof. Colin C. Schwarzwald from the Clinic for Equine Internal Medicine, Vetsuisse Faculty, for his support with the ultrasound imaging. Also, we thank Petra Seebeck, Svende Pfundstein and Stefanie Weinreich from the Zürich Integrative Rodent Physiology (ZIRP), University of Zürich for their help with the animal work.

Author Contributions

Conceived and designed the experiments: SK RPW. Performed the experiments: SK DR KM IE. Analyzed the data: SK DR MR SS RPW. Contributed reagents/materials/analysis tools: KM SS RPW. Wrote the paper: SK RPW.

References

1. Harris PC, Torres VE (2009) Polycystic kidney disease. Annu Rev Med 60: 321–337. doi: 10.1146/annurev.med.60.101707.125712 PMID: 18947299
2. Torres VE, Harris PC, Pirson Y (2007) Autosomal dominant polycystic kidney disease. Lancet 369: 1287–1301. PMID: 17434405
3. Schrier RW, McFann KK, Johnson AM (2003) Epidemiological study of kidney survival in autosomal dominant polycystic kidney disease. Kidney Int 63: 678–685. PMID: 12631134
4. Wüthrich RP, Mei C (2014) Pharmacological management of polycystic kidney disease. Expert Opin Pharmacother 15: 1085–1095. doi: 10.1517/14656566.2014.903923 PMID: 24673552
5. Devuyst O, Torres VE (2013) Osmoregulation, vasopressin, and cAMP signaling in autosomal dominant polycystic kidney disease. Curr Opin Nephrol Hypertens 22: 459–470. doi: 10.1097/MNH.0b013e3283621510 PMID: 23736843
6. Torres VE, Harris PC (2014) Strategies targeting cAMP signaling in the treatment of polycystic kidney disease. J Am Soc Nephrol 25: 18–32. doi: 10.1681/ASN.2013040398 PMID: 24335972
7. Meijer E, Gansevoort RT, de Jong PE, van der Wal AM, Leonhard WN, de Krey SR, et al. (2011) Therapeutic potential of vasopressin V2 receptor antagonist in a mouse model for autosomal dominant polycystic kidney disease: optimal timing and dosing of the drug. Nephrol Dial Transplant 26: 2445–2453. doi: 10.1093/ndt/gfr069 PMID: 21393612
8. Gattone VH 2nd, Wang X, Harris PC, Torres VE (2003) Inhibition of renal cystic disease development and progression by a vasopressin V2 receptor antagonist. Nat Med 9: 1323–1326. PMID: 14502283
9. Torres VE, Wang X, Qian Q, Somlo S, Harris PC, Gattone VH 2nd (2004) Effective treatment of an orthologous model of autosomal dominant polycystic kidney disease. Nat Med 10: 363–364. PMID: 14991049
10. Wang X, Gattone V 2nd, Harris PC, Torres VE (2005) Effectiveness of vasopressin V2 receptor antagonists OPC-31260 and OPC-41061 on polycystic kidney disease development in the PCK rat. J Am Soc Nephrol 16: 846–851. PMID: 15728778
11. Hopp K, Wang X, Ye H, Irazabal MV, Harris PC, Torres VE (2015) Effects of hydration in rats and mice with polycystic kidney disease. American Journal of Physiology—Renal Physiology 308: F261–F266.
12. Torres VE, Chapman AB, Devuyst O, Gansevoort RT, Grantham JJ, Higashihara E, et al. (2012) Tolvaptan in patients with autosomal dominant polycystic kidney disease. N Engl J Med 367: 2407–2418. doi: 10.1056/NEJMoa1205511 PMID: 23121377
13. Wang X, Wu Y, Ward CJ, Harris PC, Torres VE (2008) Vasopressin directly regulates cyst growth in polycystic kidney disease. J Am Soc Nephrol 19: 102–108. PMID: 18032793
14. Nagao S, Nishii K, Katsuyama M, Kurahashi H, Marunouchi T, Takahashi H, et al. (2006) Increased water intake decreases progression of polycystic kidney disease in the PCK rat. J Am Soc Nephrol 17: 2220–2227. PMID: 16807403
15. Ho TA, Godefroid N, Gruzon D, Haymann JP, Marechal C, Wang X, et al. (2012) Autosomal dominant polycystic kidney disease is associated with central and nephrogenic defects in osmoregulation. Kidney Int 82: 1121–1129. doi: 10.1038/ki.2012.225 PMID: 22718190
16. Torres VE, Bankir L, Grantham JJ (2009) A case for water in the treatment of polycystic kidney disease. Clin J Am Soc Nephrol 4: 1140–1150. doi: 10.2215/CJN.00790209 PMID: 19443627
17. Wang CJ, Creed C, Winklhofer FT, Grantham JJ (2011) Water prescription in autosomal dominant polycystic kidney disease: a pilot study. Clin J Am Soc Nephrol 6: 192–197. doi: 10.2215/CJN.03950510 PMID: 20876670
18. Wang X, Zhang S, Liu Y, Spichtig D, Kapoor S, Koepsell H, et al. (2013) Targeting of sodium-glucose cotransporters with phlorizin inhibits polycystic kidney disease progression in Han:SPRD rats. Kidney Int 84: 962–968. doi: 10.1038/ki.2013.199 PMID: 23715121
19. Mather A, Pollock C (2010) Renal glucose transporters: novel targets for hyperglycemia management. Nat Rev Nephrol 6: 307–311. doi: 10.1038/nrneph.2010.38 PMID: 20351704
20. Chapman AB, Johnson AM, Gabow PA, Schrier RW (1994) Overt proteinuria and microalbuminuria in autosomal dominant polycystic kidney disease. J Am Soc Nephrol 5: 1349–1354. PMID: 7894001

21. Skrtic M, Yang GK, Perkins BA, Soleymanlou N, Lytvyn Y, von Eynatten M, et al. (2014) Characterisation of glomerular haemodynamic responses to SGLT2 inhibition in patients with type 1 diabetes and renal hyperfiltration. Diabetologia 57: 2599–2602. doi: 10.1007/s00125-014-3396-4 PMID: 25280671

22. De Nicola L, Gabbai FB, Liberti ME, Sagliocca A, Conte G, Minutolo R (2014) Sodium/glucose cotransporter 2 inhibitors and prevention of diabetic nephropathy: targeting the renal tubule in diabetes. Am J Kidney Dis 64: 16–24. doi: 10.1053/j.ajkd.2014.02.010 PMID: 24673844

23. Devenny JJ, Godonis HE, Harvey SJ, Rooney S, Cullen MJ, Pelleymounter MA (2012) Weight loss induced by chronic dapagliflozin treatment is attenuated by compensatory hyperphagia in diet-induced obese (DIO) rats. Obesity (Silver Spring) 20: 1645–1652. doi: 10.1038/oby.2012.59 PMID: 22402735

24. Thomson SC, Rieg T, Miracle C, Mansoury H, Whaley J, Vallon V, et al. (2012) Acute and chronic effects of SGLT2 blockade on glomerular and tubular function in the early diabetic rat. Am J Physiol Regul Integr Comp Physiol 302: R75–83. doi: 10.1152/ajpregu.00357.2011 PMID: 21940401

25. Meng W, Ellsworth BA, Nirschl AA, McCann PJ, Patel M, Girotra RN, et al. (2008) Discovery of dapagliflozin: a potent, selective renal sodium-dependent glucose cotransporter 2 (SGLT2) inhibitor for the treatment of type 2 diabetes. J Med Chem 51: 1145–1149. doi: 10.1021/jm701272q PMID: 18260618

26. Han S, Hagan DL, Taylor JR, Xin L, Meng W, Biller SA, et al. (2008) Dapagliflozin, a selective SGLT2 inhibitor, improves glucose homeostasis in normal and diabetic rats. Diabetes 57: 1723–1729. doi: 10.2337/db07-1472 PMID: 18356408

27. Obermeier M, Yao M, Khanna A, Koplowitz B, Zhu M, Li W, et al. (2010) In vitro characterization and pharmacokinetics of dapagliflozin (BMS-512148), a potent sodium-glucose cotransporter type II inhibitor, in animals and humans. Drug Metab Dispos 38: 405–414. doi: 10.1124/dmd.109.029165 PMID: 19996149

28. Brown JH, Bihoreau MT, Hoffmann S, Kranzlin B, Tychinskaya I, Obermuller N, et al. (2005) Missense mutation in sterile alpha motif of novel protein SamCystin is associated with polycystic kidney disease in Cy/+ rat. J Am Soc Nephrol 16: 3517–3526. PMID: 16207829

29. Hoff S, Halbritter J, Epting D, Frank V, Nguyen TM, van Reeuwijk J, et al. (2013) ANKS6 is a central component of a nephronophthisis module linking NEK8 to INVS and NPHP3. Nat Genet 45: 951–956. doi: 10.1038/ng.2681 PMID: 23793029

30. Chevalier RL (1998) Pathophysiology of obstructive nephropathy in the newborn. Semin Nephrol 18: 585–593. PMID: 9819149

31. Reed B, Helal I, McFann K, Wang W, Yan XD, Schrier RW (2012) The impact of type II diabetes mellitus in patients with autosomal dominant polycystic kidney disease. Nephrol Dial Transplant 27: 2862–2865. doi: 10.1093/ndt/gfr744 PMID: 22207329

Chapter 5

High resolution ultrasonography for assessment of renal cysts in the PCK rat model of autosomal recessive polycystic kidney disease

Sarika Kapoor[1,2], Daniel Rodriguez[1,3], Katharyn Mitchell[4] and Rudolf P.Wüthrich[1,2]

[1]Division of Nephrology, University Hospital, Zürich, Switzerland
[2]Institute of Physiology, University of Zürich, Switzerland
[3]Molecular and Translational Biomedicine, Competence Center for Personalized Medicine, University of Zürich, Switzerland
[4]Clinic for Equine Internal Medicine, Vetsuisse Faculty, University of Zürich, Switzerland

Kidney Blood Press Res 2016;41:186-196

Contribution by Daniel Rodriguez:

Animal handling and assistance during high resolution ultrasonography procedures and statistical analysis of data (correlation analysis and Bland-Altman plot).

Kidney & Blood Pressure Research

Kidney Blood Press Res 2016;41:186-196
DOI: 10.1159/000443420
Published online: March 17, 2016
Accepted: February 08, 2016

Original Paper

High Resolution Ultrasonography for Assessment of Renal Cysts in the PCK Rat Model of Autosomal Recessive Polycystic Kidney Disease

Sarika Kapoor[a,b] Daniel Rodriguez[a,c] Katharyn Mitchell[d] Rudolf P. Wüthrich[a,b]

[a]Division of Nephrology, University Hospital, [b]Institute of Physiology, [c]Molecular and Translational Biomedicine, Competence Center for Personalized Medicine, [d]Clinic for Equine Internal Medicine, Vetsuisse Faculty, University of Zürich, Zürich, Switzerland

Key Words
High resolution diagnostic imaging • Total kidney volume • Total cyst volume • Polycystic kidney disease • PCK rat

Abstract
Background/Aims: The PCK rat model of polycystic kidney disease is characterized by the progressive development of renal medullary cysts. Here, we evaluated the suitability of high resolution ultrasonography (HRU) to assess the kidney and cyst volume in PCK rats, testing three different ultrasound image analysis methods, and correlating them with kidneys weights and histological examinations. Methods: After inducing anesthesia, PCK rats (n=18) were subjected to HRU to visualize the kidneys, to perform numeric and volumetric measurements of the kidney and any cysts observed, and to generate 3-dimensional images of the cysts within the kidney parenchyma. Results: HRU provided superior information in comparison to microscopic analysis of stained kidney sections. HRU-based kidney volumes correlated strongly with kidney weights (R^2=0.809; P<0.0001). Conclusion: HRU represents a useful diagnostic tool for kidney and cyst volume measurements in PCK rats. Sequential HRU examinations may be useful to study the effect of drugs on cyst growth without the need to euthanize experimental animals.

Introduction

Autosomal recessive polycystic kidney disease (ARPKD) has been estimated to have an incidence of 1:20,000 people and typically presents in utero or during the neonatal period with greatly enlarged, echogenic kidneys [1]. The disease is due to mutations in the gene

Rudolf P. Wüthrich, MD, FACP, FASN
Division of Nephrology, University Hospital, Rämistrasse 100, 8091 Zürich (Switzerland)
Tel. +41 44 255 33 84, Fax +41 44 255 45 93, E-Mail rudolf.wuethrich@usz.ch

Pkhd1 which encodes for fibrocystin, a ciliary protein. The major histological manifestation is a fusiform dilatation of the collecting ducts where cysts are attached and do not separate from the parental tubules [2].

The PCK rat model is a well-known orthologous model of ARPKD that has been widely used to assess the therapeutic effect of drugs which retard cyst development in preclinical studies [3]. PCK rats develop multiple cysts in the renal medulla but not in the cortex. As the cysts grow the renal function deteriorates progressively, reducing the life span of the rats which generally die of renal failure.

A non-invasive imaging technique that is capable of high throughput, is relatively inexpensive and provides sufficient resolution to quantify the variables of interest with high accuracy may reduce the number of experimental animals [4]. High-frequency ultrasound technology recently became more accessible, which enables high-quality imaging of anatomical structures in mice and rats, and provides excellent temporal and spatial resolution [5].

Here, we explored for the first time if high resolution ultrasonography (HRU) is a suitable method to assess the cyst burden in anesthetized PCK rats. Ultrasonography was used to image PCK rat kidneys to determine total kidney volume (TKV), total cyst volume (TCV) and total cyst number (TCN). We compared 3 different methods for HRU-based TKV assessments, namely an HRU-stereological (HRUs), an HRU-automated (HRUa) and an HRU-ellipsoid (HRUe) method and correlated the findings with total kidney weight (TKW) and histological examination (HE).

Materials and Methods

Experimental design

All animal experiments were conducted in an ethical and humane fashion, and were approved by the district veterinary office of the Canton Zurich (permit number 175-2012) that is our institutional animal care and use committee (IACUC). PCK rats (an orthologous model of autosomal recessive PKD) were obtained from Charles River Laboratories (Sulzfeld, Germany). Heterozygous Cy/+ Han:SPRD rats (a non-orthologous model of autosomal dominant PKD) and homozygous wild type +/+ rats were obtained from the Rat Resource and Research Center (Columbia, MO, USA). All animals were bred in our animal facility. Only male rats were used since cysts develop more rapidly in male than in female rats. PCK rats were examined at the age of 7 weeks (n=6) and 12 weeks (n=12) by HRU to determine their TKV, TCV and TCN. After HRU examination, the rats were euthanized and both kidneys were excised, decapsulated and weighed. Kidney slices of approximately 2 mm were then fixed in 10% buffered formalin and embedded in paraffin for histological examination. Cy/+ Han:SPRD and wild type +/+ rats were examined at the age of 10 and 12 weeks respectively to compare their renal HRU images with those of the PCK rats.

High Resolution Ultrasonography (HRU)

Animal preparation. Isoflurane (5% induction, then 1.5-2% maintenance) in oxygen (1 L/min) was used to induce and maintain anaesthesia. Physiological variables (heart rate, respiratory rate, rectal temperature) were continuously monitored during the procedure, using a physiological monitoring unit (VisualSonics, Toronto, Canada). As shown in Fig. 1A and 1B, rats were placed in dorsal recumbency and were fixed on a dedicated handling table for rats (VisualSonics) using adhesive tape. The abdomen of the rats was clipped and all hair was removed using hair removal cream (Veet).

Image acquisition

HRU images were acquired using the Vevo 2100 high resolution ultrasound system (VisualSonics) equipped with the 18-38 MHz probe (MS400) and 3-dimensional (3-D) image motor. Acoustic coupling was ensured using ultrasound coupling gel. Following image optimisation, kidneys were imaged in a ventro-dorsal plane to acquire sequential transverse 2-dimensional (2-D) and power Doppler images of each kidney, using an automated 3-D motor head and the respiratory gating feature to avoid artefacts

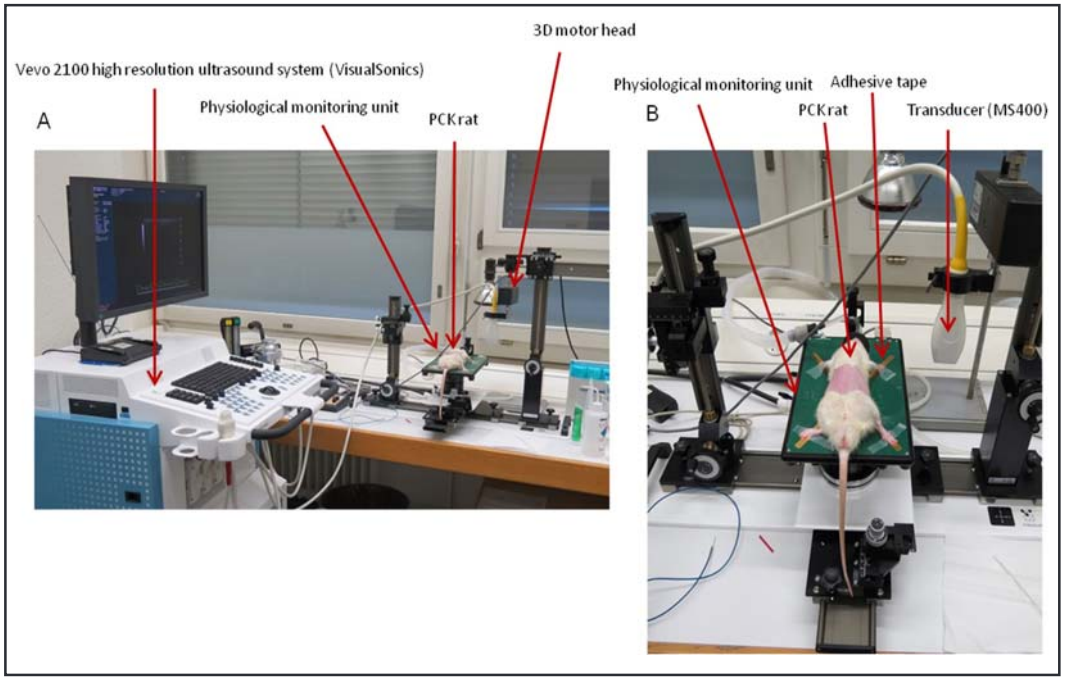

Fig. 1. Experimental set-up using high resolution ultrasonography (HRU) for the analysis of kidney and cyst volumes in anaesthetized PCK rats.

associated with respiratory motion. Care was taken to include the cranial and caudal poles of the kidney where possible (maximum scan distance 28 mm). The slice thickness between scanning planes was 0.05 mm with a maximum of 500 frames. The images were captured in digital raw format as 500 frame cineloops. Following imaging, the rats were euthanized with embutramide (T61®) via injection into the liver. All raw data files from HRU were copied to a work station and inspected to confirm complete coverage of both kidneys and image quality.

Image analysis

Stereological method. The 2-D transverse sequential cineloops were reconstructed into a rectangular 3-D model, using the VevoLab v1.6.0 software (VisualSonics). Tracing of the outer kidney surface and the outer wall of each cyst was performed manually in the 3-D reconstruction, using the volume measurement tools present in the VevoLab software as per the manufacturer's instructions. The resulting 3-D model was used to determine the stereological TKV (TKVs). Identification and measuring of all cystic structures allowed the determination of the TCV and the TCN. Finally, cystic index (CI) was calculated in percent as TCVs/ TKVs*100.

Automated method. The 2-D transverse cineloops were exported from the VevoLab software and transferred to Analyze 12.0 software (AnalyzeDirect, Inc., Overland Park, KS, USA). Here, tracing of the kidney and cyst surface was performed in the 3-D reconstruction by semi-automatic tools present in the Analyze 12.0 software as per the manufacturer's instructions. The resulting 3-D model was used to determine automated TKV (TKVa) and automated TCV (TCVa). The CI was again calculated in percent as TCVa/ TKVa*100.

Ellipsoid method. The 2-D and 3-D cineloops were used to determine the 3 renal dimensions (length, lateral diameter [width], anterior-posterior diameter [depth]). Renal length was determined from axial slices by multiplying the slice thickness by the number of slices between the cranial and caudal poles of the kidneys. Lateral diameter was measured from the lateral extent of the kidney to the renal sinus and

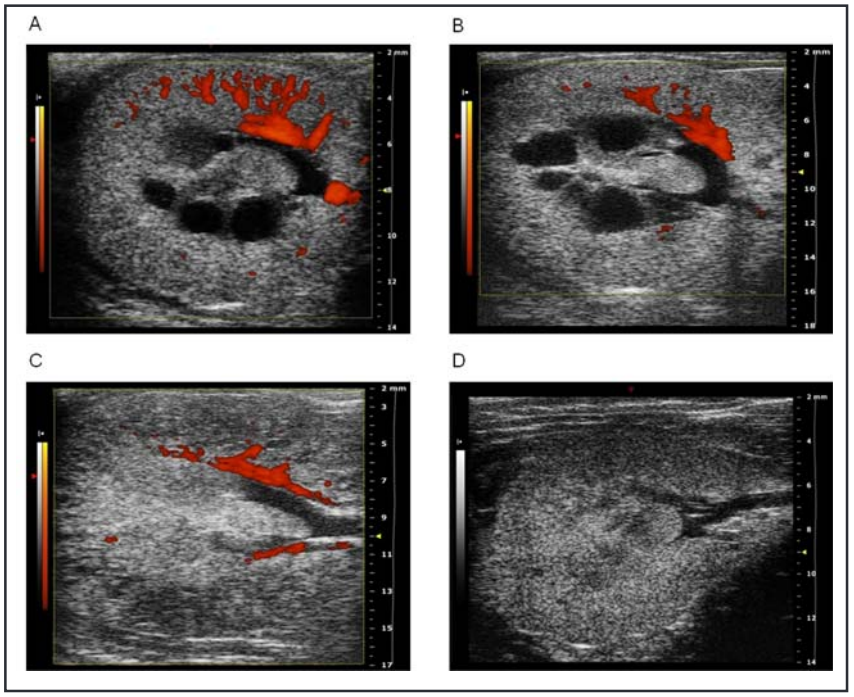

Fig. 2. Representative transverse 2-dimensional (2-D) B-mode images of the right kidney, overlaid with power Doppler (red areas) to identify blood flow within the renal parenchyma in 7-week old PCK rat (A), 12-week old PCK rat (B), 10-week old Cy/+ (Han:SPRD) rat (C) and 12-week old wild-type (+/+) rat (the latter is a 2-D B-mode image without power Doppler) (D).

anterior-posterior diameter was measured perpendicular to the lateral diameter. The ellipsoid TKV (TKVe) was calculated using the ellipsoid formula (length × lateral diameter × anterior-posterior diameter × π/6).

Histological analysis (HA)

One of the kidneys from each rat was used for the histological analysis and was sliced perpendicularly to the long axis at approximately 2 mm intervals. Slices from the mid-portion of the kidneys were fixed in 10% buffered formalin overnight, and tissues were then embedded in paraffin. Three µm sections were stained with Periodic acid–Schiff (PAS) staining following a routine protocol. The stained sections were subjected to CI analysis, using the HistoQuest image analysis software (TissueGnostics, Vienna, Austria). We calculated the total cystic and total kidney area in six full cross sections of each kidney and averaged the total cystic area (TCA) and total kidney area (TKA) in each PCK rat. The CI was calculated in percent as TCA/TKA*100.

Statistical analysis

Data are expressed as means ± SD. Different age groups were compared with two-tailed Student's t-test for unpaired data by using the GraphPad Prism version 5.0 software (GraphPad, San Diego, CA, USA). Bland–Altman plot and Pearson correlation test were used to show the differences in TKVs vs TKVa, TKVs vs TKVe, TKW vs TKVs and TKW vs TKVa. P values of <0.05 were considered statistically significant.

Results

TKV, TCV and TCN determination by stereological method

We performed HRU on 7- and 12-week old PCK rats (Fig. 2A and 2B), 10-week old heterozygous Cy/+ Han:SPRD rats (Fig. 2C) and 12-week old wild type +/+ rats (Fig. 2D). The kidney cysts were readily visible in 7- and 12-week old PCK rats. In Cy/+ Han:SPRD rats, the kidneys appeared to be enlarged compared with +/+ wild-type rats. Furthermore, the renal cortex showed an increased echogenicity in Cy/+ compared with +/+. Contrasting with PCK, individual cysts could however not be identified in Cy/+ kidneys, which is in line with the

Table 1. HRU-based stereological analysis of kidney and cyst volume in 7- and 12-week old PCK rat kidneys

	Volume of kidney (mm^3)			Volume of all cysts (mm^3)			Number of cysts			Cyst index (%)		
	Left	Right	Total	Left	Right	Total	Left	Right	Total	Left	Right	Mean
7-week old PCK rats												
1	1462	1366	2828	116	85	201	27	34	61	7.9	6.2	7.1
2	1439	1557	2996	57	68	125	26	37	63	4.0	4.4	4.2
3	1607	1636	3243	57	68	126	19	37	56	3.5	4.2	3.9
4	1587	1808	3394	77	70	147	24	34	58	4.9	3.9	4.4
5	1842	1812	3654	101	128	230	22	33	55	5.5	7.1	6.3
6	1973	1843	3815	93	160	253	30	38	68	4.7	8.7	6.7
Mean	1652	1670	3322	84	97	180	25	36	60	5.1	5.7	5.4
SD	194	171	345	22	35	50	4	2	4	1.4	1.8	1.3
12-week old PCK rats												
1	1767	2029	3796	50	110	160	22	29	51	2.8	5.4	4.1
2	1906	1902	3808	89	75	163	33	27	60	4.7	3.9	4.3
3	1963	1961	3924	96	102	198	26	25	51	4.9	5.2	5.0
4	1813	2205	4018	60	96	156	23	32	55	3.3	4.3	3.8
5	2078	2052	4130	156	73	229	41	36	77	7.5	3.6	5.5
6	2021	2427	4448	114	151	265	54	39	93	5.6	6.2	5.9
7	2365	2141	4506	119	70	189	21	27	48	5.0	3.3	4.2
8	2001	2543	4544	95	157	252	43	40	83	4.7	6.2	5.5
9	2620	2440	5060	61	94	155	28	25	53	2.3	3.9	3.1
10	2487	2588	5075	56	75	130	29	27	56	2.2	2.9	2.6
11	3106	2366	5472	141	84	225	20	29	49	4.6	3.5	4.1
12	2947	2923	5870	153	98	251	42	50	92	5.2	3.4	4.3
Mean	2256	2298	4554	99	99	198	32	32	64	4.4	4.3	4.4
SD	428	291	653	37	28	44	10	7	16	1.5	1.1	1.0

known histological observations. Thus, the PCK model appeared suitable for determining the TCV and TCN in addition to TKV by HRU, whereas in the Cy/+ only the TKV could be determined.

Thus, we then focused on PCK rats to determine TKV, TVC and TCN in 7- and 12-week old rats by the stereological image analysis method (Table 1). As expected, there was a significant increase in TKVs with age from 3322 ± 345 mm^3 at 7 weeks to 4554 ± 653 mm^3 at 12 weeks (P=0.0009), whereas the TCVs (180 ± 50 vs 198 ± 44 mm^3; P=0.4861), the TCNs (60 ± 4 vs 64 ± 16; P=0.6048) and the CI (5.4 ± 1.3 vs 4.4 ± 1.0%; P=0.0786) did not change between 7- and 12- weeks of age.

Altogether our findings demonstrate that TKVs, TCVs and TCNs can easily be measured by HRU in the PCK rat model, whereas HRU only allows to determine TKVs in the Cy/+ rat model because the cysts are too small to be detected by HRU.

TKV determination by automated and ellipsoid methods

We then determined the TKV by the automated (TKVa) and the ellipsoid (TKVe) method in 7- and 12-week old PCK rats, as well as in 10-week old Cy/+ Han:SPRD rats, and compared the values to the stereologically determined TKVs. These volumes were then correlated with the TKW which was obtained after euthanizing the animals. The time needed to measure TKVs was 20-30 minutes per animal, compared with 15-20 minutes for TKVa and 10-12 minutes for TKVe. Table 2 shows that the TKV analyzed by these three methods showed similar values, but with highest value for TKVs followed by TKVa and TKVe in 7-weeks old (3322 >3141>2937 mm^3) and in 12-weeks old (4554 >4308>3871 mm^3) PCK rats as well as in 10-weeks old (6610>6442>6035 mm^3) Cy/+ rats. The TKV detected by these three methods (TKVs, TKVa, and TKVe) were also in good agreement with the TKW (Table 2).

Fig. 3A and 3C show that there was a strong correlation of TKVs with TKVa (R^2=0.991, P<0.0001) and TKVe (R^2=0.966, P<0.0001) in PCK rats (n=18). The corresponding Bland-Altman plots (Fig. 3B and 3D) show that the TKVs exceeds the TKVa by 5.6 ± 2.1% (95% confidence interval, 1.5% to 9.9%) and the TKVe by 15.0 ± 3.8% (95% confidence interval, 7.6% to 22.4%). In Cy/+ rats (n=5) we also found a strong correlation of TKVs with TKVa (R^2=0.973, P=0.0019) and TKVe (R^2=0.999, P<0.0001) (graphs not shown).

TKV correlation with TKW

We then correlated TKVs and TKVa with TKW (Fig. 4A and 4B). TKW correlated well with TKVs (R^2=0.809, P<0.0001) and TKVa (R^2=0.782, P<0.0001) in PCK rats (n=18). The TKW (in mg) exceeded TKVs and TKVa (in mm^3) which is consistent with the specific weight of kidney tissue that is higher than water. In Cy/+ rats (n=5) the TKW also correlated well with TKVs (R^2=0.961, P=0.0033) and TKVa (R^2=0.940, P=0.0176) (graphs not shown).

Comparison of HRU with histological analysis (HA)

Using HA, the cyst burden in the PCK model can be estimated by CI determination which is calculated by dividing TCA with TKA and multiplying by 100. We were interested to determine the correlation of this area-based CI by HA with the volume-based CI which is obtained by HRUs and HRUa by dividing the TCV with TKV, multiplied by 100. The CI was significantly higher by HA in comparison to HRUs- and HRUa-based CI in 7- and 12- week old PCK rats (Table 3). Fig. 5A and 5B illustrate the histological view in a 7- and a 12-week old PCK rat and demonstrate the cyst growth between 7- and 12- weeks. Fig. 5C shows that the correlation between the area-based CI and the volume-based CI was weak (R^2=0.026, P=0.5247) (n=18).

3-D reconstruction from HRU

We finally generated 3-D reconstructions of HRU images which were acquired from PCK rat kidneys. Fig. 6A shows the tracings of the outer kidney and cyst wall used for the final reconstruction of the kidney and all cysts. Fig. 6B illustrates the types of 3-D images that can be obtained, revealing excellent spatial resolution of the cysts within the renal parenchyma in PCK rats (see also video clip of 3-D reconstructed kidney with cysts in a 12-week old PCK rat shown at the right QR-Code).

Table 2. Comparison of total kidney volumes as determined by stereological (TKVs), automated (TKVa) and ellipsoid (TKVe) methods with total kidney weight (TKW) in 7- and 12-week old PCK rats and in 10 weeks old Cy/+ Han:SPRD rats

	TKVs (mm^3)	TKVa (mm^3)	TKVe (mm^3)	TKW (mg)
7-week old PCK rats				
1	2828	2695	2513	3470
2	2996	2678	2526	3400
3	3243	3111	2883	4080
4	3394	3215	3073	3430
5	3654	3501	3233	3700
6	3815	3645	3395	4210
Mean	3322	3141	2937	3715
SD	345	366	334	321
12-week old PCK rats				
1	3796	3544	3268	4190
2	3808	3701	3347	3920
3	3924	3592	3147	4140
4	4018	3856	3424	3700
5	4130	3859	3345	3900
6	4448	4212	4056	4500
7	4506	4121	3642	5440
8	4544	4389	3846	4200
9	5060	4834	4455	5630
10	5075	4777	4304	5010
11	5472	5195	4664	6090
12	5870	5610	4950	5900
Mean	4554	4308	3871	4718
SD	653	639	581	816
10-week old Han:SPRD rats				
1	4470	4529	4098	3900
2	6488	6297	5951	6300
3	6973	6515	6321	7600
4	7053	6761	6438	7100
5	8067	8106	7366	8100
Mean	6610	6442	6035	6600
SD	1187	1145	1075	1475

Video clip. Video clip of 3-D reconstructed kidney with cysts in a 12-week old PCK rat.

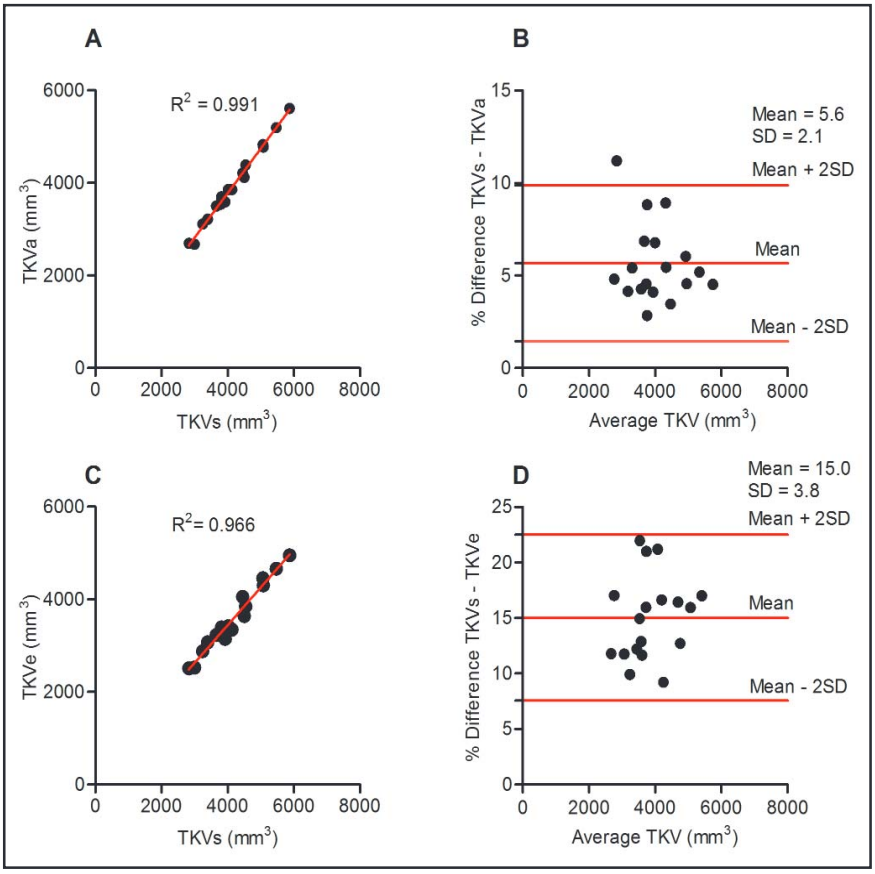

Fig. 3. Correlation of stereological total kidney volume (TKVs) with automated total kidney volume (TKVa) (A and B) and with ellipsoid total kidney volume (TKVe) (C and D) in 7- and 12-week old PCK rats (n=18).

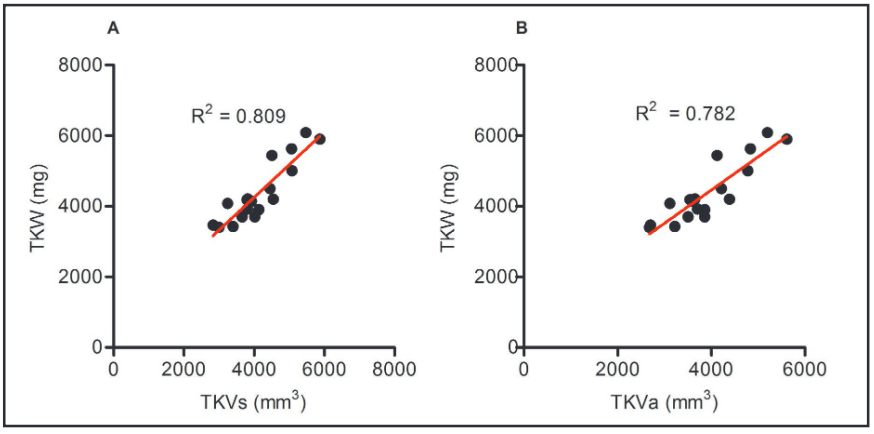

Fig. 4. Correlation of total kidney weight (TKW) with stereological total kidney volume (TKVs) (A) and with automated total kidney volume (TKVa) (B) in 7- and 12-week old PCK rats (n=18).

Discussion

In this study, we tested the utility of HRU in two different rat models of PKD, the PCK and the Han:SPRD rats. HRU allowed to visualize renal cysts and to determine the kidney and cyst volume and the number of cysts in PCK rats, whereas HRU did not allow to visualize the cysts in the Han:SPRD rat model of PKD since the cysts are too small to be visualized with the 18-38 MHz ultrasound probe. Nevertheless, the kidney volumes could be determined by HRU in Han:SPRD rat. Thus, the method could therefore be useful to follow kidney volume changes over time as well as in response to experimental therapies.

Among the three different types of HRU-based volumetric measurements (stereological, automated and ellipsoid) the stereological method was the most time consuming. Assuming that TKVs might provide the most precise volume measurements, the TKVa and the TKVe appeared to systematically underestimate the "true" TKV. All three methods correlated well with each other, and also with kidney weights. HRU also allowed accurate quantification of the number of cysts in each kidney, a parameter that cannot be obtained with the 2-D histological analysis that is unable to represent the entire kidney.

The HRU-based cyst volume determinations yielded cystic indices (CI) which did not correlate with the indices obtained by histological analysis. Assuming a more precise estimation of the cyst burden by determining the CI with the volumetric method, we believe that HRU improves precision over the histological method. This may be particularly relevant for experimental research which tests novel drugs to retard PKD disease progression.

PKD research has increased exponentially in the last three decades and has led to the development of several candidate drugs to prevent disease progression (i.e. cyst growth). Recent clinical trials with some of these drugs provided modest but encouraging results. However the management of most patients with ADPKD continues to be restricted to the detection and treatment of renal and extra-renal complications, and timely initiation of renal

Table 3. HRU-based cystic index (CI) determination using stereological (HRUs) and automated (HRUa) method, and comparison with histological analysis (HA)-based CI in 7- and 12- week old PCK rats

	HRUs (%)	HRUa (%)	HA (%)
7-week old PCK rats			
1	3.9	3.6	8.5
2	4.1	3.9	9.4
3	4.4	4.1	9.5
4	6.3	5.9	9.6
5	6.7	6.4	9.7
6	7.1	6.8	6.8
Mean	5.4	5.1	8.9
SD	1.3	1.3	1.1
12-week old PCK rats			
1	2.6	2.5	6.7
2	3.1	2.9	4.4
3	4.1	3.7	6.6
4	4.1	3.3	7.3
5	4.2	3.9	6.9
6	4.3	4.1	5.7
7	5.0	4.8	7.6
Mean	3.9	3.6	6.5
SD	0.8	0.7	1.0

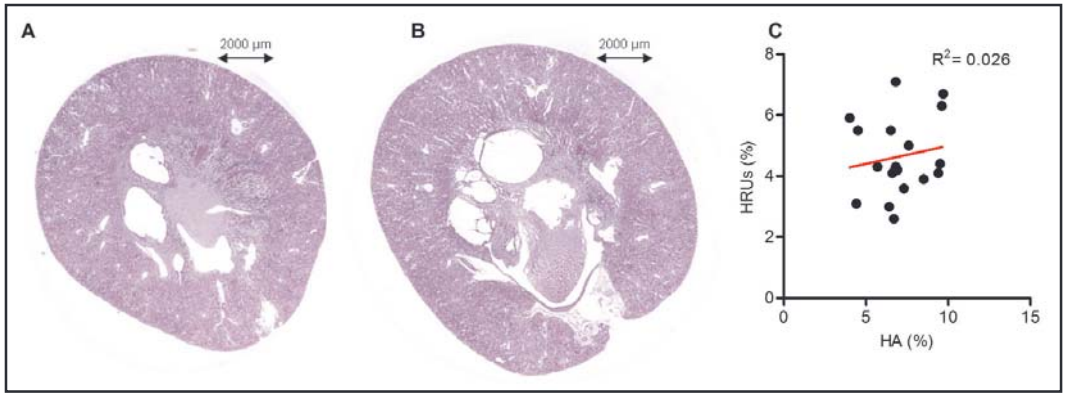

Fig. 5. Detection of cysts in male PCK rats by histology using Periodic acid–Schiff (PAS) staining in 7-week old (A) and 12-week old (B) PCK rats. Correlation of areal cystic index (%) obtained from histological analysis (HA) with volumetric cystic index (%) obtained from high resolution ultrasonography (HRU) using stereological method (HRUs) in PCK rats (C) (n=18).

replacement therapy which includes dialysis and transplantation [6]. The PCK rat represents a reliable experimental model of PKD that has been widely used to evaluate the efficacy of pharmacological interventions designed to ameliorate PKD. Thus, several drugs have been tested in PCK rats, including vasopressin V_2 receptor antagonists which were shown to be

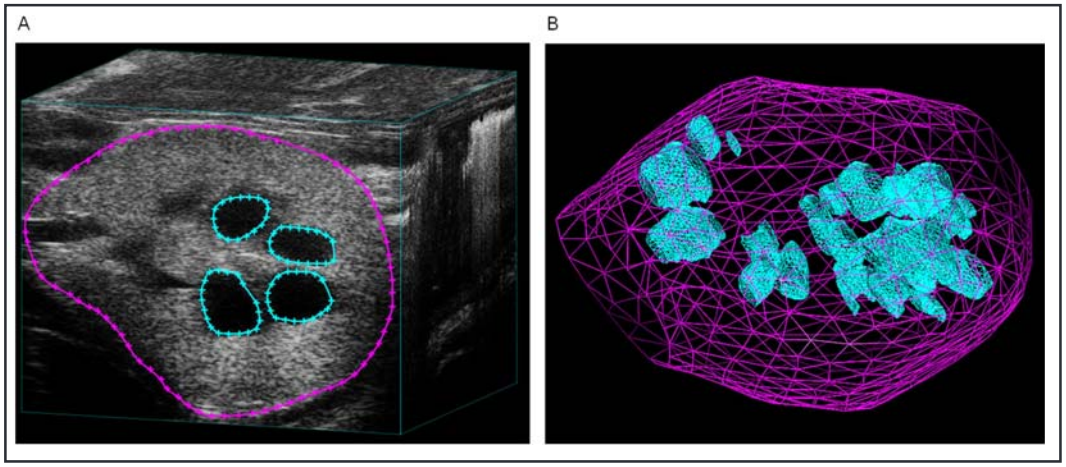

Fig. 6. A 3-dimensional (3-D) reconstruction from a PCK rat kidney showing the tracings of the outer cyst wall used for the final reconstruction (A), allowing visualisation of the kidney and the intra-parenchymal cysts and their spatial orientation (B).

effective in reducing cyst growth and slowing the decline of kidney function [7-9]. Other examples include chronic water loading which also ameliorated the renal pathology by an inhibition of vasopressin secretion [10] and the somatostatin agonists octreotide and pasireotide [11, 12]. In all these studies disease progression was monitored by histological analysis and not by ultrasound imaging. HRU offers the advantage over histological analyses to be more accurate and to be used repetitively without the need to euthanize the experimental animals. In previous studies, we examined the effect of dapagliflozin, an inhibitor of the renal sodium-glucose cotransporter 2 (SGLT2), in Han:SPRD [13] and in PCK rats [14] and found quite surprisingly that the drug had opposing effects. In PCK rats we evaluated the utility of HRU and found that HRU was very robust in evaluating the effect of the drug. Based on our results, we therefore recommend HRU in the PCK rat strain to precisely monitor cyst progression and to study the effect of novel drug therapies.

Our study is extending data from another study where it was shown that volume changes in the rat kidney can be measured in vivo with 3-D ultrasound using a position sensor [15, 16]. Furthermore, ultrasonography examination was shown to be useful and reliable for diagnosing PKD in cats with polycystic kidney [17-19]. It has also been shown that the resistive index which measures the arterial resistance in the peripheral vessels by Duplex-ultrasound is a valuable diagnostic tool to detect renal diseases in cats [20]. It is only by the HRU method however that intrarenal cysts can be visualized in rats. HRU therefore opens new possibilities for measurements of the volumes of organs in small animals such as rats.

As there is a great need to reduce the number of experimental animals, HRU might contribute to using a lower number of rats when examining cyst progression in PCK rats, since HRU offers sequential visualization of the cystic disease process in these rats over time. Thus, PCK rat kidneys can be examined at various intervals along a given treatment time, allowing dose adaptations and treatment prolongations without the need to sacrifice the experimental animals. In addition, since PCK also suffer liver disease, the HRU technique could also be used for sequential liver volume measurements. Thus, additional information can be gained in a single experimental animal with the advantage of a potentially lower number of rats.

In summary, we have shown that HRU is a very useful tool for measuring kidney and cyst volume in the PCK rat model of ARPKD, facilitating future pharmacological studies and offering the advantage to use a lower number of experimental animals.

Conclusion

HRU was used to determine total kidney and cyst volumes in PCK rats with polycystic kidney disease. HRU allows generating 3-D models from the sequentially obtained 2-D cineloops which scan each kidney from its cranial to caudal pole. This represents an excellent technique for visualizing the spatial orientation of the cysts within the kidney. Moreover, HRU-based TKV showed strong correlation with the respective kidney weights. HRU appears to be a suitable method to assess the progression of disease without euthanizing animals.

Abbreviations

ARPKD- autosomal recessive polycystic kidney disease; CI- cystic index; HA- histological analysis; HRU- high resolution ultrasonography; TCA- total cystic area; TKA- total kidney area; TCN- total cyst number; TCV- total cyst volume; TKV- total kidney volume; TKW- total kidney weight.

Disclosure Statement

The authors declare that they have no competing financial interest in the work presented here.

Acknowledgments

We thank Prof. Colin C. Schwarzwald from the Clinic for Equine Internal Medicine, Vetsuisse Faculty, for his support with the high resolution ultrasound system. Also, we thank Petra Seebeck and Svende Pfundstein from the Zürich Integrative Rodent Physiology (ZIRP), University of Zürich, for their help with the animal work. We also thank Andrea Brown from AnalyzeDirect, Inc. (Overland Park, KS) and the applications specialists and software developers from FUJIFILM VisualSonics, Inc. for their help in automated image analysis using both the VevoLab and the updated Analyze 12.0 software. The project was supported by the Swiss National Science Foundation (grant number 320030_144093) to RPW, and by the Hartmann Müller Foundation to SK.

References

1 Harris PC, Torres VE: Polycystic kidney disease. Annu Rev Med 2009;60:321-337.
2 Bergmann C: ARPKD and early manifestations of ADPKD: The original polycystic kidney disease and phenocopies. Pediatr Nephrol 2015;30:15-30.
3 Mason SB, Liang Y, Sinders RM, Miller CA, Eggleston-Gulyas T, Crisler-Roberts R, Harris PC, Gattone VH, 2nd: Disease stage characterization of hepatorenal fibrocystic pathology in the PCK rat model of ARPKD. Anat Rec (Hoboken) 2010;293:1279-1288.
4 Moran CM, Pye SD, Ellis W, Janeczko A, Morris KD, McNeilly AS, Fraser HM: A comparison of the imaging performance of high resolution ultrasound scanners for preclinical imaging. Ultrasound Med Biol 2011;37:493-501.
5 Khankin EV, Hacker MR, Zelop CM, Karumanchi SA, Rana S: Intravital high-frequency ultrasonography to evaluate cardiovascular and uteroplacental blood flow in mouse pregnancy. Pregnancy Hypertens 2012;2:84-92.
6 Chebib FT, Sussman CR, Wang X, Harris PC, Torres VE: Vasopressin and disruption of calcium signalling in polycystic kidney disease. Nat Rev Nephrol 2015;11:451-464.

7 Wang X, Gattone V, 2nd, Harris PC, Torres VE: Effectiveness of vasopressin V2 receptor antagonists OPC-31260 and OPC-41061 on polycystic kidney disease development in the PCK rat. J Am Soc Nephrol 2005;16:846-851.
8 Gattone VH, 2nd, Wang X, Harris PC, Torres VE: Inhibition of renal cystic disease development and progression by a vasopressin V_2 receptor antagonist. Nat Med 2003;9:1323-1326.
9 Torres VE, Chapman AB, Devuyst O, Gansevoort RT, Grantham JJ, Higashihara E, Perrone RD, Krasa HB, Ouyang J, Czerwiec FS, Investigators TT: Tolvaptan in patients with autosomal dominant polycystic kidney disease. N Engl J Med 2012;367:2407-2418.
10 Nagao S, Nishii K, Katsuyama M, Kurahashi H, Marunouchi T, Takahashi H, Wallace DP: Increased water intake decreases progression of polycystic kidney disease in the PCK rat. J Am Soc Nephrol 2006;17:2220-2227.
11 Masyuk TV, Radtke BN, Stroope AJ, Banales JM, Gradilone SA, Huang B, Masyuk AI, Hogan MC, Torres VE, Larusso NF: Pasireotide is more effective than octreotide in reducing hepatorenal cystogenesis in rodents with polycystic kidney and liver diseases. Hepatology 2013;58:409-421.
12 Masyuk TV, Masyuk AI, Torres VE, Harris PC, Larusso NF: Octreotide inhibits hepatic cystogenesis in a rodent model of polycystic liver disease by reducing cholangiocyte adenosine 3',5'-cyclic monophosphate. Gastroenterology 2007;132:1104-1116.
13 Rodriguez D, Kapoor S, Riwanto M, Edenhofer I, Segerer S, Mitchell K, Wüthrich RP: Inhibition of sodium-glucose cotransporter 2 with dapagliflozin in Han: SPRD rats with polycystic kidney disease. Kidney Blood Press Res 2015;40:638-647.
14 Kapoor S, Rodriguez D, Riwanto M, Edenhofer I, Segerer S, Mitchell K, Wüthrich RP: Effect of sodium-glucose cotransport inhibition on polycystic kidney disease progression in PCK rats. PLoS One 2015;10:e0125603.
15 Stormark TA, Strommen K, Iversen BM, Matre K: Three-dimensional ultrasonography can detect the modulation of kidney volume in two-kidney, one-clip hypertensive rats. Ultrasound Med Biol 2007;33:1882-1888.
16 Bakker J, Olree M, Kaatee R, de Lange EE, Moons KG, Beutler JJ, Beek FJ: Renal volume measurements: Accuracy and repeatability of US compared with that of MR imaging. Radiology 1999;211:623-628.
17 Biller DS, DiBartola SP, Eaton KA, Pflueger S, Wellman ML, Radin MJ: Inheritance of polycystic kidney disease in Persian cats. J Hered 1996;87:1-5.
18 Bonazzi M, Volta A, Gnudi G, Bottarelli E, Gazzola M, Bertoni G: Prevalence of the polycystic kidney disease and renal and urinary bladder ultrasonographic abnormalities in Persian and Exotic Shorthair cats in Italy. J Feline Med Surg 2007;9:387-391.
19 Lee YJ, Chen HY, Hsu WL, Ou CM, Wong ML: Diagnosis of feline polycystic kidney disease by a combination of ultrasonographic examination and PKD1 gene analysis. Vet Rec 2010;167:614-618.
20 Tipisca V, Murino C, Cortese L, Mennonna G, Auletta L, Vulpe V, Meomartino L: Resistive index for kidney evaluation in normal and diseased cats. J Feline Med Surg 2016, in press.

Chapter 6

Inhibition of aerobic glycolysis attenuates disease progression in polycystic kidney disease

Meliana Riwanto[1,2], Sarika Kapoor[1], Daniel Rodriguez[1], Ilka Edenhofer[1], Stephan Segerer[1,2], Rudolf P. Wüthrich[1,2]

[1] Nephrology, Institute of Physiology, University of Zürich, Zürich, Switzerland,
[2] Division of Nephrology, University Hospital Zürich, Zürich, Switzerland

PLoS ONE 11(1): e0146654

Contribution by Daniel Rodriguez:

Animal treatment assistance and histological analysis with image analysis software.

PLOS | ONE

RESEARCH ARTICLE

Inhibition of Aerobic Glycolysis Attenuates Disease Progression in Polycystic Kidney Disease

Meliana Riwanto[1,2], Sarika Kapoor[1], Daniel Rodriguez[1], Ilka Edenhofer[1], Stephan Segerer[1,2], Rudolf P. Wüthrich[1,2]*

1 Nephrology, Institute of Physiology, University of Zurich, Zurich, Switzerland, 2 Division of Nephrology, University Hospital Zurich, Zurich, Switzerland

* rudolf.wuethrich@usz.ch

Citation: Riwanto M, Kapoor S, Rodriguez D, Edenhofer I, Segerer S, Wüthrich RP (2016) Inhibition of Aerobic Glycolysis Attenuates Disease Progression in Polycystic Kidney Disease. PLoS ONE 11(1): e0146654. doi:10.1371/journal.pone.0146654

Editor: Eric Feraille, University of Geneva, SWITZERLAND

Received: August 4, 2015

Accepted: December 21, 2015

Published: January 11, 2016

Data Availability Statement: All relevant data are within the paper and the results of our microarray analysis to the NCBI's Gene Expression Omnibus (GEO). The microarray results are available online (accession number GSE75578) at the NCBI GEO (http://www.ncbi.nlm.nih.gov/geo/query/acc.cgi?acc=GSE75578).

Funding: This study was supported by funding from the Forschungkredit Postdoc grant to MR, grants by the CKM-Stiftung and Fundação Pesquisa e Desenvolvimento Humanitário to SS, the Novartis Foundation for medical-biological research and the

Abstract

Dysregulated signaling cascades alter energy metabolism and promote cell proliferation and cyst expansion in polycystic kidney disease (PKD). Here we tested whether metabolic reprogramming towards aerobic glycolysis ("Warburg effect") plays a pathogenic role in male heterozygous Han:SPRD rats (Cy/+), a chronic progressive model of PKD. Using microarray analysis and qPCR, we found an upregulation of genes involved in glycolysis (Hk1, Hk2, Ldha) and a downregulation of genes involved in gluconeogenesis (G6pc, Lbp1) in cystic kidneys of Cy/+ rats compared with wild-type (+/+) rats. We then tested the effect of inhibiting glycolysis with 2-deoxyglucose (2DG) on renal functional loss and cyst progression in 5-week-old male Cy/+ rats. Treatment with 2DG (500 mg/kg/day) for 5 weeks resulted in significantly lower kidney weights (-27%) and 2-kidney/total-body-weight ratios (-20%) and decreased renal cyst index (-48%) compared with vehicle treatment. Cy/+ rats treated with 2DG also showed higher clearances of creatinine (1.98±0.67 vs 1.41±0.37 ml/min), BUN (0.69±0.26 vs 0.40±0.10 ml/min) and uric acid (0.38±0.20 vs 0.21±0.10 ml/min), and reduced albuminuria. Immunoblotting analysis of kidney tissues harvested from 2DG-treated Cy/+ rats showed increased phosphorylation of AMPK-α, a negative regulator of mTOR, and restoration of ERK signaling. Assessment of Ki-67 staining indicated that 2DG limits cyst progression through inhibition of epithelial cell proliferation. Taken together, our results show that targeting the glycolytic pathway may represent a promising therapeutic strategy to control cyst growth in PKD.

Introduction

Autosomal dominant polycystic kidney disease (ADPKD) is the most common genetic renal disease, characterized by progressive development of innumerable cysts in both kidneys. The development and relentless growth of cysts lead to kidney enlargement and compression of renal parenchyma, leading to subsequent loss of renal function [1,2]. Recent studies have indicated that various signaling cascades are dysregulated in ADPKD, including activation of

Swiss National Science Foundation (grant number 320030_144093) to RPW. The funders had no role in study design, data collection and analysis, decision to publish, or preparation of the manuscript.

Competing Interests: The authors have declared that no competing interests exist.

mTOR and downregulation of AMPK signaling, and enhanced vasopressin-mediated cAMP and ERK signaling [3,4,5,6]. Favourable results from several clinical trials targeting these pathways have led to the development of therapeutic concepts for ADPKD, yet treatment is not available for the majority of patients [7].

A promising strategy to achieve therapeutic selectivity and efficacy in ADPKD is to take advantage of the fundamental difference between cyst epithelial cells and normal epithelial cells in their energy metabolism. A recent study by Rowe et al. has shown that glycolysis was enhanced in a mouse model of ADPKD and also in kidney tissues from patients with ADPKD [8]. Metabolomic profiling of extracellular medium of embryonic fibroblast cultures derived from *Pkd1*$^{-/-}$ and *Pkd1*$^{+/+}$ mice indicated increased glucose uptake and lactate production and enhanced glycolytic enzyme gene expression in the mutant cells [8]. Using 2-deoxyglucose (2DG), an analog of glucose that blocks glycolysis, they found that cyst growth could be inhibited in rapidly progressing mouse models of polycystic kidney disease (PKD). Although the tested models did not allow for assessment of renal function, the data suggested that targeting glycolysis might represent a novel therapeutic strategy in ADPKD.

The purpose of the present study was to extend the above observations and to examine whether 2DG could be used in a chronic progressive rat model of PKD. Here we show that cystic kidneys in Han:SPRD rats display metabolic reprogramming in the sense of a 'Warburg effect' and that 2DG improved renal functional loss and cyst progression through normalization of intracellular signaling pathways.

Methods

Animals

The Han:SPRD rat colony was established in our animal facility from a litter which was obtained from the Rat Resource and Research Center (Columbia, MO, USA). Heterozygous cystic (Cy/+) and wild type normal (+/+) rats were used in this study. Han:SPRD rats carry a missense mutation in *Anks6* (also called *Pkdr1*), leading to an R823W substitution in SamCystin, a protein that contains ankyrin repeats and a sterile alpha motif (SAM) [9]. Han:SPRD Cy/+ rats develop a slowly progressing form of PKD which resembles phenotypically human ADPKD [10]. Only male rats were used in this study since cysts develop more rapidly in male compared with female rats [11]. The protocol has been approved by the committee on the Ethics of Animals Experiments at the University of Zurich (Licence Number: 174–2013). Rats had free access to tap water and standard rat diet.

Genechip expression analysis

Affymetrix GeneChip® rat genome 230 2.0 arrays were used according to the manufacturer's instructions (Affymetrix Inc., Santa Clara, CA, USA). Briefly, 5 μg of total RNA from 5-week old Cy/+ and +/+ rat kidneys was used as starting material to generate biotin-labeled cRNA samples, which includes cDNA synthesis using oligo-dT/T7 primers, followed by *in vitro* transcription (one-cycle labeling protocol). Labeled cRNA samples (15 μg) were randomly fragmented to 35–200 bp and hybridized on arrays for 16 h. After washing the arrays the fluorescent intensity emitted by the labeled targets was measured by an Affymetrix GeneChip® Scanner 3000. Finally, the hybridization images were analyzed using Affymetrix GCOS 1.2 software.

Reverse transcription and real-time PCR

RT-PCR analyses were performed as described previously [12,13]. Total RNA was reverse-transcribed and PCR was carried out using SYBR® Green JumpStart Taq ReadyMix (Sigma-

Aldrich, St Louis, MO, USA). Real-time PCR analyses were performed with the ABI PRISM 7500 Sequence Detection System (Applied Biosystems, Rotkreuz, Switzerland), according to the instructions of Applied Biosystems. The expression levels of β-actin were used as a house-keeping gene. Relative quantification of all targets was calculated by the comparative cycle threshold method outlined by the manufacturer (User Bulletin No. 2; Applied Biosystems, Rotkreuz, Switzerland).

Experimental protocol

Male Cy/+ and +/+ rats were weaned and then treated at 5 weeks of age with 500 mg/kg/day 2DG (Cy/+: n = 10; +/+: n = 10) or vehicle NaCl (Cy/+: n = 10; +/+: n = 10) by daily subcutaneous injection for 5 weeks throughout the treatment phase. The dose of 2DG or vehicle was adjusted daily to the body weight of the rats. For blood collection, rats were anesthetized with inhalation of 1.5–3.5% isoflurane. Metabolic cages were used to collect 24-hour urine samples and to monitor food and fluid intake. Rats were acclimatized to the metabolic cage for an hour every day for three consecutive days prior to the actual metabolic cage experiment. All animals were sacrificed at week 10 by CO_2 euthanasia.

Blood and urine chemistries

Plasma and 24-hour urines were collected from rats at week 5, 7.5 and 10 and aliquots were rapidly frozen and stored at -80°C until measurement. Glucose, sodium, chloride, creatinine, blood urea nitrogen (BUN) and uric acid concentrations were determined in plasma and urine using a Cobas 8000 Modular Analyzer from Roche Diagnostics AG (Rotkreuz, Switzerland). Plasma and urine osmolality were measured by using an Advanced Osmometer Model 2020 (Advanced Instruments Inc., Norwood, MA, USA). Urinary albumin concentration was determined using a rat albumin ELISA kit (Genway, San Diego, CA, USA), as previously described [14]. Albuminuria was expressed as total urinary albumin excretion over 24-hour. Urine proteins were also analyzed by non-reducing SDS-PAGE and Coomassie blue staining.

Tissue processing, periodic acid-Schiff staining, and cyst index measurement

At the age of 10 weeks, all rats were sacrificed and kidneys were excised, decapsulated and weighed. For histological examination, one of the kidneys from each animal was sliced perpendicularly to the long axis at approximately 2 mm intervals. Slices from the midportion of the kidneys were fixed in 4% buffered formalin and submitted to subsequent paraffin embedding. Serial sections of 3 μm thickness per paraffin block were cut and stained with periodic acid-Schiff (PAS) following a routine protocol. The stained sections were subjected to cyst index analysis, using the HistoQuest image analysis software (TissueGnostics, Vienna, Austria) to determine the cyst area (CA) and the total area (TA). The cyst index was calculated as CA/TA□100.

Immunohistochemical detection of proliferation

Immunohistochemistry for Ki67 was performed on 3-μm tissue sections. In brief, the tissue sections were deparaffinized and rehydrated. The antigen retrieval was performed in an autoclave oven. Primary mouse anti-Ki67 antibody (BD Pharmingen, San Jose, CA, USA) and biotinylated secondary antibody (Vector, Los Angeles, CA, USA) were used. This was followed by the application of the ABC reagent, using 3,3'-diaminobenzidine with metal enhancement as the detection reagent. The stained sections were subjected to analysis using the HistoQuest

image analysis software (TissueGnostics, Vienna, Austria) to quantify the number of Ki67-positive nuclei over the total area of the kidney section.

Primary TEC cultures

Primary cultures of renal tubular epithelial cells (TECs) from 10-week-old +/+ and Cy/+ kidneys were prepared by mincing the kidneys and digesting the tissues with 1 mg/ml collagenase with gentle agitation for 1 h at 37°C. The suspension was allowed to sediment for 1 min. Cells were collected by harvesting the supernatant twice, and were then washed three times with 10% fetal bovine serum (FBS)/Hanks balanced salt solution. Isolated cells were resuspended in K1 medium (1:1 mixture of Dulbecco's modified Eagle's medium and Ham's F-12 medium supplemented with 5% FBS, 10 mmol/l HEPES, 42 mmol/l sodium bicarbonate, 50 ng/ml insulin, 50 nmol/l hydrocortisone, 50 ng/ml transferrin, 5 pmol/l triiodothyronine, 20 ng/ml rat EGF, 100 IU/ml penicillin, and 100 μg/ml streptomycin). Cells were then seeded in collagen type 1–precoated culture dishes and grown to confluence. The medium was changed to a K1 medium with 0.5% FBS for 24 h, and the cells were then incubated with 2DG at various concentrations for 24 h. Cell viability was assessed by MTS assay following standard protocols.

Normal human kidney epithelial cells (NHK) were obtained from ATCC (ATCC® PCS-400-010™, Manassas, VA, USA). ADPKD cells were prepared from nephrectomy material as previously described [15], after obtaining ethical approval from the ethics committee of the canton of Zurich, Switzerland, and informed oral consent. The culture conditions for ADPKD and NHK cells were similar to that of rat primary renal tubular epithelial cells.

Western blotting analysis

Snap frozen kidney tissue was homogenized and tissue lysates or cell culture lysates were resolved by SDS–polyacrylamide gel electrophoresis, transferred to nitrocellulose membranes, and probed with primary antibodies. Mouse anti-Phospho-p70-S6K (Thr389), rabbit anti-p70-S6K mouse anti-Phospho-Erk1/2 (Thr202/Tyr24), rabbit anti-Erk1/2, rabbit anti-Phospho-AMPKα (Thr172), mouse-anti-Phospho-Akt (Ser473), rabbit anti-Akt and anti-caspase-3 antibodies were obtained from Cell signaling Technology, Beverly, MA, USA. Mouse anti-AMPKα was obtained from Santa Cruz Biotechnology (Santa Cruz, CA, USA). Anti-mouse and anti-rabbit secondary antibodies were purchased from Licor Biosciences (Lincoln, Nebraska, USA).

ATP and lactate quantification

Intracellular ATP was quantified by luciferase activity according to the standard protocol in the ATP Determination kit (Invitrogen, Life Technologies, Zug, Switzerland). The concentration of lactate in cell culture supernatants and in kidney tissue from Han:SPRD rats was measured using the EnzyChrom L-lactate Assay Kit (BioAssay Systems, Hayward, USA), according to the manufacturer's instructions.

In vitro BrdU Proliferation Assay

In vitro proliferation of primary TEC was analyzed with the colorimetric cell proliferation BrdU assay kit (Roche Applied Science, Indianapolis, USA) according to the manufacturer's instruction. Briefly, cells were cultured in 96-well plates with or without 2DG. After 48 hours, cells were labeled using 10 μM BrdU per well and re-incubated overnight at 37°C in a humidified atmosphere. The next day, the culture media was removed, the cells were fixed, and the DNA was denatured in one step by adding FixDenat solution. Cells were incubated with anti-

BrdU-POD antibody, washed and the substrate solution was added. The reaction product was quantified by measuring the absorbance using a spectrophotometer at 370 nm with a reference wavelength of 492 nm.

In vitro Cell Apoptosis Assay

Cells were cultured in 6-well plates with or without 2DG at a concentration of 1, 5, and 10 mM. After 24 hours, cells were collected following detachment with trypsin, resuspended in 140 mM NaCl, 10 mM HEPES, and 2.5 mM $CaCl_2$ and incubated with annexin V-FITC (Roche Diagnostics, Basel, Switzerland) for 30 minutes at room temperature according to the manufacturer's instructions. Flow cytometric analyses were performed using a BD-FACScan flow cytometer (BD Biosciences, San Jose, CA, USA). Data were analyzed using FlowJo software (Treestar Inc., Ashland, OR, USA.).

Statistical analyses

All data are expressed as means ± SEM unless otherwise stated. Statistical analyses were performed using Student's-t-test and ANOVA with Dunnett post-hoc test for multiple comparison analysis using GraphPad Prism version 5.0 (Graph Pad Inc., San Diego, CA, USA). A value of $P < 0.05$ was considered as statistically significant.

Results

Increased glycolysis and decreased gluconeogenesis in polycystic kidney disease

First we performed microarray gene expression analysis on mRNA transcripts from kidney tissues from Han:SPRD Cy/+ and wild-type +/+ male rats to examine the glycolysis and the gluconeogenesis pathways of glucose metabolism. The microarray results are available online (accession number GSE75578) at the NCBI Gene Expression Omnibus (GEO). The mRNA levels of several genes involved in the glycolysis pathway were upregulated, whereas transcript levels of genes encoding for enzymes in gluconeogenesis were significantly donwregulated (Fig 1A and 1B). This observation was confirmed by quantitative real-time PCR analysis which demonstrated upregulation of key genes involved in the glycolysis pathway (*Hk1*, *Hk2*, *Ldha*) and downregulation of key genes involved in the gluconeogenesis pathway (*Fbp1*, *Fbp2*, *G6pc*) in the kidney tissues of Cy/+ rats versus +/+ rats (Fig 1C). Furthermore, upregulation of *Hk1* and *Hk2* genes was also observed in primary cell cultures of human ADPKD as compared to control primary cultures of normal human kidney (NHK) epithelial cells (Fig 1D).

To extend these observations we measured the intracellular ATP levels and the production of lactate *in vitro* using primary cell cultures of tubular epithelial cells isolated from kidneys of Cy/+ versus +/+ rats. The intracellular ATP levels were significantly increased in the Cy/+ cell cultures as compared to +/+ cell cultures, and were decreased upon incubation of Cy/+ cells with 2DG (Fig 2A). Furthermore, the lactate content in the cell culture media was higher in Cy/+ cell cultures in comparison to +/+ cell cultures, and was also decreased upon incubation of Cy/+ cells with 2DG (Fig 2B). No significant changes in the intracellular ATP levels or lactate content in the cell culture media were observed when +/+ cells were incubated with 2DG (Fig 2A and 2B). Similar observations were obtained in the primary cell cultures of human ADPKD and NHK cells; intracellular ATP levels and lactate in the cellular medium were higher in ADPKD cells as compared to NHK cells, and the levels were diminished upon incubation of ADPKD cells with 2DG (Fig 2D and 2E).

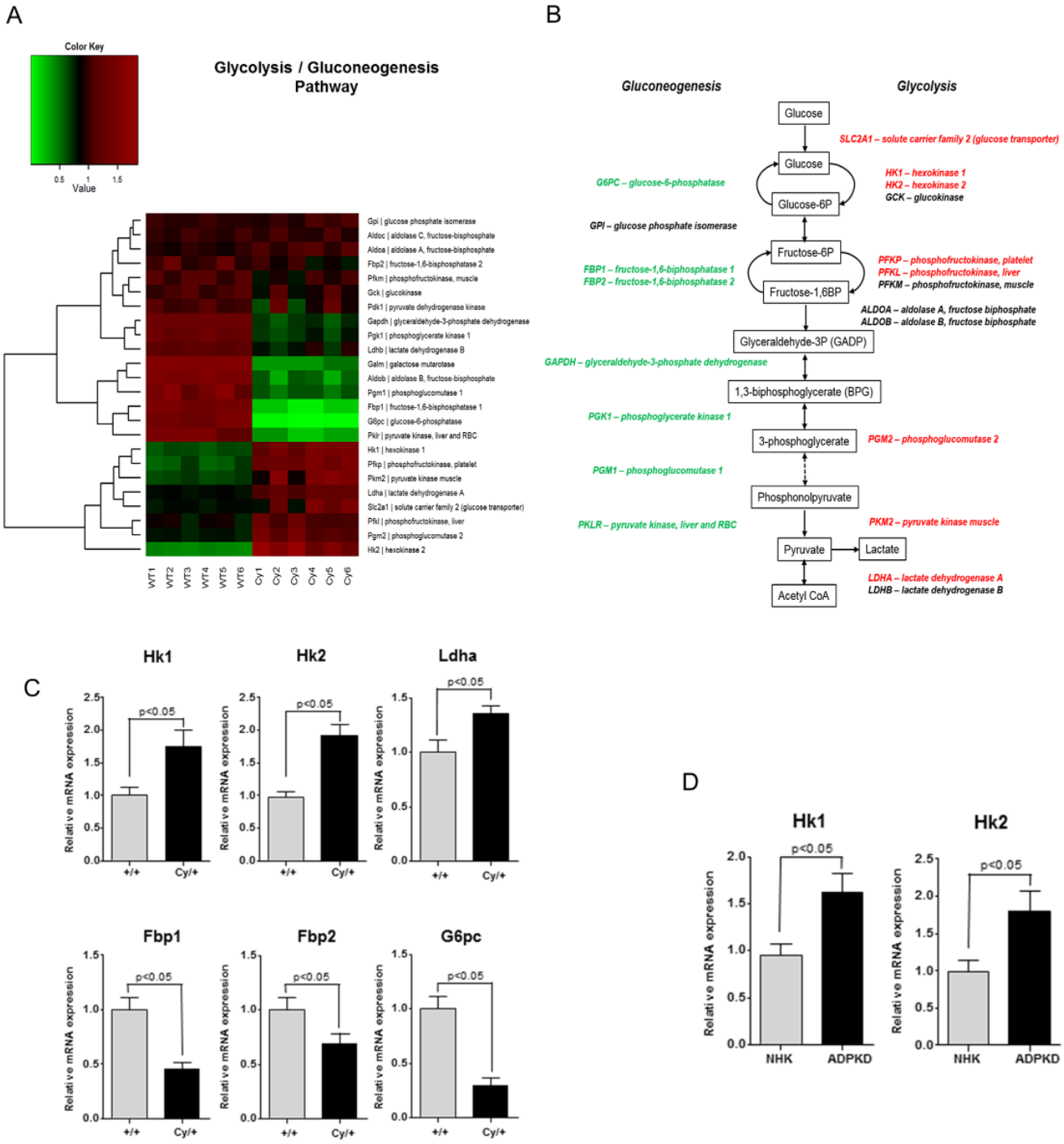

Fig 1. Dysregulation of the glycolysis and gluconeogenesis pathways in rat polycystic kidney disease. (A) Microarray analysis showing differential expression of genes coding for glycolysis and gluconeogenesis enzymes in Han:SPRD Cy/+ and wild-type +/+ kidneys. Upregulated genes are shown in red, and downregulated genes are shown in green. (B) Schematic diagram showing the glycolysis/gluconeogenesis cascades. In red, upregulated genes; green, downregulated genes; black, genes unchanged in kidneys from Cy/+ rats compared with wild-type +/+ kidneys. (C) Real-time quantitative PCR analysis of genes coding for key enzymes involved in glycolysis/gluconeogenesis in kidneys from Cy/+ rats and +/+ rats. (D) Real-time quantitative PCR analysis of the hexokinase-1 (Hk1) and hexokinase-2 (Hk2) genes in primary cell cultures of human ADPKD and control NHK cells. The expression levels of β-actin were used as a housekeeping gene.

doi:10.1371/journal.pone.0146654.g001

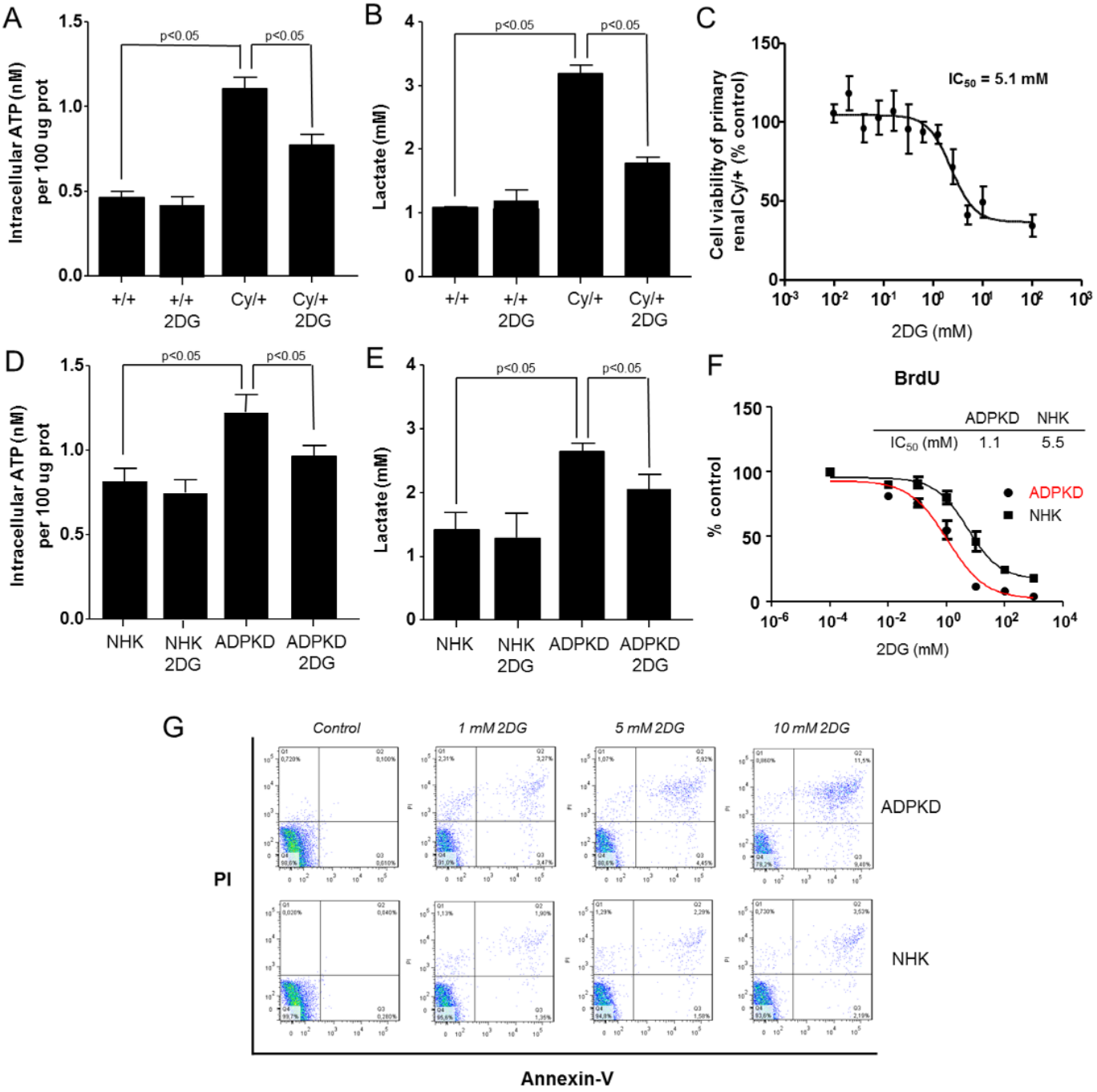

Fig 2. Increased glycolytic phenotype in polycystic kidney disease. (A) Intracellular ATP content in primary cell cultures of tubular epithelial cells isolated from kidneys of Cy/+ and +/+ rats. (B) Lactate concentration in the medium of primary cell cultures of tubular epithelial cells isolated from kidneys of Cy/+ and +/+ rats. (C) Cell growth of primary renal Cy/+ cells upon incubation with increasing concentrations of 2DG, as assessed by the MTS assay. (D) Intracellular ATP content in primary cell cultures of ADPKD and NHK cells. (E) Lactate concentration in the medium of primary cell cultures of ADPKD and NHK cells. (F) Effect of 2DG on cell proliferation of human ADPKD cells and control NHK cells, as quantified by BrdU assay. (G) Effect of 2DG on apoptosis of human ADPKD cells and control NHK cells, as analyzed with annexin-V/propidium iodide (PI) staining using flow cytometry.

doi:10.1371/journal.pone.0146654.g002

To analyze the effect of 2DG on cell proliferation and apoptosis we incubated primary renal tubular epithelial cells from Cy/+ rats with increasing concentrations of 2DG and found reduced cellular growth, as measured by the MTS assay (IC_{50} = 5.1 mM, Fig 2C). We also evaluated the effect of 2DG on cell proliferation and apoptosis of primary cultures of human ADPKD cells and control NHK cells. Incubation with 2DG limited cell proliferation (BrdU assay) and increased apoptosis (annexin-V staining) of primary human ADPKD cells in concentration-dependent manner (Fig 2F and 2G). Of note, the effects of 2DG on cell proliferation and apoptosis were more pronounced on ADPKD cells than on NHK cells, indicating a therapeutic potential of 2DG in human ADPKD (Fig 2F and 2G).

In vivo effect of 2DG treatment

Effect of 2DG treatment on kidney weight and morphology. To assess the *in vivo* effect of glycolysis inhibition on cyst development and disease progression, we examined the effects of 2DG treatment in Han:SPRD Cy/+ and +/+ control rats. Rats were treated with 500 mg/kg/day 2DG or vehicle NaCl daily for 5 weeks. Based on the human equivalent dose [16], the amount of 2DG administered is equivalent to approximately 81 mg/kg/day in human. A previous study has reported 63 mg/kg/day to be the clinically tolerable dose for human clinical trials, with reversible side effects observed at a dose range of 63–88 mg/kg/day [17]. The dose used in the current proof-of-concept study should therefore not lead to any significant irreversible adverse effects.

The 5-week treatment with 2DG was generally well tolerated in both animal groups. Side effects included lower body weight and mildly increased diuresis in 2DG-treated Cy/+ and +/+ rats. There were no significant changes in the plasma Na^+ and Cl^-, and no difference in plasma glucose levels between 2DG- and vehicle-treated Cy/+ and +/+ rats. At the end of the 5-week treatment phase, the total weight of both kidneys was significantly lower in 2DG-treated Cy/+ rats in comparison with vehicle-treated Cy/+ rats (-27.2%, P< 0.001; Table 1). The 2-kidneys/body weight ratio was also lower upon 2DG treatment in Cy/+ rats as compared to vehicle treatment (-20.4%, P< 0.01; Table 1, Fig 3A and 3B).

Table 1. Effect of 2DG treatment on kidney and body weight.

	+/+					Cy/+				
	Baseline	Week 2.5		Week 5		Baseline	Week 2.5		Week 5	
		Vehicle	2DG	Vehicle	2DG		Vehicle	2DG	Vehicle	2DG
Number of animals (n)	20	10	10	10	10	20	10	10	10	10
Age (in weeks)	5	7.5	7.5	10	10		7.5	7.5	10	10
Body Weight (g)	161.4 (17.5)	284.7 (17.9)	266.8 (25.5)	339.2 (28.2)	328 (24.6)	167.4 (20.0)	290.1 (33.2)	263.1 (25.3)	345.0 (31.5)	317.1* (26.0)
Total kidney weight (g)				2.38 (2.66)	2.35 (1.75)				8.67 (1.46)	6.31*** (1.14)
%TKW/BW				0.70 (0.06)	0.72 (0.04)				2.50 (0.29)	1.99** (0.30)

Data are presented as means and standard deviations (in parentheses).

*P<0.05,

**P<0.01,

***P<0.001 when comparing 2DG- versus vehicle-treated groups at each time point. TKW/BW, total kidney weight divided by body weight.

doi:10.1371/journal.pone.0146654.t001

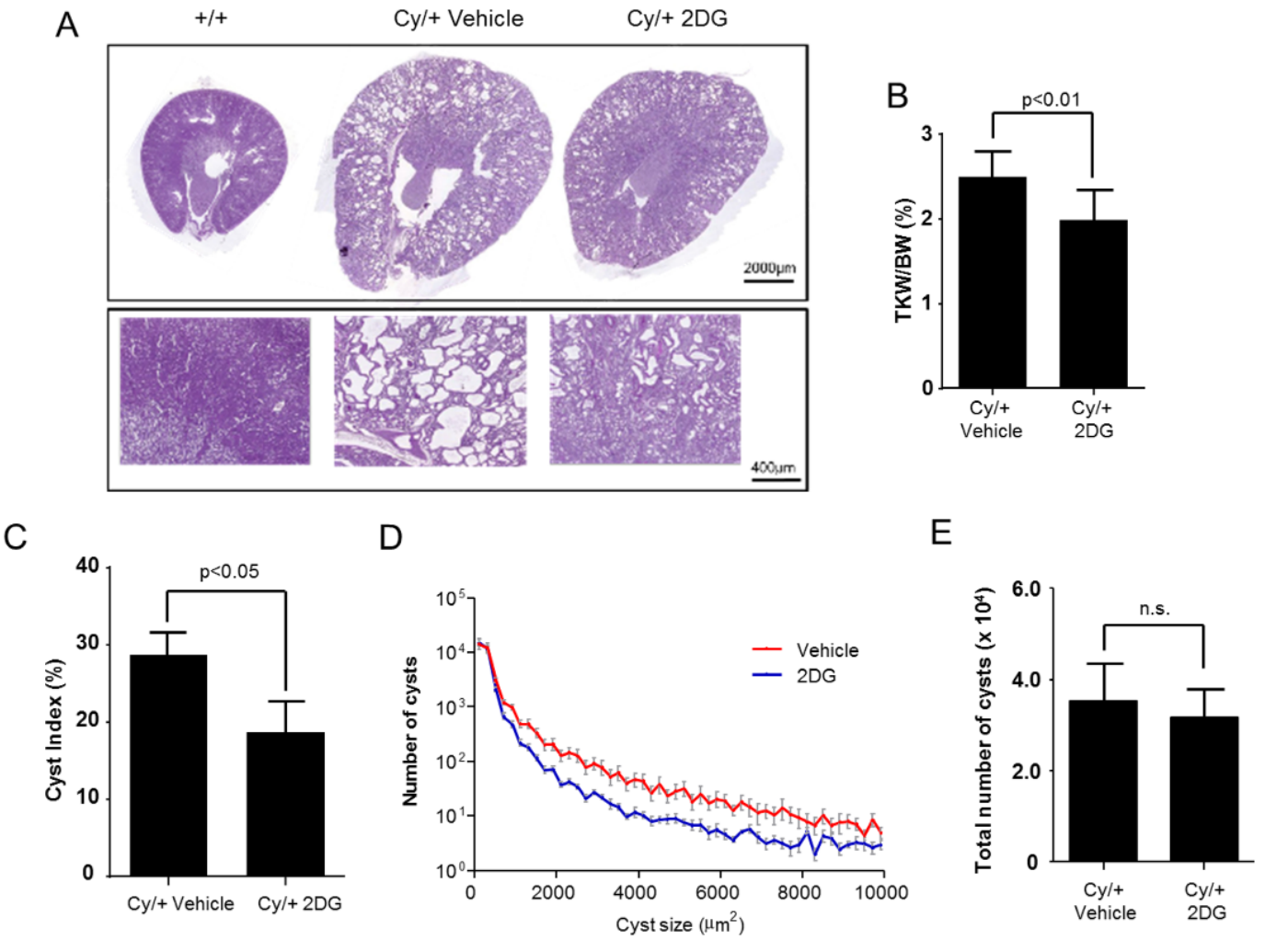

Fig 3. Effect of 2DG treatment on kidney weight and morphology in Han:SPRD Cy/+ rats. (A) Representative images of periodic acid-Schiff staining of kidneys from 10 week old +/+ and Cy/+ rats after 5-week treatment with 2DG or vehicle. (B) Ratio of total kidney weight (TKW) to body weight (BW) in 10 week old Cy/+ rats after 5-week treatment with 2DG or vehicle. (C). Cyst index in kidneys from Cy/+ rats after 5-week treatment with 2DG or vehicle. (D) Frequency distribution of the cyst size, and (E) total number of cysts, in kidneys from Cy/+ rats following 5-week treatment with 2DG or vehicle.

doi:10.1371/journal.pone.0146654.g003

Histomorphological examination of the kidney sections showed that vehicle-treated Cy/+ rats had enlarged kidneys with multiple cysts which were not present in +/+ rats, as expected (Fig 3A). Treatment with 2DG resulted in a reduced size of the kidneys and reduced cyst sizes in Cy/+ rats compared with vehicle treatment (Fig 3A). Furthermore, quantification of the number of cysts on periodic acid Schiff-stained sections showed a significant reduction of the cyst index in 2DG-treated Cy/+ rats as compared to vehicle treatment (Fig 3C). Frequency distribution analysis of the cyst size showed that treatment with 2DG led to a shift in the size profile of the cysts (Fig 3D). The total number of cysts was similar in 2DG- and vehicle-treated rats (Fig 3E), suggesting that 2DG treatment affected cyst growth rather than cyst development in Cy/+ rats.

Effect of 2DG treatment on renal function. We then evaluated the effects of 2DG treatment on the parameters of renal function. Cy/+ rats developed significant impairment of renal function as compared to +/+ rats (Fig 4A, 4B and 4C). Following treatment with 2DG, Cy/

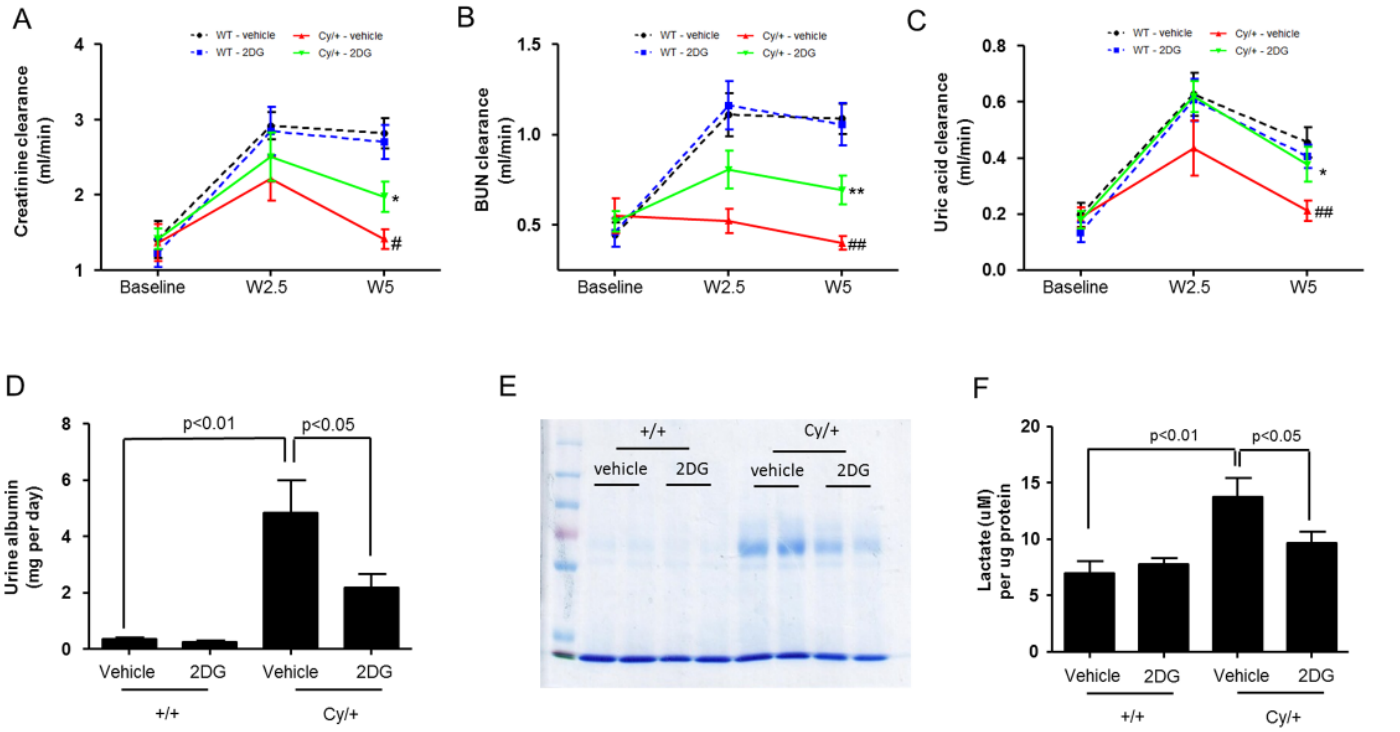

Fig 4. Effect of 2DG treatment on parameters of renal function. Measurement of (A) creatinine clearance, (B) BUN clearance, and (C) uric acid clearance, in +/+ and Cy/+ rats upon treatment with 2DG or vehicle at baseline, 2.5 weeks and 5 weeks. Black, +/+ treated with vehicle; blue, +/+ treated with 2DG; red, Cy/+ treated with vehicle; green, Cy/+ treated with 2DG. *P<0.05, **P<0.01 when comparing Cy/+ 2DG and Cy/+ vehicle at each time point. #P<0.05, ## P<0.01 when comparing Cy/+ and +/+ group. (D) Urine albumin excretion in Cy/+ and +/+ rats after 5-week treatment with 2DG or vehicle. (E) SDS-polyacrylamide gel electrophoresis of urine samples from Cy/+ and +/+ rats after 5-week treatment with 2DG or vehicle. (F) Lactate content in the kidneys of Cy/+ and +/+ rats after treatment with 2DG or vehicle.

doi:10.1371/journal.pone.0146654.g004

+ rats had lower plasma creatinine levels as compared to vehicle treatment, with significantly higher clearances for creatinine (Fig 4A), BUN (Fig 4B) and uric acid (Fig 4C). Furthermore, the albumin excretion following treatment with 2DG was significantly lower as compared to vehicle-treated Cy/+ rats (Fig 4D and 4E). Lactate content in the kidneys of vehicle-treated Cy/+ rats were significantly higher than in vehicle-treated +/+ rats (Fig 4F). Treatment with 2DG reduced the level of lactate in the kidneys of Cy/+ rats when compared to vehicle treatment (Fig 4F).

Effect of 2DG treatment on cell proliferation and apoptosis. To examine whether 2DG reduces cyst epithelial cell proliferation we stained kidney sections for Ki67 and found a marked reduction in Ki67-positive nuclei in the tubular epithelium of Cy/+ kidneys as compared to vehicle treatment (Fig 5A and 5B). We also tested for apoptosis, examining active caspase-3 expression by Western blot analysis of kidney tissues from the Cy/+ rats. We found no difference in the level of active caspase-3 expression after treatment with 2DG as compared to vehicle treatment (Fig 5C). These data suggest that 2DG limits cyst growth in Cy/+ rats by inhibiting cell proliferation rather than by promoting apoptosis in the cystic epithelium.

Effect of 2DG treatment on cellular signaling pathways. To further characterize the mechanisms of the increased glycolysis observed in Han:SPRD rats, we assessed the effect of 2DG on important signaling pathways that have previously been shown to be dysregulated in ADPKD. First, we examined the effect of 2DG on the phosphorylation of AMPK-α, an important negative regulator of mTOR, which has been shown to be reduced in PKD.

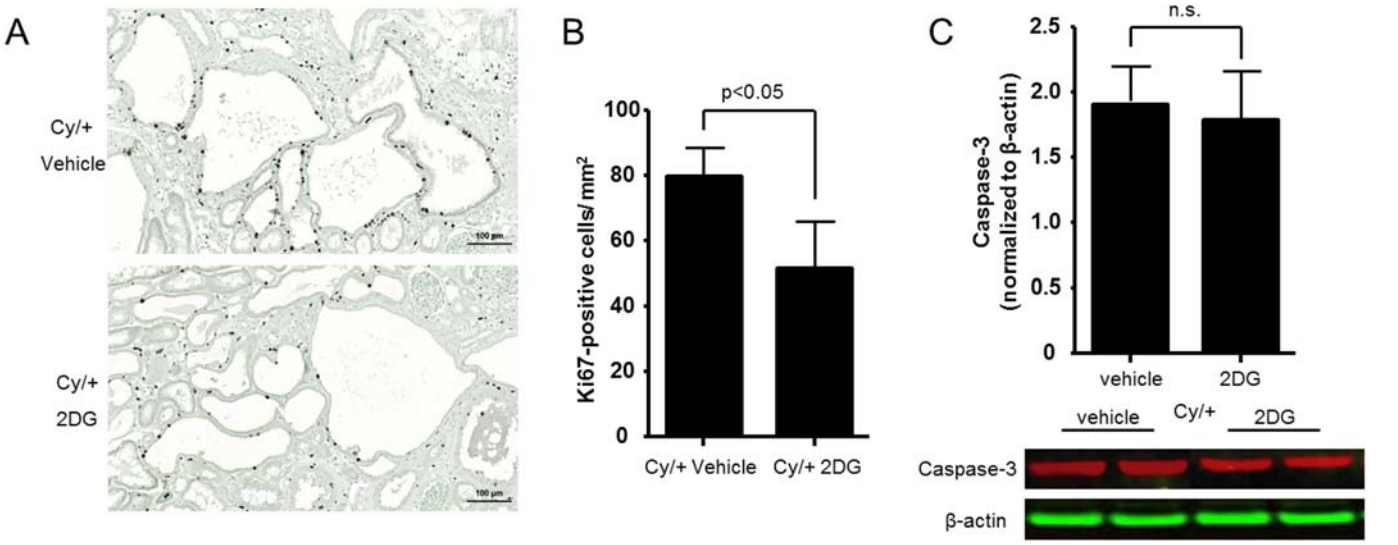

Fig 5. Effect of 2DG treatment on cell proliferation and apoptosis in Han:SPRD Cy/+ rats. (A) Representative images of Ki67 staining of cyst-lining epithelium in kidneys of Cy/+ rats treated with 2DG or vehicle. (B) Quantification of Ki67-positive nuclei in kidneys of Cy/+ rats after 5-week treatment with 2DG or vehicle. (C) Western blot analysis of active caspase-3 in kidneys from Cy/+ rats after treatment with 2DG or vehicle.

doi:10.1371/journal.pone.0146654.g005

Phosphorylation of AMPK-α was reduced in the kidney lysate from Cy/+ rats as compared to +/+ rats. Treatment with 2DG significantly increased AMPK-α phosphorylation in the kidneys of Cy/+ rats (Fig 6A). Next, we studied the effect of 2DG on the phosphorylation of two key kinases previously known to be activated in PKD, i.e. extracellular signal-regulated kinase (ERK; mitogen-activated protein kinase [MAPK] pathway) and p70 S6K (mTOR pathway). As shown in Fig 6B and 6C, phosphorylation of both ERK and p70 S6K were increased in the kidney of Cy/+ rats as compared to +/+ rats. Treatment with 2DG led to a significant reduction in the phosphorylation of ERK (Fig 6B), but there was no effect on the phosphorylation of p70 S6K (Fig 6C). Interestingly, 2DG treatment led to increased Akt phosphorylation (Fig 6D), which may likely explain the lack of an observable effect on p70 S6K as activation of Akt is known to counteract the effect of increased AMPK phosphorylation on p70 S6K activation.

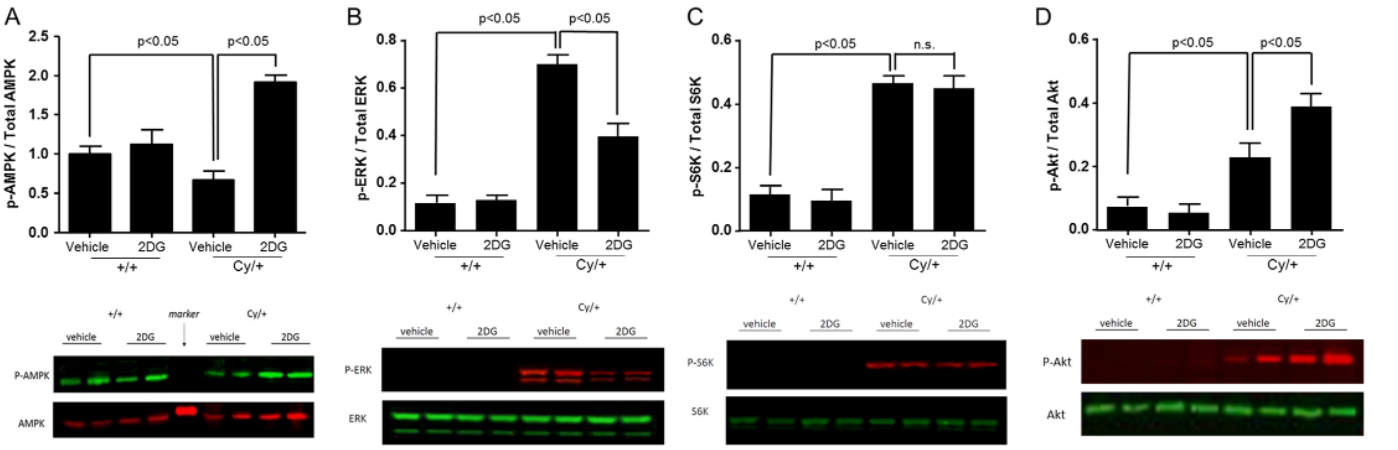

Fig 6. Effect of 2DG treatment on cellular signaling pathways in vivo. Measurements of phosphorylation levels of (A) AMPK, (B) ERK, (C) S6K, and (D) Akt using Western blot analysis in the kidneys of 10 week old +/+ and Cy/+ rats following 5-week treatment with 2DG or vehicle.

doi:10.1371/journal.pone.0146654.g006

Previous studies have shown that activation of mTOR signaling is connected to enhanced glycolysis [18]. We therefore examined the effect of direct mTOR inhibition on the enhanced glycolysis which we observed in primary human cell cultures of ADPKD cells. Treatment with the mTOR inhibitor rapamycin (50 nM) reduced the enhanced mRNA expression of glycolytic genes (*Hk1*, *Hk2*, *Pkm2*) in ADPKD cells and also reduced the enhanced levels of lactate in the cell culture medium (Fig 7A–7D). In line with this, the expression of glycolytic genes and lactate production was also inhibited with the AMPK agonist metformin (2 mM), further emphasizing the importance of mTOR in glycolysis regulation (Fig 7A–7D).

Discussion

In the present study we show that Han:SPRD Cy/+ rats display increased transcript levels for glycolysis enzymes and decreased transcript levels for gluconeogenesis enzymes in the kidney. Lactate and ATP levels were also increased in the kidneys and in TEC cultures of Cy/+ rats compared to wild type +/+ kidneys. Similar findings were obtained in cultured TEC derived from patients with ADPKD. Importantly, administration of 2DG, a glycolytic inhibitor, retarded cyst progression, improved renal function in Han:SPRD Cy/+ rats and was associated with reduced intrarenal lactate levels and normalization of altered signaling pathways. Taken together our data suggest that in PKD there is metabolic reprogramming towards enhanced aerobic glycolysis, a phenomenon which is known as the Warburg effect, after its discoverer Otto Warburg.

Recently, Rowe et al. reported that mutation of *Pkd1* results in enhanced glycolysis in a mouse model of PKD and in kidneys from patients with ADPKD [8,19]. Metabolomic profiling of the cell culture medium of *Pkd1*-deficient mouse embryonic fibroblasts showed increased glucose uptake and lactate production. The authors also found that treatment with 2DG delayed cyst growth in two rapidly progressive mouse models of PKD. However, the duration of the treatment with 2DG was extremely short (2 days), which does not account for the slowly progressive nature of the disease. In addition, the effect of 2DG on renal function could not be assessed due to the rapidly progressive nature of the models. More recently, Chiaravalli et al. used an orthologous and slowly progressive murine PKD model created by inducible inactivation of the Pkd1 gene postnatally and found that 2DG also had beneficial effects on cyst growth at a lower dose (100 mg/kg for 5 days per week for 2 months) [20].

Increased glycolysis has been previously reported in proliferating cells which require altered metabolism to efficiently incorporate nutrients such as glucose into biomass. Cancer cells, for instance, primarily metabolize glucose by glycolysis, whereas most normal cells completely catabolize glucose by oxidative phosphorylation [21]. This shift to aerobic glycolysis with increased lactate production, coupled with increased glucose uptake, is likely used by proliferating cells to promote the efficient conversion of glucose into the macromolecules needed to construct a new cell [22].

It has been shown that the Warburg effect is associated with defective mitochondrial respiration in the context of a hypoxic environment [23]. Similar to cancer cells, cyst epithelial cells in polycystic kidney disease are exposed to hypoxia and display mitochondrial dysfunction [24,25,26,27]. Furthermore it has been shown that cyst epithelial cells display a high rate of apoptosis, a process which is tightly regulated at the level of mitochondria [28]. Increased apoptosis in polycystic Han:SPRD rat kidneys was shown to be due to the activation of caspase-3 and dysregulation of the balance between pro- and anti-apoptotic Bcl-2 family members, specifically a down-regulation of anti-apoptotic Bcl-XL [29]. Zamzami et al. have shown that apoptosis is closely related to mitochondrial impairment [30]. There is also a high level of mitochondrial DNA (mtDNA) damage in apoptotic cells [31]. It is therefore conceivable that

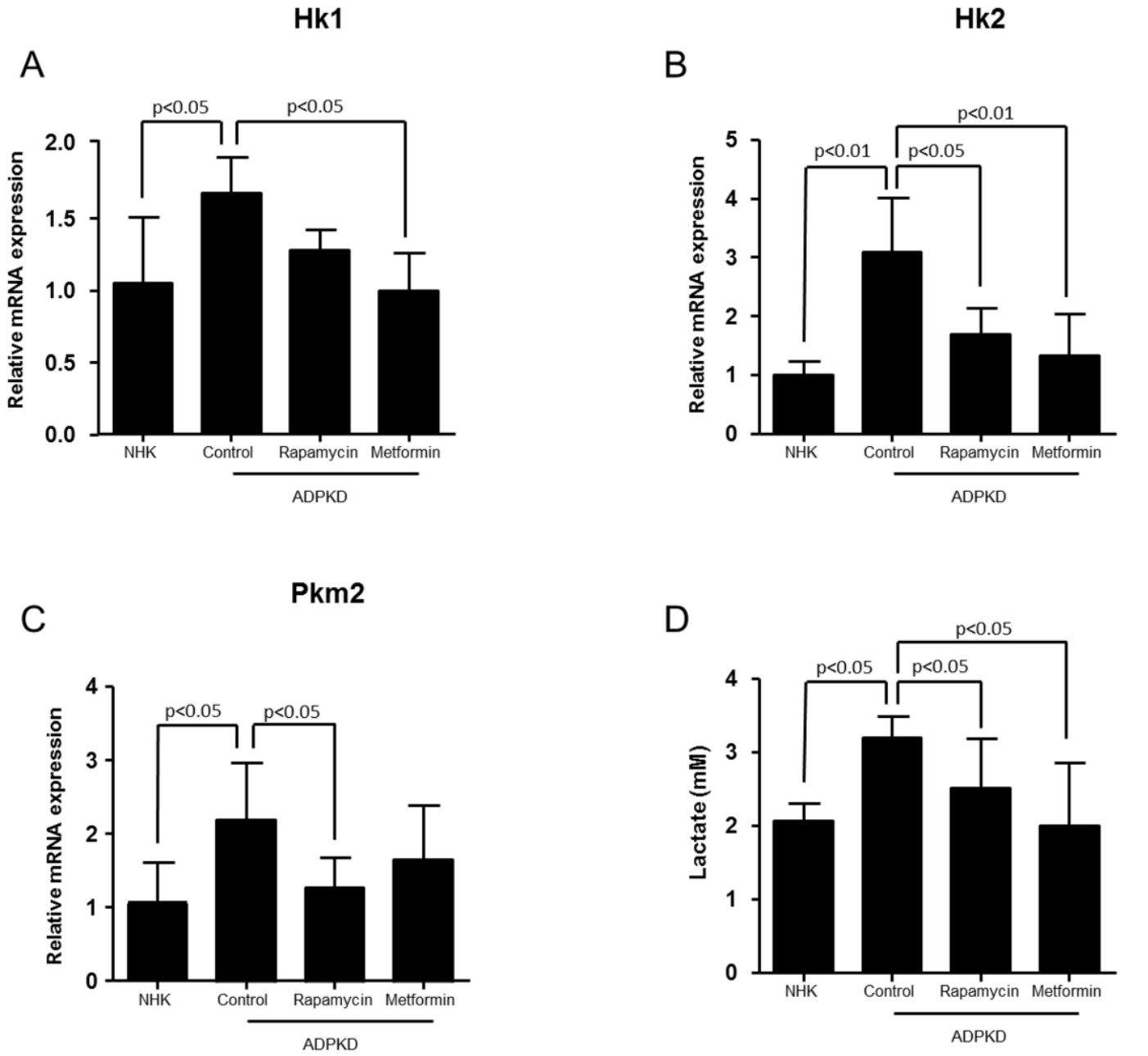

Fig 7. Effect of selected inhibitors on the glycolysis pathway in vitro. Real-time quantitative PCR analysis of the genes coding for glycolytic enzymes (A) Hk1, (B) Hk2, and (C) Pkm2 in primary cell cultures of human ADPKD cells following incubation with rapamycin (50 nM) or metformin (2 mM). (D) Lactate production in the supernatant of NHK and ADPKD cells, and response to inhibitors.

doi:10.1371/journal.pone.0146654.g007

damage to the mtDNA would cause malfunction in the respiratory chain in PKD, forcing the cyst epithelial cells to use the aerobic glycolysis pathway to generate ATP.

The glucose analog 2-deoxyglucose (2DG) acts as a competitive inhibitor of glucose metabolism.[32] Upon transport into the cells, 2DG is phosphorylated by hexokinase to 2DG-P. However, unlike G-6-P, 2DG-P cannot be further metabolized by phosphohexose isomerase, which converts G-6-P to fructose-6-phosphate [33]. Thus 2DG-P is trapped and accumulates in the

cells, leading to inhibition of glycolysis mainly at the step of phosphorylation of glucose by hexokinase. Inhibition of this rate-limiting step by 2DG causes a depletion of cellular ATP, leading to blockage of cell cycle progression and cell death *in vitro* [34]. The anti-tumor effect of 2DG has been well characterized in animal models and human clinical trials [35,36,37]. The feasibility of using a glycolytic inhibitor in a defined and progressive rat model of PKD has not been tested yet. In the current study, we investigated the therapeutic potential of 2-deoxyglucose (2DG) in Han:SPRD Cy/+ rats, a well-known animal model of PKD which develop slowly progressing renal cysts resembling human ADPKD.

A major complication of polycystic kidney disease is the deterioration of renal function. Glomerular filtration rate (GFR) significantly decreases towards the later stage of the disease, requiring the patients to initiate renal replacement therapy. Delaying the loss of renal function has therefore been a major therapeutic aim in PKD. In our study we show for the first time that 2DG improved different parameters of renal function (clearances for creatinine, BUN and uric acid). 2DG also ameliorated albuminuria, a common biomarker of altered and progressively deteriorating renal function in PKD. Taken together our data suggest that 2DG or related molecules may have a beneficial therapeutic potential for patients with ADPKD.

Interestingly, we observed that either direct inhibition of mTOR signaling using rapamycin or indirect inhibition using the AMPK agonist metformin reversed the glycolytic phenotype in ADPKD cells *in vitro*. Furthermore, we found that phosphorylation of ERK1/2 was significantly reduced in Cy/+ upon treatment with 2DG, which likely explains the observed effect of 2DG on cell proliferation. Interestingly, treatment of 2DG did not affect the phosphorylation status of S6K which is highly enhanced in Cy/+ kidneys as compared to wild-type rats. This could be explained by 2DG-mediated activation of the survival signal PI3K/Akt pathway, which counteracts the effect of 2DG via ERK and AMPK. As previously described, mTOR functions as a central node in a complex net of signaling pathways; it integrates signals from the Akt, ERK, and AMPK pathways and plays an important role in regulating protein biosynthesis, cellular growth, and proliferation [38,39]. Fig 8 summarizes the various signaling

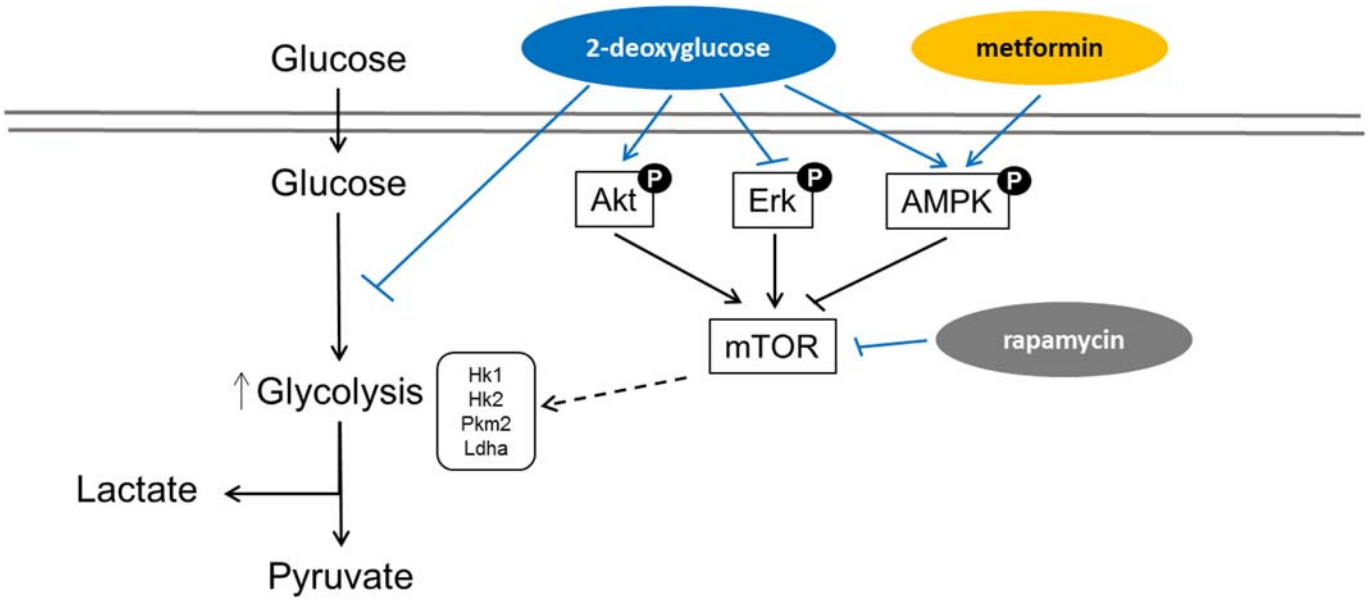

Fig 8. Schematic diagram showing the interplay of various signaling pathways involved in the regulation of glycolysis in polycystic kidney disease.

doi:10.1371/journal.pone.0146654.g008

pathways involved in the regulation of glycolysis in ADPKD that have been investigated in this study.

Taken together, our results show that the cystic kidneys of Han:SPRD Cy/+ rats display enhanced aerobic glycolysis which likely plays an important role in the pathogenesis of PKD. The administration of 2DG, a potent glycolytic inhibitor, markedly delayed the loss of renal function and retarded cyst development Han:SPRD Cy/+ rats with PKD. Targeting the glycolytic pathway may therefore present a novel therapeutic strategy to control cyst growth in polycystic kidney disease.

Acknowledgments

We thank Petra Seebeck, Herbert Passmann and Svende Pfundstein from the Zurich Integrative Rodent Physiology for their help with the animal work. We thank the Functional Genomics Center for their technical support.

Author Contributions

Conceived and designed the experiments: MR RPW. Performed the experiments: MR DR IE. Analyzed the data: MR. Contributed reagents/materials/analysis tools: MR SK DR IE. Wrote the paper: MR SS RPW.

References

1. Torres VE, Harris PC, Pirson Y (2007) Autosomal dominant polycystic kidney disease. Lancet 369: 1287–1301. PMID: 17434405
2. Grantham JJ (2008) Clinical practice. Autosomal dominant polycystic kidney disease. N Engl J Med 359: 1477–1485. doi: 10.1056/NEJMcp0804458 PMID: 18832246
3. Serra AL, Poster D, Kistler AD, Krauer F, Raina S, Young J, et al. (2010) Sirolimus and kidney growth in autosomal dominant polycystic kidney disease. N Engl J Med 363: 820–829. doi: 10.1056/NEJMoa0907419 PMID: 20581391
4. Wuthrich RP, Kistler AD, Serra AL (2010) Impact of mammalian target of rapamycin inhibition on autosomal-dominant polycystic kidney disease. Transplantation proceedings 42: S44–46. doi: 10.1016/j.transproceed.2010.07.008 PMID: 21095452
5. Devuyst O, Torres VE (2013) Osmoregulation, vasopressin, and cAMP signaling in autosomal dominant polycystic kidney disease. Current opinion in nephrology and hypertension 22: 459–470. doi: 10.1097/MNH.0b013e3283621510 PMID: 23736843
6. Torres VE, Harris PC (2014) Strategies targeting cAMP signaling in the treatment of polycystic kidney disease. Journal of the American Society of Nephrology: JASN 25: 18–32. doi: 10.1681/ASN.2013040398 PMID: 24335972
7. Wuthrich RP, Mei C (2014) Pharmacological management of polycystic kidney disease. Expert opinion on pharmacotherapy 15: 1085–1095. doi: 10.1517/14656566.2014.903923 PMID: 24673552
8. Rowe I, Chiaravalli M, Mannella V, Ulisse V, Quilici G, Pema M, et al. (2013) Defective glucose metabolism in polycystic kidney disease identifies a new therapeutic strategy. Nat Med 19: 488–493. doi: 10.1038/nm.3092 PMID: 23524344
9. Brown JH, Bihoreau MT, Hoffmann S, Kranzlin B, Tychinskaya I, Obermuller N, et al. (2005) Missense mutation in sterile alpha motif of novel protein SamCystin is associated with polycystic kidney disease in (cy/+) rat. J Am Soc Nephrol 16: 3517–3526. PMID: 16207829
10. Guay-Woodford LM (2003) Murine models of polycystic kidney disease: molecular and therapeutic insights. Am J Physiol Renal Physiol 285: F1034–1049. PMID: 14600027
11. Gretz N, Kranzlin B, Pey R, Schieren G, Bach J, Obermuller N, et al. (1996) Rat models of autosomal dominant polycystic kidney disease. Nephrol Dial Transplant 11 Suppl 6: 46–51. PMID: 9044328
12. Berthier CC, Lods N, Joosten SA, van Kooten C, Leppert D, Lindberg RL, et al. (2006) Differential regulation of metzincins in experimental chronic renal allograft rejection: potential markers and novel therapeutic targets. Kidney Int 69: 358–368. PMID: 16408127
13. Berthier CC, Wahl PR, Le Hir M, Marti HP, Wagner U, Rehrauer H, et al. (2008) Sirolimus ameliorates the enhanced expression of metalloproteinases in a rat model of autosomal dominant polycystic kidney disease. Nephrol Dial Transplant 23: 880–889. PMID: 18042615

14. Wang X, Zhang S, Liu Y, Spichtig D, Kapoor S, Koepsell H, et al. (2013) Targeting of sodium-glucose cotransporters with phlorizin inhibits polycystic kidney disease progression in Han:SPRD rats. Kidney Int 84: 962–968. doi: 10.1038/ki.2013.199 PMID: 23715121
15. Wallace DP, Grantham JJ, Sullivan LP (1996) Chloride and fluid secretion by cultured human polycystic kidney cells. Kidney Int 50: 1327–1336. PMID: 8887295
16. Center for Drug Evaluation and Research (2002) Estimating the safe starting dose in clinical trials for therapeutics in adult healthy volunteers. US Food and Drug Administration Rockville, Maryland, USA.
17. Raez LE, Papadopoulos K, Ricart AD, Chiorean EG, Dipaola RS, Stein MN, et al. (2013) A phase I dose-escalation trial of 2-deoxy-D-glucose alone or combined with docetaxel in patients with advanced solid tumors. Cancer Chemother Pharmacol 71: 523–530. doi: 10.1007/s00280-012-2045-1 PMID: 23228990
18. Cairns RA, Harris IS, Mak TW (2011) Regulation of cancer cell metabolism. Nat Rev Cancer 11: 85–95. doi: 10.1038/nrc2981 PMID: 21258394
19. Rowe I, Boletta A (2014) Defective metabolism in polycystic kidney disease: potential for therapy and open questions. Nephrol Dial Transplant 29: 1480–1486. doi: 10.1093/ndt/gft521 PMID: 24459136
20. Chiaravalli M, Rowe I, Mannella V, Quilici G, Canu T, Bianchi V, et al. (2015) 2-Deoxy-d-Glucose Ameliorates PKD Progression. J Am Soc Nephrol.
21. Jones RG, Thompson CB (2009) Tumor suppressors and cell metabolism: a recipe for cancer growth. Genes Dev 23: 537–548. doi: 10.1101/gad.1756509 PMID: 19270154
22. Vander Heiden MG, Cantley LC, Thompson CB (2009) Understanding the Warburg effect: the metabolic requirements of cell proliferation. Science 324: 1029–1033. doi: 10.1126/science.1160809 PMID: 19460998
23. Xu RH, Pelicano H, Zhou Y, Carew JS, Feng L, Bhalla KN, et al. (2005) Inhibition of glycolysis in cancer cells: a novel strategy to overcome drug resistance associated with mitochondrial respiratory defect and hypoxia. Cancer Research 65: 613–621. PMID: 15695406
24. Che R, Yuan Y, Huang S, Zhang A (2014) Mitochondrial dysfunction in the pathophysiology of renal diseases. American journal of physiology Renal physiology 306: F367–378. doi: 10.1152/ajprenal.00571.2013 PMID: 24305473
25. Li QW, Lu XY, You Y, Sun H, Liu XY, Ai JZ, et al. (2012) Comparative proteomic analysis suggests that mitochondria are involved in autosomal recessive polycystic kidney disease. Proteomics 12: 2556–2570. doi: 10.1002/pmic.201100590 PMID: 22718539
26. Bernhardt WM, Wiesener MS, Weidemann A, Schmitt R, Weichert W, Lechler P, et al. (2007) Involvement of hypoxia-inducible transcription factors in polycystic kidney disease. The American journal of pathology 170: 830–842. PMID: 17322369
27. Buchholz B, Schley G, Faria D, Kroening S, Willam C, Schreiber R, et al. (2014) Hypoxia-inducible factor-1alpha causes renal cyst expansion through calcium-activated chloride secretion. Journal of the American Society of Nephrology: JASN 25: 465–474. doi: 10.1681/ASN.2013030209 PMID: 24203996
28. Woo D (1995) Apoptosis and loss of renal tissue in polycystic kidney diseases. N Engl J Med 333: 18–25. PMID: 7776989
29. Ecder T, Melnikov VY, Stanley M, Korular D, Lucia MS, Schrier RW, et al. (2002) Caspases, Bcl-2 proteins and apoptosis in autosomal-dominant polycystic kidney disease. Kidney Int 61: 1220–1230. PMID: 11918728
30. Zamzami N, Susin SA, Marchetti P, Hirsch T, Gomez-Monterrey I, Castedo M, et al. (1996) Mitochondrial control of nuclear apoptosis. J Exp Med 183: 1533–1544. PMID: 8666911
31. Esteve JM, Mompo J, Garcia de la Asuncion J, Sastre J, Asensi M, Boix J, et al. (1999) Oxidative damage to mitochondrial DNA and glutathione oxidation in apoptosis: studies in vivo and in vitro. FASEB J 13: 1055–1064. PMID: 10336888
32. Brown J (1962) Effects of 2-deoxyglucose on carbohydrate metablism: review of the literature and studies in the rat. Metabolism 11: 1098–1112. PMID: 13873661
33. Weindruch R, Keenan KP, Carney JM, Fernandes G, Feuers RJ, Floyd RA, et al. (2001) Caloric restriction mimetics: metabolic interventions. J Gerontol A Biol Sci Med Sci 56 Spec No 1: 20–33. PMID: 12088209
34. Maher JC, Krishan A, Lampidis TJ (2004) Greater cell cycle inhibition and cytotoxicity induced by 2-deoxy-D-glucose in tumor cells treated under hypoxic vs aerobic conditions. Cancer Chemother Pharmacol 53: 116–122. PMID: 14605866
35. Maschek G, Savaraj N, Priebe W, Braunschweiger P, Hamilton K, Tidmarsh GF, et al. (2004) 2-deoxy-D-glucose increases the efficacy of adriamycin and paclitaxel in human osteosarcoma and non-small cell lung cancers in vivo. Cancer Research 64: 31–34. PMID: 14729604

36. Singh D, Banerji AK, Dwarakanath BS, Tripathi RP, Gupta JP, Mathew TL, et al. (2005) Optimizing cancer radiotherapy with 2-deoxy-d-glucose dose escalation studies in patients with glioblastoma multiforme. Strahlenther Onkol 181: 507–514. PMID: 16044218

37. Mohanti BK, Rath GK, Anantha N, Kannan V, Das BS, Chandramouli BA, et al. (1996) Improving cancer radiotherapy with 2-deoxy-D-glucose: phase I/II clinical trials on human cerebral gliomas. Int J Radiat Oncol Biol Phys 35: 103–111. PMID: 8641905

38. Hardie DG (2008) AMPK and Raptor: matching cell growth to energy supply. Molecular cell 30: 263–265. doi: 10.1016/j.molcel.2008.04.012 PMID: 18471972

39. Ma XM, Blenis J (2009) Molecular mechanisms of mTOR-mediated translational control. Nature reviews Molecular cell biology 10: 307–318. doi: 10.1038/nrm2672 PMID: 19339977

Chapter 7

Prediction of glomerular filtration rate decline in patients with autosomal dominant polycystic kidney disease

Daniel Rodriguez[1-3], Borja Garrido[4], Sandra Mischler[1], and Rudolf P. Wüthrich[1]

[1]Division of Nephrology, University Hospital, Zürich, Switzerland
[2]Institute of Physiology, University of Zürich, Switzerland
[3]Competence Center for Personalized Medicine, Zürich, Switzerland
[4]Electrical Engineering Department, University of Oviedo, Gijón, Spain

Contribution by Daniel Rodriguez:

Hypothesis proposal, analysis of basic characteristic of patients, classification of patient by $hTKV_0$, analysis of the eGFR prediction, correlation between predicted eGFR and observed eGFR, analysis of the prediction in time, interpretation of results, writing of the first draft of the manuscript.

Prediction of glomerular filtration rate decline in patients with autosomal dominant polycystic kidney disease

Daniel Rodriguez[1-3], Borja Garrido[4], Sandra Mischler[1] and Rudolf P. Wüthrich[1*]

[1]Division of Nephrology, University Hospital, Zürich, Switzerland
[2]Institute of Physiology, University of Zürich, Switzerland
[3]Competence Center for Personalized Medicine, University of Zürich, Switzerland
[4]Electrical Engineering Department, University of Oviedo, Gijon, Spain

*Corresponding author:

Rudolf P. Wüthrich, MD, FACP, FASN
Division of Nephrology
University Hospital
Rämistrasse 100
8091 Zürich
Switzerland
Phone: +41 44 255 33 84
Fax: +41 44 255 45 93
E-mail: rudolf.wuethrich@usz.ch

Abstract

A novel kidney imaging classification and estimated glomerular filtration rate (eGFR) prediction model for patients with autosomal dominant polycystic kidney disease (ADPKD) was recently proposed by the Mayo Clinic (Irazabal M. et al., J Am Soc Nephrol 2015; 26: 160-172). This classification and prediction model has demonstrated an accurate eGFR prediction for the American population. The objective of this study was to apply this same imaging classification to test the Mayo Clinic prediction model in a Swiss cohort of 203 ADPKD patients that had clinical follow-up data for up to 10 years. The eGFR prediction model showed an accurate correlation with the observed eGFR in Swiss ADPKD patients for up to 5 years of follow-up, but tended to underestimate observed eGFR values beyond 5 years, particularly in patients with less severe disease. In summary, our study shows that the Mayo Clinic prediction model appropriately predicts the eGFR decline in the short term in Swiss patients with ADPKD.

Introduction

Autosomal Dominant Polycystic Kidney Disease (ADPKD) is the most common form of cystic renal diseases. With an incidence of 1:400 to 1:1.000, ADPKD it is one of the leading causes of end-stage renal disease (ESRD) in adults and affects all ethnic groups worldwide [1,2]. An early and accurate prediction of chronic kidney disease (CKD) progression may help to develop more efficient strategies to confront the disease and the progression to ESRD [3].

Recently, a prediction model for eGFR decline in ADPKD has been developed at the Mayo Clinic by Irazabal et al. [4]. The model uses the parameters age, sex and height-adjusted total kidney volume at baseline ($hTKV_0$) to predict eGFR decline over time in a longitudinal mixed-effects regression equation. The model was derived from two different ADPKD populations in the United States, the Consortium for Radiologic Imaging Study of PKD (CRISP) and the Mayo Clinic Translational Polycystic Kidney Disease Center (MTPC) cohorts. In the present study, we tested whether this longitudinal mixed-effects regression model also correctly predicts the eGFR decline in a cohort of Swiss ADPKD patients.

Materials and methods

Patients

The clinical data from well-characterized patients with ADPKD from the University Hospital in Zürich, Switzerland, were used in this study. All participants gave their written informed consent. Patients younger than 20 years were excluded since eGFR estimation equations tend to be unreliable in these patients [5,6]. Baseline data included age, gender, body height, magnetic resonance imaging-based total kidney volume (TKV) and serum creatinine. The eGFR was calculated according to the Chronic Kidney Disease Epidemiology Collaboration (CKD-EPI) equation. Patients had yearly follow-up visits for creatinine/eGFR determinations for up to 10 years.

Classification of patients into classes 1A, 1B, 1C, 1D and 1E

Based on the radiological classification as proposed by M. Irazabal et al. [4] we selected 203 ADPKD patients with class 1 (typical) ADPKD, and excluding the class 2 (atypical) cases. The class 1 patients were then stratified into 5 subclasses (1A to 1E) of ADPKD according to the estimated yearly hTKV growth rates: <1.5% (1A), 1.5-3.0% (1B), 3.0-4.5% (1C), 4.5-6.0 (1D) and >6.0% (1E).

eGFR prediction equation

Irazabal et al. developed and reported to us (personal communication) their longitudinal mixed-effects regression equation [4]. This formula is based on the age, sex and height-adjusted total kidney volume at baseline ($hTKV_0$) and includes the patients' classification in subclasses (1A-1E).

A prototype software application was developed to analyze the patients' data from a single database. This software compiles date of birth, date of visit, gender, height and blood creatinine measurements and reports the eGFR estimation using the longitudinal mixed-effect prediction equation. The class ranges were computed by fitting the hTKV at baseline into the ranges defined by log ($hTKV_n/hTKV_{n-1}$) limits between classes (A<1.5, B<3.0, C<4.5, D<6.0, E>6.0).

Statistical analyses

Quantitative variables are described as means ± SD. Correlation by linear regression and Bland-Altmann analyses were used to show the relationship between predicted eGFR and observed eGFR. A $P<0.05$ was considered statistically significant. GraphPad Prism version 5.0 software (GraphPad, San Diego, CA, USA) was used for data analysis.

Results

Baseline data of Swiss ADPKD patients

All class 1 ADPKD patients were subdivided into the classes 1A to 1E according to their age and their $hTKV_0$ at baseline. Table 1 shows the baseline data of the patients, stratified according to the classes 1A to 1E. From the total of 203 included patients, 13% were classified in class 1A, 29% in class 1B, 31% in class 1C, 20% in class 1D and 8% in class 1E. The percentage of males increased from the least pronounced class 1A (34.6%) to the most severe class 1E (81.3%). Mean age (35 ± 10 years) and height (175 ± 9 cm) did not show significant differences among the classes. The eGFR declined from class 1A to class 1E, whereas the hTKV increased, as expected. The distribution of patients by age and hTKV according to the classes 1A to 1E is graphically presented in Figure 1.

Predicted and observed eGFR decline

Based on the baseline data we calculated the predicted eGFR decline in the different classes 1A to 1E of the 203 Swiss ADPKD patients. As shown in Figure 2A, the predicted eGFR decline differed significantly among the different subclasses. Next, we analyzed the decline of the observed eGFR in the different classes (Figure 2B). Again we found that the observed eGFR decline differed significantly among the different classes. Thus, in a first approximation we found that the longitudinal mixed-effects equation generated predicted eGFR values which paralleled the observed eGFR decline.

Correlation between predicted and observed eGFR decline

When we correlated the predicted with the observed eGFR decline according to the longitudinal mixed-effects regression equation, we observed a strong overall correlation ($r=0.884$, $R^2=0.781$) (Figure 3A). When classes were analyzed separately, the classes 1B, 1C, 1D and 1E showed a strong correlation ($R^2>0.7$, $p<0.0001$), whereas class 1A showed only a weak but still significant correlation ($R^2=0.518$, $p<0.0001$) (Table 2). Figure 3B shows the Bland-Altman analysis where dots represent the difference between predicted and observed values of individual

patients. This analysis show a tendency to underestimate the observed eGFR, especially in patients with higher eGFR values (>60 ml/min/1.73 m^2).

Accuracy of eGFR prediction over time

To analyze the precision of the prediction model over time we calculated the observed and the predicted eGFR for each year of follow-up, up to a maximum of 10 years. Figure 4 shows the differences between observed eGFR and predicted eGFR in the different classes along 10 years of follow-up. During the first 5 years of follow up, the predicted eGFR closely matched the observed eGFR in all classes (maximum mean difference of -7.9 ± 15.6 ml/min/1.73 m^2 in class 1A). Beyond 5 years, the prediction tended to slightly underestimate the observed eGFR in classes 1A, 1C and 1E (maximum mean difference of -19.0 ± 11.5 ml/min/1.73 m^2 in class 1A).

Discussion

Formulas which predict the decline in eGFR are of great importance to counsel patients with various diseases that cause CKD [7,8]. Long term prediction equations may serve as useful tools to identify patients at risk for progression and to define optimal treatment in individual patients. Consequently, there is an increased demand of accurate prediction models for the different patient populations. As demonstrated by Tangri et al. [9], estimations based exclusively on creatinine are not sufficient to correctly predict kidney function. The inclusion of more classification parameters which can easily be obtained, such as different laboratory tests, may result in more accurate prediction models. In the case of ADPKD, the TKV in combination with age proved to be the most powerful parameters for predicting kidney function decline [10-13].

In this study, the novel longitudinal mixed-effects equation proposed by M. Irazabal et al. was tested in a population of ADPKD patients from the University Hospital in Zürich. This novel prediction equation uses age, sex and hTKV at baseline to predict kidney function decline. Irazabal and colleagues determined the TKV by ellipsoid equation, with the limitation that there is a certain imprecision in comparison with the stereological method for TKV determination. However, the two volume

measurements seem to correlate quite well [14,15]. Our TKV values were based on the stereological method, and are therefore very precise [16,17].

The Mayo Clinic model as developed by Irazabel et al. was less accurate in ADPKD patients with close to normal kidney function. In addition, some patients may change to a more severe class and should be reevaluated. Only 3.7% of the Swiss patients changed to a worse subclass during the follow up (data not shown). Our analysis in the Swiss population shows that the overall predicted eGFR correlates well with the observed eGFR. However, our data of the predicted eGFR over 10 years reveal a tendency to underestimate the observed eGFR when the prediction time is beyond 5 years. This was most pronounced in patients with better renal function (eGFR>60 ml/min/1.73 m^2). A clear limitation of this study resides in the number of patients included, especially for subclass 1E. Due to this limited sample size a larger cohort and a longer follow up may be required to clarify the magnitude of this effect.

A novel model, the PROPKD score [18], was proposed to classify PKD patients according to their risk of kidney failure. This model uses genetic and clinical variables, including type of PKD mutation, hypertension before 35 years and first urologic event before 35 years of age to score patients into 3 different classes: low-risk, intermediate-risk and high-risk of ESRD. The PROPKD score accurately predicts an evolution without ESRD before 60 years for patients in the low-risk category, with a negative predictive value (NPP) of 81.4%. The model was not found to be suitable for patients younger than 20 years old. A comparison of the Mayo and the PROPKD models [15] suggested that due to the cost and limited availability of genetic analysis, it would be difficult to implement the PROPKD model routinely at the present time, but it might become a helpful tool in the future.

In summary, the new longitudinal mixed-effects equation predicts the eGFR decline with accuracy over a reasonable time period in ADPKD patients of the Swiss population. The eGFR in the subclasses 1C, 1D and 1E seemed to be predicted best by the mixed-effects equation, whereas the eGFR of patients in the subclasses 1A or 1B could be predicted with much less precision. The inclusion of additional (yet to be defined) clinical or laboratory parameters to the Mayo model may improve the

prediction of the critical groups and help to paint a better picture of ADPKD patient prognosis in the future.

References

1. Torres VE, Harris PC, Pirson Y (2007) Autosomal dominant polycystic kidney disease. Lancet 369: 1287-1301.
2. Gabow PA (1993) Autosomal dominant polycystic kidney disease. N Engl J Med 329: 332-342.
3. Chapman AB, Bost JE, Torres VE, Guay-Woodford L, Bae KT, Landsittel D, Li J, King BF, Martin D, Wetzel LH, Lockhart ME, Harris PC, Moxey-Mims M, Flessner M, Bennett WM, Grantham JJ (2012) Kidney volume and functional outcomes in autosomal dominant polycystic kidney disease. Clin J Am Soc Nephrol 7: 479-486.
4. Irazabal MV, Rangel LJ, Bergstralh EJ, Osborn SL, Harmon AJ, Sundsbak JL, Bae KT, Chapman AB, Grantham JJ, Mrug M, Hogan MC, El-Zoghby ZM, Harris PC, Erickson BJ, King BF, Torres VE (2015) Imaging classification of autosomal dominant polycystic kidney disease: a simple model for selecting patients for clinical trials. J Am Soc Nephrol 26: 160-172.
5. Selistre L, De Souza V, Cochat P, Antonello IC, Hadj-Aissa A, Ranchin B, Dolomanova O, Varennes A, Beyerle F, Bacchetta J, Dubourg L (2012) GFR estimation in adolescents and young adults. J Am Soc Nephrol 23: 989-996.
6. Matsushita K, Tonelli M, Lloyd A, Levey AS, Coresh J, Hemmelgarn BR (2012) Clinical risk implications of the CKD Epidemiology Collaboration (CKD-EPI) equation compared with the Modification of Diet in Renal Disease (MDRD) Study equation for estimated GFR. Am J Kidney Dis 60: 241-249.
7. Lin J, Knight EL, Hogan ML, Singh AK (2003) A comparison of prediction equations for estimating glomerular filtration rate in adults without kidney disease. J Am Soc Nephrol 14: 2573-2580.
8. Bostom AG, Kronenberg F, Ritz E (2002) Predictive performance of renal function equations for patients with chronic kidney disease and normal serum creatinine levels. J Am Soc Nephrol 13: 2140-2144.
9. Tangri N, Stevens LA, Griffith J, Tighiouart H, Djurdjev O, Naimark D, Levin A, Levey AS (2011) A predictive model for progression of chronic kidney disease to kidney failure. JAMA 305: 1553-1559.
10. Ars E, Bernis C, Fraga G, Martinez V, Martins J, Ortiz A, Rodriguez-Perez JC, Sans L, Torra R (2014) Spanish guidelines for the management of autosomal dominant polycystic kidney disease. Nephrol Dial Transplant 29 Suppl 4: iv95-105.
11. Grantham JJ, Chapman AB, Torres VE (2006) Volume progression in autosomal dominant polycystic kidney disease: the major factor determining clinical outcomes. Clin J Am Soc Nephrol 1: 148-157.

12. Grantham JJ, Torres VE, Chapman AB, Guay-Woodford LM, Bae KT, King BF, Jr., Wetzel LH, Baumgarten DA, Kenney PJ, Harris PC, Klahr S, Bennett WM, Hirschman GN, Meyers CM, Zhang X, Zhu F, Miller JP (2006) Volume progression in polycystic kidney disease. N Engl J Med 354: 2122-2130.
13. Kistler AD, Serra AL, Siwy J, Poster D, Krauer F, Torres VE, Mrug M, Grantham JJ, Bae KT, Bost JE, Mullen W, Wuthrich RP, Mischak H, Chapman AB (2013) Urinary proteomic biomarkers for diagnosis and risk stratification of autosomal dominant polycystic kidney disease: a multicentric study. PLoS One 8: e53016.
14. Higashihara E, Nutahara K, Okegawa T, Tanbo M, Hara H, Miyazaki I, Kobayasi K, Nitatori T (2015) Kidney volume estimations with ellipsoid equations by magnetic resonance imaging in autosomal dominant polycystic kidney disease. Nephron 129: 253-262.
15. Gansevoort RT, Arici M, Benzing T, Birn H, Capasso G, Covic A, Devuyst O, Drechsler C, Eckardt KU, Emma F, Knebelmann B, Le Meur Y, Massy ZA, Ong AC, Ortiz A, Schaefer F, Torra R, Vanholder R, Wiecek A, Zoccali C, Van Biesen W (2016) Recommendations for the use of tolvaptan in autosomal dominant polycystic kidney disease: a position statement on behalf of the ERA-EDTA Working Groups on Inherited Kidney Disorders and European Renal Best Practice. Nephrol Dial Transplant 31: 337-348.
16. Bae KT, Tao C, Zhu F, Bost JE, Chapman AB, Grantham JJ, Torres VE, Guay-Woodford LM, Meyers CM, Bennett WM (2009) MRI-based kidney volume measurements in ADPKD: reliability and effect of gadolinium enhancement. Clin J Am Soc Nephrol 4: 719-725.
17. Mignani R, Corsi C, De Marco M, Caiani EG, Santucci G, Cavagna E, Severi S, Cagnoli L (2011) Assessment of kidney volume in polycystic kidney disease using magnetic resonance imaging without contrast medium. Am J Nephrol 33: 176-184.
18. Cornec-Le Gall E, Audrezet MP, Rousseau A, Hourmant M, Renaudineau E, Charasse C, Morin MP, Moal MC, Dantal J, Wehbe B, Perrichot R, Frouget T, Vigneau C, Potier J, Jousset P, Guillodo MP, Siohan P, Terki N, Sawadogo T, Legrand D, Menoyo-Calonge V, Benarbia S, Besnier D, Longuet H, Ferec C, Le Meur Y (2016) The PROPKD Score: A new algorithm to predict renal survival in autosomal dominant polycystic kidney disease. J Am Soc Nephrol 27: 942-951.

Tables

	ADPKD subclasses					
	1A	1B	1C	1D	1E	All
Patients (%)	26 (12.8%)	58 (28.6%)	63 (31.0%)	40 (19.7%)	16 (7.9%)	203 (100.0%)
Sex (% males)	34.6%	41.4%	60.3%	75.0%	81.3%	56.2%
Age (years)	30.0 ± 8.8	33.0 ± 9.3	34.0 ± 8.4	32.0 ± 7.9	26.0±7.0	34.8 ± 9.7
Height (cm)	173.0 ± 7.2	174.0 ± 8.3	176.0 ± 9.9	177.0 ± 10.4	179.0 ± 6.2	174.9 ± 9.1
hTKV (cm^3/m)	207.0 ± 32.7	343.0 ± 92.8	546.0 ± 181.7	835.0 ± 404.7	1085.0±362.0	636.8 ± 455.3
eGFR (ml/min/1.73 m^2)	98.8 ± 16.9	94.2 ± 19.7	91.4 ± 19.3	86.7 ± 19.7	85.6 ± 24.8	96.7 ± 38.3
Follow up (years)*	4 (2-6)	4 (2-5)	3 (2-5)	5 (3-6)	4 (3-5)	4 (2-5)

Table 1: Basic characteristics of Swiss cohort of ADPKD patients organized by subclasses (1A to 1E). Data are derived from a total of 203 Swiss ADPKD patients. The eGFR is based on the CKD-EPI equation. Age, height, hTKV and eGFR are means ± SD. *Follow up are median (interquartile range).

	Subclasses					
	1A	1B	1C	1D	1E	All
Number of patients	26	58	63	40	16	203
r	0.720	0.895	0.887	0.873	0.865	0.884
R^2	0.518	0.800	0.791	0.763	0.748	0.781
P value (two-tailed)	<0.0001	<0.0001	<0.0001	<0.0001	<0.0001	<0.0001

Table 2 Correlation coefficients (r) and coefficients of determination (R^2) between predicted and observed eGFR in the different subclasses (1A to 1E).

Figures

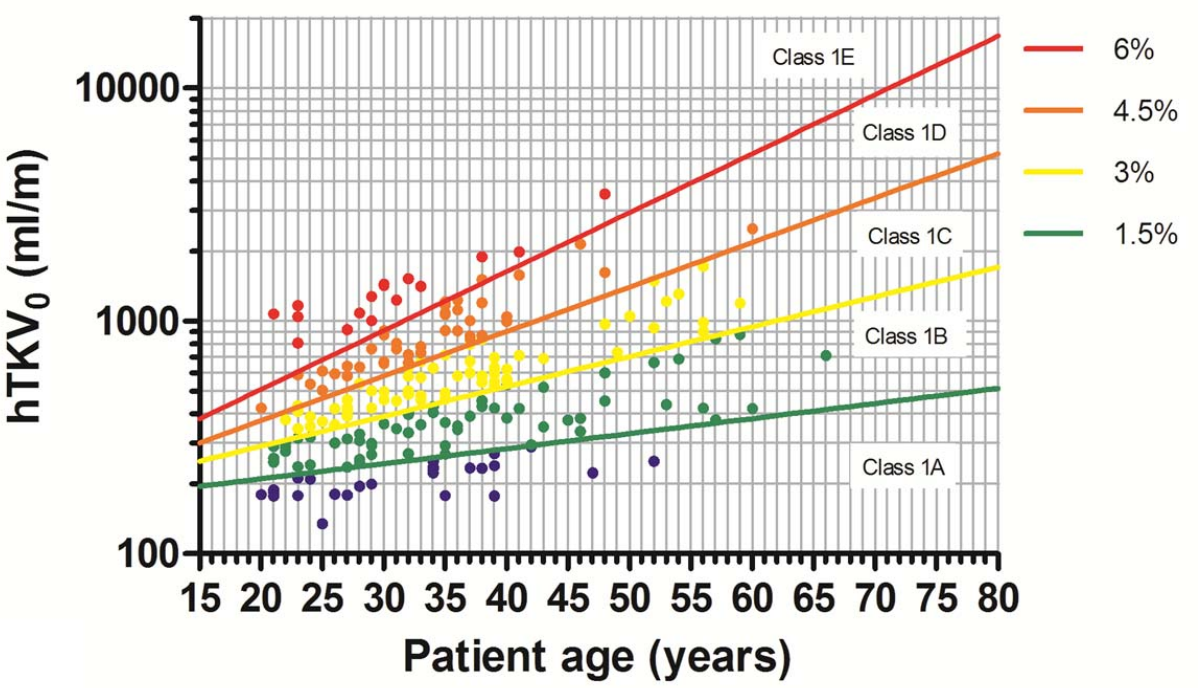

Figure 1: Classification of 203 Swiss ADPKD patients by age and TKV at baseline ($hTKV_0$). The classes 1A to 1E are defined by their kidney growth rate ranges, i.e. <1.5% (1A), 1.5-3.0% (1B), 3.0-4.5% (1C), 4.5-6.0 (1D) and >6.0% (1E).

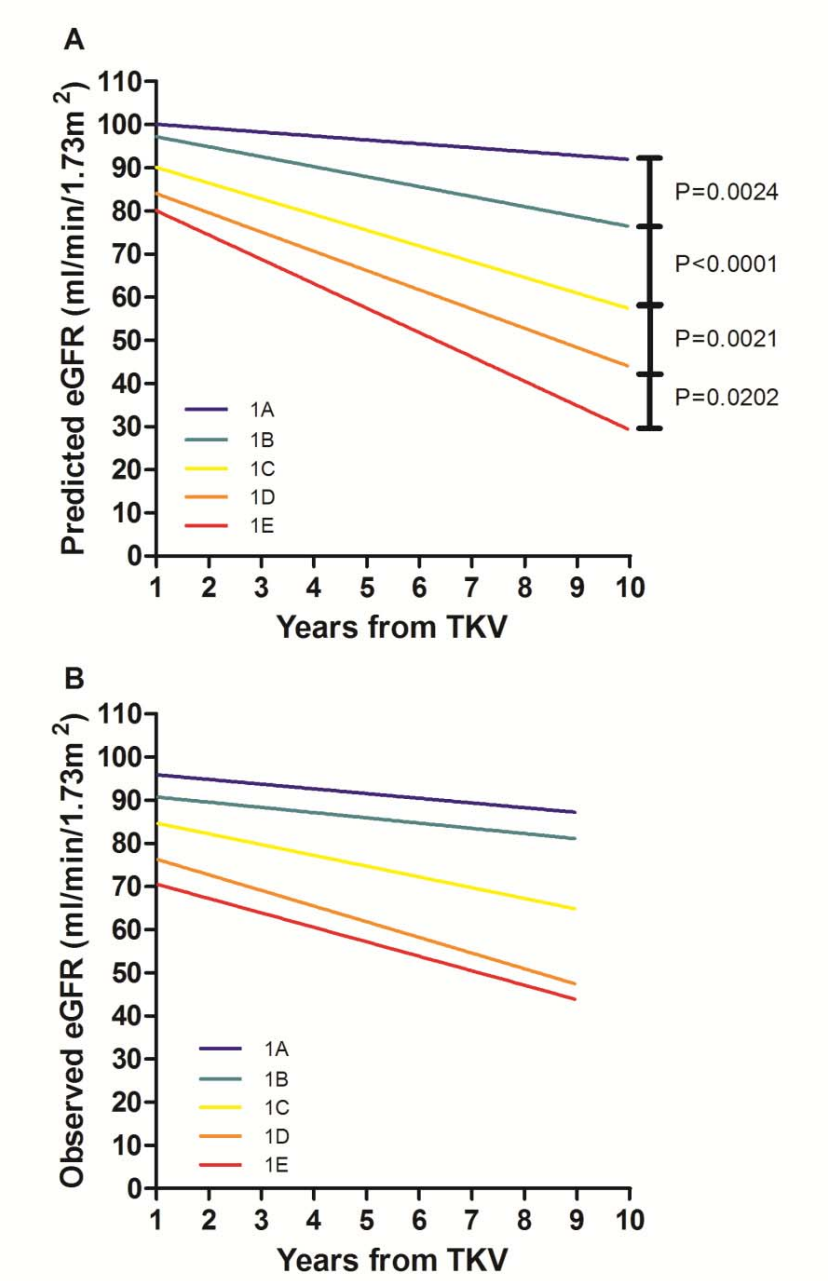

Figure 2: Predicted and observed eGFR over time. A) Average predicted eGFR (ml/min per 1.73 m^2) over time by subclasses. B) Average observed eGFR (ml/min per 1.73 m^2) over time by subclasses.

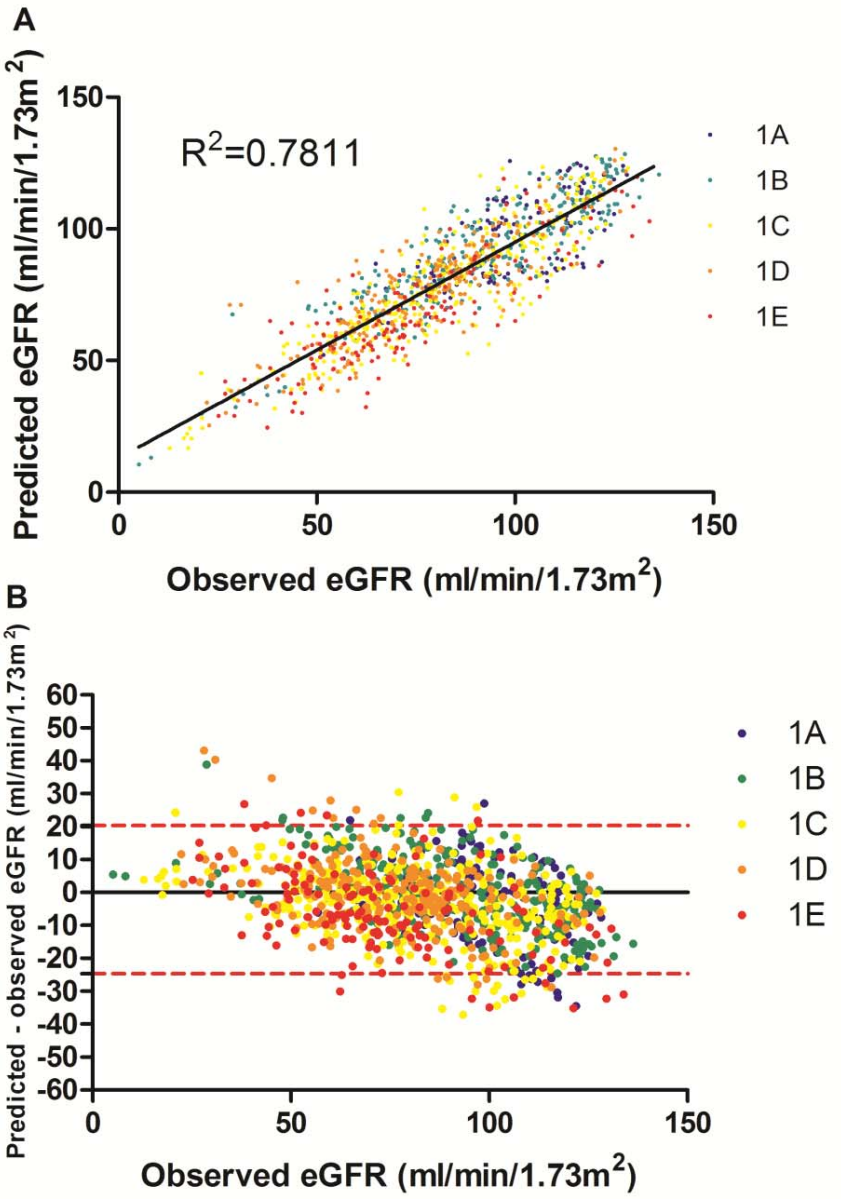

Figure 3: Correlation between observed and predicted eGFR (ml/min per 1.73 m^2). A) Linear correlation between observed and predicted eGFR. Black line represents the overall linear regression. Each dot represents an individual patient and is colored according to its class. B) Bland-Altman analysis of eGFR, showing differences between observed and predicted eGFR against the observed eGFR by CKD-EPI equation. Dotted lines means 95% limits of agreement

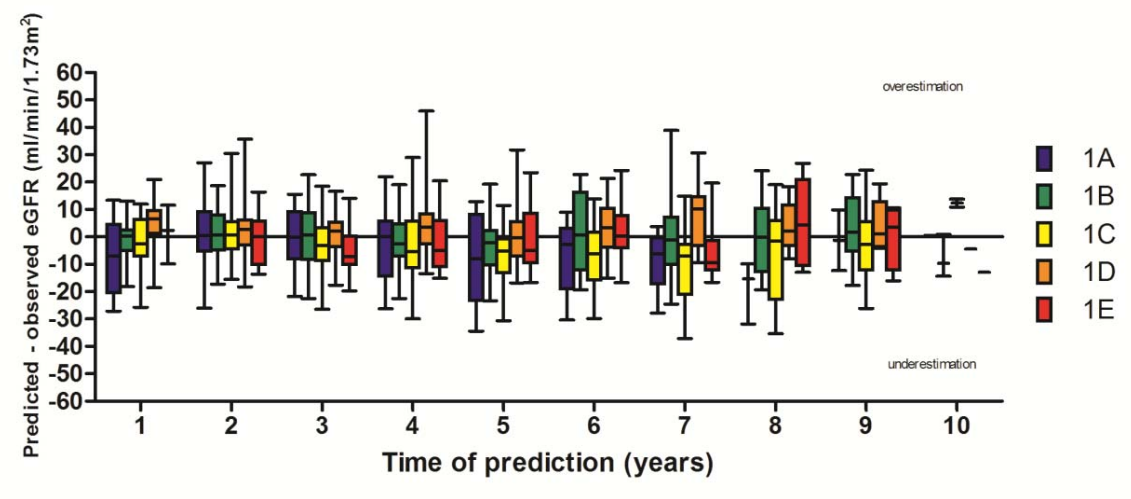

Figure 4: Differences between predicted and observed eGFR (ml/min per 1.73 m^2) over time from a minimum of 1 year (n=203) to a maximum of 10 years (n=9) of follow-up. Data are means ± SD. Data points below 0 signify underestimated values, data points above 0 mean overestimated values.

Chapter 8

Summarizing discussion

Contents

Summarizing discussion

Polycystic kidney disease is characterized by formation of multiple cysts throughout the kidney parenchyma. Two essential mechanisms play a key role in the disease progression: the proliferation of cystic epithelial cells and the cyst fluid secretion. Both processes lead to cyst expansion. Recent research efforts resulted in the discovery of many potential targets to limit cyst expansion. Various drugs were shown to ameliorate PKD progression, but an effective treatment to stop PKD disease progression has still not been identified. Glucose transport and metabolism emerges now as an innovative way to approach the disease. In this thesis we demonstrate that the inhibition of glucose transport or glucose metabolism both reduce cyst expansion and disease progression in animal models of PKD. Figure 8.1 provides a scheme which depicts the essential steps in these pathways of glucose transport and metabolism and the interactions with intracellular signaling cascades.

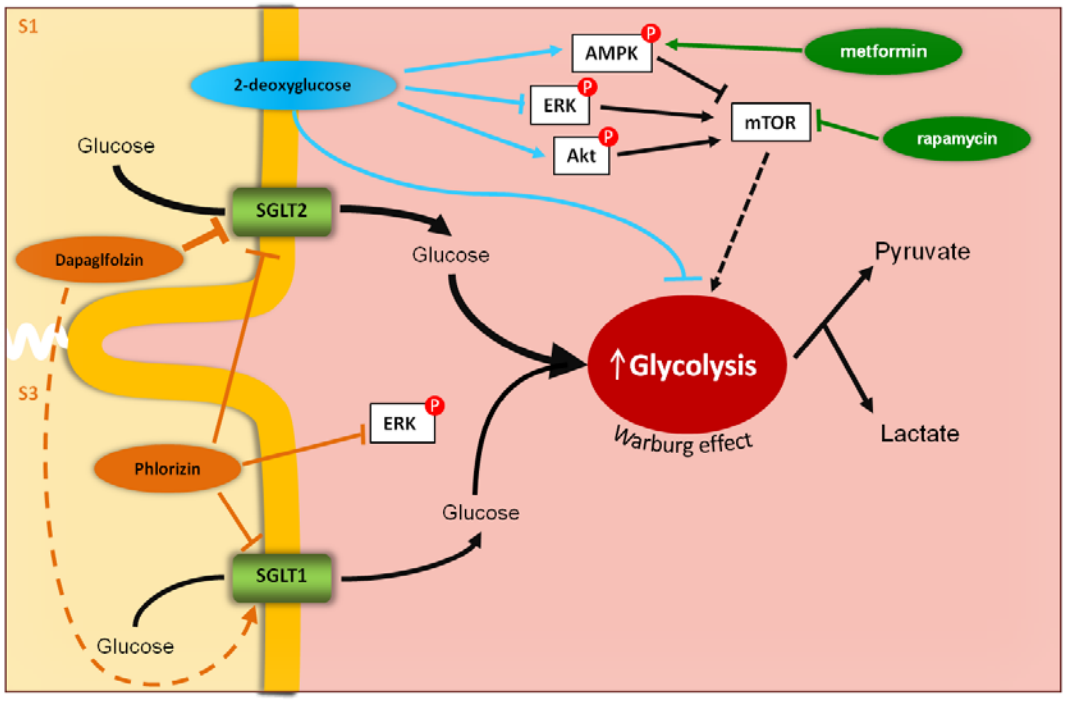

Figure 8.1: Glucose transport and metabolism in cyst epithelial cell. SGLT inhibitors (phlorizin, dapagliflozin) block glucose reabsorption in proximal tubules of nephrons, creating an osmotic gradient that forces the cyst fluid to reenter the tubular lumen, thereby reducing cyst expansion. Glucose analogs (2-deoxyglucose, 2DG) inhibit the enhanced aerobic glycolysis present in proliferative tissues of PKD. Additionally 2DG reduces ERK phosphorylation and stimulates AMPK phosphorylation, both inhibiting mTOR activity. Potential combination of SGLT inhibitors or 2DG with metformin or rapamycin may generate synergistic effects on cell proliferation.

Non selective SGLT inhibition

In Chapter 2, the dual inhibition of SGLT1 and SGLT2 with phlorizin was tested in Han:SPRD rats. Phlorizin exercises a specific and competitive inhibition of both SGLT1 and SGLT2 cotransporters without affecting GLUT transporters. We hypothesized that by inhibition of glucose transport through the epithelium, glucose concentration in the lumen of tubules may increase considerably and could create a gradient that forces fluid transfer from adjacent cysts to the lumen, ameliorating cyst expansion. In Han:SPRD rats, a model for ADPKD, we observed that chronic inhibition with phlorizin, a non selective SGLT inhibitor,

effectively caused glycosuria and osmotic diuresis. Although phlorizin did not completely stop disease progression, it improved renal function, albuminuria and reduced total kidney weight. Additionally, phlorizin decreased cell proliferation and inhibited the MAPK pathway.

These experiments with phlorizin demonstrated that SGLT inhibition is a potential therapy that can reduce the disease progression and partially limit the decline in kidney function in experimental rats with PKD. Nevertheless, phlorizin presents several limitations. It is poorly absorbed orally since it reacts with hydrolytic enzymes and is then converted to phloretin in the small intestine. Thus it must be administrated via subcutaneous injections (1). Phlorizin is therefore not the best choice for a potential PKD treatment.

As mentioned, phlorizin is a competitive inhibitor of both SGLT1 and SGLT2. Nevertheless, SGLT2 is responsible for the most of glucose reabsorption in the kidney (90%) while SGLT1 only manages a small portion (10%). The specific inhibition of SGLT2 with a selective drug may therefore achieve a similar increase in the glucose concentration in the lumen. Based on the structure of phlorizin, several SGLT2-specific inhibitors have been developed (Table 8.1). Dapagliflozin (DAPA) is one of these specific SGLT2 inhibitors that has the advantage of being effectively absorbed by the enteral route. DAPA has been developed and marketed for the treatment of type 2 diabetes mellitus (2). Thus we tested DAPA in Han:SPRD rats and a second model (PCK rats) to examine whether it provided similar beneficial effects on PKD progression. In Chapter 3 and Chapter 4 we report the results from testing the effects of DAPA in Han:SPRD and PCK rats.

Compound	SGLT-2 (AMG)	SGLT-1 (AMG)	SGLT-4 (AMG)	SGLT-5 (mannose)	SGLT-6 (myo-inositol)
C-glucosides			IC_{50} $pIC_{50} \pm SEM$		
Empagliflozin	3.1	8300	11000	1100	2000
(BI 10773)	8.50 ± 0.02	5.08 ± 0.03	4.94 ± 0.09	5.98 ± 0.15	5.70 ± 0.08
Dapagliflozin	1.2	1400	9100	820	1300
(BMS-512148)	8.94 ± 0.06	5.86 ± 0.07	5.04 ± 0.12	6.09 ± 0.22	5.88 ± 0.09
Canagliflozin	2.7	710	7900	1700	240
(JNJ-28431754;TA-7284)	8.56 ± 0.02	6.15 ± 0.06	5.10 ± 0.02	5.77 ± 0.12	6.61 ± 0.09
Ipragliflozin	5.3	3000	16000	740	7800
(ASP-1941)	8.27 ± 0.04	5.53 ± 0.02	4.80 ± 0.07	6.13 ± 0.11	5.11 ± 0.06
Tofogliflozin	6.4	12000	14000	3000	n.d.
(CSG-452, RG-7201)	8.18 ± 0.12	4.92 ± 0.09	4.84 ± 0.12	5.53 ± 0.25	
O-glucosides			IC_{50} $pIC_{50} \pm SEM$		
Sergliflozin	7.5	2100	6000	1100	14000
	8.12 ± 0.01	5.69 ± 0.11	5.22 ± 0.23	5.95 (n = 1)	4.84 ± 0.08
Remogliflozin	12	6500	1500	190	6200
	7.93 ± 0.13	5.19 ± 0.19	5.81 ± 0.24	6.72 ± 0.19	5.21 ± 0.11
T-1095A	4.4	260	2300	1100	3300
	8.36 ± 0.08	6.58 ± 0.04	6.63 ± 0.22	5.97 ± 0.19	5.48 ± 0.15
Phlorizin	21	290	6100	1500	10000
	7.67 ± 0.03	6.54 ± 0.05	5.22 ± 0.32	5.82 ± 0.18	4.99 ± 0.10

Table 8.1: Potency and selectivity of diverse SGLT inhibitors. Data are shown as mean IC_{50} and pIC_{50}. Abbreviations: AMG, α-methyl glucose; SEM, standard error mean. Table is from R. Rempler: Empagliflozin, a novel selective sodium glucose cotransporter-2 (SGLT-2) inhibitor: characterization and comparison with other SGLT-2 inhibitors. Diabetes, Obesity and Metabolism 14: 83–90, 2012.

Selective SGLT2 inhibition

In Chapter 3 we tested whether DAPA can stimulate a similar osmotic diuresis, thereby also reducing cyst expansion in Han:SPRD rats, a rat model of PKD that phenotypically resembles human ADPKD. In contrast to phlorizin, DAPA is well absorbed orally, thus rats received daily oral doses during 5 weeks.

Compared with phlorizin, DAPA treatment resulted in a lesser increase of glucosuria and osmotic diuresis. Thus glucosuria (18.0±4.6 PHLO vs. 15.8±4.5 mmol/day DAPA) and diuresis (65.0±2.2 PHLO vs. 42.7±7.0 ml/day DAPA) increased less in DAPA-treated Han:SPRD. Surprisingly, DAPA increased the kidney mass in Han:SPRD, an effect that was also seen in normal rats treated with DAPA. These hypertrophic effects of DAPA seemed not to be associated with an increased severity of the cystic disease, since no differences in cyst index or cyst number were observed between groups. Histological analyses for cell proliferation, macrophages infiltration and interstitial fibrosis did not reveal significant differences when DAPA- and vehicle-treated Han:SPRD rats were compared.

Several studies have described the apparently reduced effect of selective SGLT2 inhibitors over dual SGLT1/2 inhibitors in animal and humans (3-5). Abdul-Ghani et al. (6) suggested that when SGLT2 is inhibited, SGLT1 can increase its glucose absorption activity (Figure 8.12). SGLT1 is located more distally in the S3 segment of proximal tubules. Due to the main absorption of glucose by SGLT2 in the S1 segment, SGLT1 normally operates at submaximal transport capacity but with inhibition or absence of SGLT2, SGLT1 is forced to reach full capacity. In consequence, the total amount of glucose absorbed in the kidney is greater than expected with SGLT2 inhibition. It appears therefore that the potential effect of DAPA on SGLT2 is blunted by compensatory SGLT1 activity.

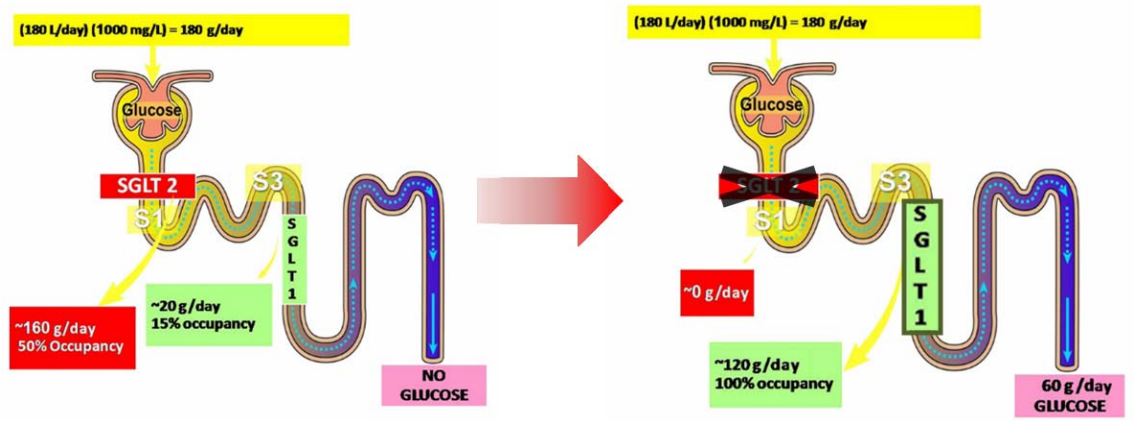

Figure 8.2: Selective inhibition of SGLT2 cotrantsporter in the S1 segment stimulates compensatory glucose reabsorption via SGLT1 in the S3 segment of the proximal tubule. Figure is from Muhammad A. Abdul-Ghani, Novel hypothesis to explain why SGLT2 inhibitors inhibit only 30–50% of filtered glucose load in humans. Diabetes 62:3324–3328, 2013.

How DAPA increases the kidney mass without affecting cyst expansion or proliferation remains unclear. Such a hypertrophic effect was also seen in SGLT2 knock-out mice (7). In addition, a hypertrophic response was also noticed in SGLT1-overexpressing cardiomyocytes (8). Likewise the increased activity of SGLT1 may stimulate a hypertrophic response in the tubular epithelial cells of the S3 segment during inhibition of SGLT2, resulting in an increase of the total kidney mass.

The lack of a significant effect of DAPA on cell proliferation, macrophage infiltration and interstitial fibrosis is in contrast to the effects of phlorizin which was demonstrated to have an effect on proliferation via direct inhibition of ERK1/2 phosphorylation. This effect might be exclusive to phlorizin and is probably not related to the osmotic diuresis caused by SGLT inhibition. Whether more potent dual SGLT inhibitors can also inhibit cell proliferation via MAPK pathway remains to be studied.

In Chapter 4 we describe the effect of DAPA in PCK rats, an animal model of ARPKD. Daily doses of DAPA were administered orally over a period of 6 weeks. Dapa effectively caused osmotic diuresis and glycosuria in PCK rats exceeding values obtained with DAPA in Han:SPRD (23.6±4.3 mmol/day of urine glucose and 57±7 ml/day of diuresis). However, kidney function deteriorated more rapidly with DAPA in PCK rats, and lead to a marked increase in cyst size. Using a new imaging technology (high resolution ultrasound) we could accurately measure kidney and cyst volume in vivo. The details of this new approach are described in Chapter 5. Unexpectedly, DAPA-treated kidneys showed 2-fold bigger cysts than vehicle-treated kidneys. There was no difference in the number of cysts between DAPA- and vehicle-treated kidneys. The total kidney weight and the cyst index increased significantly under DAPA treatment. In contrast with this increased cyst burden, DAPA did not lead to significantly increased intrarenal cAMP levels or enhanced cyst epithelial cell proliferation.

The PCK model is characterized by the development of multiple large cysts in the medullary area of the kidney. Cysts are originating from the collecting duct and most of them remain connected to the tubular lumen (9). This permanent connection could play a key role in the cyst-expanding effect of DAPA. The osmotic pressure in the collecting duct may force fluid to enter the cysts and increase their size. In agreement with this hypothesis, several studies have demonstrated a relationship between luminal pressure and proliferation of intestinal epithelial cells (10, 11). Likewise, the osmotic pressure may be responsible for cyst expansion in DAPA-treated PCK rats.

Taking it together, the results exposed in Chapters 2, 3 and 4 demonstrate that SGLT inhibition cannot effectively stop or reverse cyst progression in rat models of PKD. However, it opens a new way to explore the pathogenesis of the disease. Currently, many others SGLT inhibitors are being developed (12-15) and it appears that less selective SGLT2 inhibitors with a strong inhibition of SGLT2 and partial inhibition of SGLT1 might be most effective. Sotagliflozin (16, 17) is a non-selective SGLT inhibitor currently in phase 3 for treatment of type 1 diabetes mellitus. More potent than phlorizin, sotagliflozin is well tolerated orally and might become a promising drug for PKD, potentially in combination with drugs that also target cyst proliferation like metformin or rapamycin.

Aerobic glycolysis inhibition by 2 deoxyglucose

As explained in Chapter 1, cancer and proliferative tissues show an increased aerobic glycolysis, a phenomenon known as Warburg effect (18). This enhanced aerobic glycolysis, observed in proliferative ADPKD tissues by Rowe et al. (19), offers a unique chance to achieve therapeutic selectivity in PKD. In the same study, they demonstrated efficacy of 2-deoxyglucose (2DG), an analogue of glucose, blocking glycolysis and inhibiting cyst growth in mouse models. In Chapter 6 we have expanded the previous observations and tested whether 2DG is effective in the Han:SPRD rat model of PKD.

We observed at the mRNA level that glycolysis was indeed increased while gluconeogenesis was decreased in cystic kidneys of Han:SPRD rats. After treatment with daily subcutaneous injections of 2DG over 5 weeks, the production of lactate derived from aerobic glycolysis decreased significantly in Cy/+ rats. Significant reductions of kidney weight and cyst index were also noticed. 2DG-treated rats also showed improved kidney function, with increased creatinine and BUN clearances. Furthermore, 2DG reduced cyst epithelial cell proliferation in Cy/+ kidneys while apoptosis was not affected. Attending to the pathways involved that had been demonstrated to be enhanced in Cy/+ rats, 2DG enhanced the phosphorylation of AMPK (which is reduced in untreated Cy/+). Additionally, 2DG reduced significantly the phosphorylation of ERK (MAPK pathway) but increase the phosphorylation of Akt (mTOR pathway).

These results demonstrate that the Warburg effect phenomenon is actively taking place in PKD animal models and can be targeted by analogues of glucose that block the enhanced glycolysis. 2DG effectively delayed the loss of kidney function and cyst progression in the Han:SPRD rat model. Nevertheless, the 2DG-induced activation of Akt may have counteracting effects since Akt phosphorylation promotes cell survival via apoptosis inhibition (20, 21).

A combination treatment of 2DG and metformin was reported to have significant synergistic apoptotic effects on a variety of cancer types in vitro (22, 23). Interestingly, 2DG/metformin combined treatment leads to an increase in caspase-3 activity which stimulates apoptosis in cancer cells. Thus, the potential of combination therapy with 2DG and metformin or rapamycin should be tested in further experiments.

ADPKD patient classification and prediction of kidney function

Our studies on glucose transport and metabolism may have a potential application in the treatment of patients with ADPKD. During development of clinical studies, the use of well defined inclusion criteria and an accurate measurement of critical progression parameters are fundamental. In particular the estimated glomerular filtration rate (eGFR) and the prediction of its course over time is a powerful tool that offers investigators an accurate estimation of the decline in kidney function (24, 25). Through Chapter 7 we tested the applicability of a novel longitudinal mixed-effects equation to predict the eGFR decline over 10 years of follow up of Swiss ADPKD patients. By classifying patients within the different subclasses of ADPKD according their height-normalized total kidney volume (hTKV), an accurate prediction of the eGFR decline during the first 5 years was possible. However we

found that there was a tendency to underestimate the observed eGFR in the long-term, and this was most pronounced in patients with preserved renal function (i.e. an eGFR >60 ml/min/1.73 m^2). Our data suggest that the longitudinal mixed-effects equation is a useful tool for eGFR prediction, especially when it is lower than 60 ml/min/1.73 m^2. Furthermore, our study suggests that the severe subclasses (1D and 1E) might benefit most from future treatments. These patients should therefore be considered for inclusion in future studies.

Concluding remarks

The transport and metabolism of glucose opens a new branch of opportunities to treat PKD. The advances in developing dual SGLT inhibitors which can generate a strong inhibition of SGLT2 and partial inhibition of SGLT1 could be used to achieve similar benefits which were observed with phlorizin. Furthermore, the existence of an enhanced glycolysis in PKD cells provides another opportunity to target the disease.

Together with novel drugs that target the affected signaling pathways, SGLT inhibitors and 2DG may improve the effectiveness of the treatments of PKD. Thus it seems that we may be a step closer in the long way of finding a cure for PKD.

References

1. Crespy V, Aprikian O, Morand C, Besson C, et al. Bioavailability of phloretin and phloridzin in rats. J Nutr 2001; 131: 3227-3230.

2. Han S, Hagan DL, Taylor JR, Xin L, et al. Dapagliflozin, a selective SGLT2 inhibitor, improves glucose homeostasis in normal and diabetic rats. Diabetes 2008; 57: 1723-1729.

3. Liu JJ, Lee T, DeFronzo RA. Why Do SGLT2 inhibitors inhibit only 30-50% of renal glucose reabsorption in humans? Diabetes 2012; 61: 2199-2204.

4. Komoroski B, Vachharajani N, Boulton D, Kornhauser D, et al. Dapagliflozin, a novel SGLT2 inhibitor, induces dose-dependent glucosuria in healthy subjects. Clin Pharmacol Ther 2009; 85: 520-526.

5. Sha S, Devineni D, Ghosh A, Polidori D, et al. Canagliflozin, a novel inhibitor of sodium glucose co-transporter 2, dose dependently reduces calculated renal threshold for glucose excretion and increases urinary glucose excretion in healthy subjects. Diabetes Obes Metab 2011; 13: 669-672.

6. Abdul-Ghani MA, DeFronzo RA, Norton L. Novel hypothesis to explain why SGLT2 inhibitors inhibit only 30-50% of filtered glucose load in humans. Diabetes 2013; 62: 3324-3328.

7. Vallon V, Rose M, Gerasimova M, Satriano J, et al. Knockout of Na-glucose transporter SGLT2 attenuates hyperglycemia and glomerular hyperfiltration but not kidney growth or injury in diabetes mellitus. Am J Physiol Renal Physiol 2012; 304: F156-167.

8. Ramratnam M, Sharma RK, D'Auria S, Lee SJ, et al. Transgenic knockdown of cardiac sodium/glucose cotransporter 1 (SGLT1) attenuates PRKAG2 cardiomyopathy, whereas transgenic overexpression of cardiac SGLT1 causes pathologic hypertrophy and dysfunction in mice. J Am Heart Assoc 2014; 3. pii: e000899

9. Rohatgi R, Greenberg A, Burrow CR, Wilson PD, et al. Na transport in autosomal recessive polycystic kidney disease (ARPKD) cyst lining epithelial cells. J Am Soc Nephrol 2003; 14: 827-836.

10. Hirokawa M, Miura S, Shigematsu T, Yoshida H, et al. Pressure stimulates proliferation and DNA synthesis in rat intestinal epithelial cells. Life Sci 1997; 61: 667-672.

11. Walsh MF, Woo RK, Gomez R, Basson MD. Extracellular pressure stimulates colon cancer cell proliferation via a mechanism requiring PKC and tyrosine kinase signals. Cell Prolif 2004; 37: 427-441.

12. Elkinson S, Scott LJ. Canagliflozin: first global approval. Drugs 2013; 73: 979-988.

13. Markham A, Elkinson S. Luseogliflozin: first global approval. Drugs 2014; 74: 945-950.

14. Poole RM, Dungo RT. Ipragliflozin: first global approval. Drugs 2014; 74: 611-617.

15. Poole RM, Prossler JE. Tofogliflozin: first global approval. Drugs 2014; 74: 939-944.

16. Powell DR, Doree D, Jeter-Jones S, Ding ZM, et al. Sotagliflozin improves glycemic control in nonobese diabetes-prone mice with type 1 diabetes. Diabetes Metab Syndr Obes 2015 8: 121-127.

17. Lapuerta P, Zambrowicz B, Strumph P, Sands A. Development of sotagliflozin, a dual sodium-dependent glucose transporter 1/2 inhibitor. Diab Vasc Dis Res 2015 12: 101-110.

18. Warburg O. On the origin of cancer cells. Science 1956; 123: 309-314.

19. Rowe I, Chiaravalli M, Mannella V, Ulisse V, et al. Defective glucose metabolism in polycystic kidney disease identifies a new therapeutic strategy. Nat Med 2013; 19: 488-493.

20. Datta SR, Dudek H, Tao X, Masters S, et al. Akt phosphorylation of BAD couples survival signals to the cell-intrinsic death machinery. Cell 1997; 91: 231-241.

21. Kim AH, Khursigara G, Sun X, Franke TF, et al. Akt phosphorylates and negatively regulates apoptosis signal-regulating kinase 1. Mol Cell Biol 2001; 21: 893-901.

22. Ben Sahra I, Laurent K, Giuliano S, Larbret F, et al. Targeting cancer cell metabolism: the combination of metformin and 2-deoxyglucose induces p53-dependent apoptosis in prostate cancer cells. Cancer Res 2010; 70: 2465-2475.

23. Cheong JH, Park ES, Liang J, Dennison JB, et al. Dual inhibition of tumor energy pathway by 2-deoxyglucose and metformin is effective against a broad spectrum of preclinical cancer models. Mol Cancer Ther 2011; 10: 2350-2362.

24. Bostom AG, Kronenberg F, Ritz E. Predictive performance of renal function equations for patients with chronic kidney disease and normal serum creatinine levels. J Am Soc Nephrol 2002; 13: 2140-2144.

25. Chapman AB, Bost JE, Torres VE, Guay-Woodford L, et al. Kidney volume and functional outcomes in autosomal dominant polycystic kidney disease. Clin J Am Soc Nephrol 2012; 7: 479-486.

Chapter 9

Curriculum vitae

Curriculum vitae

Daniel Rodríguez Gutiérrez

—DOB: April 23th, 1988 in Santander, Spain.

—2000-2006: High school studies in health science at Santander, Spain.

—2006-2012: Licenciature in Biology with a mayor in health science at the University of Oviedo, Spain.

—2011: Internship in the Units of Microbiology and Biochemistry in Monte Naranco Hospital under the supervision of Prof. Dr. med. Fernando Vazquez Valdes, Oviedo, Spain.

—2012: Erasmus practices grant for an internship in the Department of Cardiology of the University of Zurich under the supervision of PD Dr. Giovanni G. Camici, Zurich, Switzerland.

—2013-2016: PhD position under the molecular and translational biomedicine PhD program in the Division of Nephrology at the University Hospital Zurich, Switzerland, under the direction of Prof. Dr. med. Rudolf P. Wüthrich.

Chapter 10

List of publications

List of publications

- Rodriguez D., Garrido B., Mischler S., and Wüthrich R.P. Prediction of glomerular filtration rate decline in patients with autosomal dominant polycystic kidney disease. (in preparation)

- Riwanto M., Kapoor S., Rodriguez D., Edenhofer I., Segerer S. and Wüthrich R.P. Inhibition of aerobic glycolysis with 2-deoxyglucose retards polycystic kidney disease progression in Han:SPRD rats. PLoS One 11 (1): e0146654, 2016

- Kapoor S., Rodriguez D., Mitchell K. and Wüthrich R.P. High resolution ultrasonography for assessment of renal cysts in the PCK rat model of autosomal recessive polycystic kidney disease. Kidney Blood Press Res 41:186-196, 2016

- Rodriguez D., Kapoor S., Edenhofer I., Segerer S., Riwanto M., Kipar A, Yang M., Mei C. and Wüthrich R.P. Inhibition of sodium-glucose cotransporter 2 with dapagliflozin in Han:SPRD rats with polycystic kidney disease. Kidney Blood Press Res 40:638-647, 2015

- Kapoor S., Rodriguez D., Riwanto M., Edenhofer I., Segerer S., Mitchell K. and Wüthrich R.P. Effect of sodium-glucose cotransport inhibition on polycystic kidney disease progression in PCK rats PLoS ONE 10(4): e0125603, 2015

- Wüthrich R.P., Kistler A.D., Rodriguez D., Kapoor S and Mei C. Blood Pressure Control for Polycystic Kidney Disease. (Book chapter 5) Polycystic Kidney Disease: ISBN 978-0-9944381-0-2, 2015

- Spescha R.D., Klohs J., Semerano A., Giacalone G., Derungs R.S., Reiner M.F., Rodriguez D., Mendez-Carmona N., Glanzmann M., Savarese G., Kränkel N., Akhmedov A., Keller S., Mocharla P., Kaufmann M.R., Wenger R.H., Vogel J., Kulic L., Nitsch R.M., Beer J.H., Peruzzotti-Jametti L., Sessa M., Lüscher T.F., and Camici G.G. Post-ischaemic silencing of p66Shc reduces ischaemia/reperfusion brain injury and its expression correlates to clinical outcome in stroke. European Heart Journal 36, 1590–1600, 2015

- Bonani M., Rodriguez D., Fehr T., Mohebbi N., Brockmann J., Blum M., Graf N., Frey D. and Wüthrich R.P. Sclerostin blood levels before and after kidney transplantation. Kidney Blood Press Res 39:230-239, 2014

- Wang X., Zhang S., Liu Y., Spichtig D., Kapoor S., Koepsell H., Mohebbi N., Segerer S., Serra A.L., Rodriguez D, Devuyst O., Mei C and Wüthrich R.P. Targeting of sodium-glucose cotransporters with phlorizin inhibits polycystic kidney disease progression in Han:SPRD rats. Kidney Int. 84, 962–968, 2013

Chapter 11

Acknowledgements

Acknowledgements

I am extremely grateful to my parents for giving me an extraordinary education and the opportunity of studying in a foreign country, supporting me in every step and decision. I am also grateful to my girlfriend Natalia whom I dearly love for accompanying me in this adventure and being there for me during the best and worst of times.

I would like to sincerely thank Professor Rudolf P. Wüthrich of University of Zurich who has been an exceptional mentor, dissertation advisor and friend. Without his generous guidance and continuous help this dissertation would not have been possible.

I would like to express my cordial appreciation to my committee chair, Prof. Arnold von Eckardstein and to the committee members Prof. Carsten A. Wagner and Prof. Ian Frew for being so kind and for showing interest in my research and for giving precious advice and guidance.

I would like to specially thank Sarika Kapoor and Meliana Riwanto who contributed enormously to this project and helped me with an excellent advice and support.

And big thanks to all my friends and colleagues who helped me to survive the worries and difficulties of my work, and who gave me their support over these years.